A COMPARATIVE ANALYSIS OF TERRESTRIAL LASER SCANNING (TLS) AND STRUCTURE FROM MOTION (SfM) PHOTOGRAMMETRY FOR MEASURING FLUVIAL SEDIMENTS

NEIL Burrows

Contents

List of Figures

List of Tables

<u>Acknowledgements</u>

Declaration

I certify that this thesis consist of my own original work. All quotations from published and unpublished sources are acknowledged as such in the text. Material derived from other sources is also indicated.

Total number of words in main text: 17,705

Name _____

Signature_____

Date_____

Abstract

A precise, time-efficient, cost-effective method for quantifying riverbed roughness and sediment size distribution has hitherto eluded river scientists. Traditional techniques (e.g., Wolman counts) have high potential for error brought about by operator bias and subjectivity when presented with complex facies assemblages, poor spatial coverage, insufficient sample sizes, and misrepresentation of bedforms. The application of LiDAR facilitated accurate observation of micro-scale habitats, and has been successfully employed in quantifying sediment grain size at the local level. However, despite considerable success of LiDAR instruments in remotely sensing riverine landscapes, and the obvious benefits they offer – very high spatial and temporal resolution, rapid data acquisition, and minimal disturbance in the field – procurement of these apparatus and their respective computer software comes at high financial cost, and extensive user training is generally necessary in order to operate such devices. Recent developments in computer software have led to advancements in digital photogrammetry over a broad range of scales, with Structure from Motion (SfM) techniques enabling production of precise DEMs based on point-clouds analogous to, and even denser than, those produced by LiDAR, at significantly reduced cost and convolution during post-processing. This study has employed both an SfM-photogrammetry and Terrestrial Laser Scanning (TLS) approach in a comparative analysis of sediment grain size, where LiDAR-derived data has previously provided a reliable reference of grain size. Total Station EDM theodolite provided the parent coordinate system for both SfM and meshing of TLS point-clouds. For each data set, a 0.19 m moving window (consistent with the largest sediment clast b axis) was applied to the resulting point-clouds. Two times standard deviation of elevation was calculated in order to provide a surrogate measure of grain protrusion, from which sediment frequency distribution curves were drawn. Results through semi-variance analyses elucidated continuity of each data set. Where univariate statistics failed to reveal disparity between the two data sets, semi-variance analysis exposed considerable variability in roughness, thus revealing a greater degree of detail in SfM-derived data.

Chapter 1: Introduction

1.1. River Restoration and The European Water Framework Directive

Hydrogeomorphic impacts of man-made hydraulic structures on the streams in which they reside are poorly understood and seldom quantified. In addition, morphological channel response following river restoration procedures has rarely been monitored to a reasonable standard, both as a consequence of insufficient data acquisition, and unsatisfactory timeframes over which data is collected. However, over the last decade, advent of the European Water Framework Directive (WFD) (European Commission, 2000) has provided impetus to restore rivers and monitor their subsequent ecological and hydromorphological response; hence, a requirement for accurate monitoring is necessary to demonstrate adequate completion of WFD aims and objectives (Skinner and Bruce-Burges, 2005).

Effective river restoration monitoring under guidance of the WFD relies on identification of a set of parameters relating to, for example, geomorphological, hydrological, and ecological objectives (England *et al.,* 2008). In order to more satisfactorily encompass interactions between hydrologic and geomorphic fluvial processes, the concept of 'hydromorphology' (European Commission 2000; Newson and Large, 2006) was introduced in order to better assess physical habitat quality (England *et al.,* 2008; Orr *et al.,* 2008). Thus, linkages between physical and ecological components of rivers are brought together by holistic management practices and common objectives of a wide array of practitioners of varying disciplines (Vaughn *et al.,* 2009) (Figure 1.1.) The result of this is an arrangement whereby a 'good ecological status' or, in instances where a water body is classed as 'heavily modified', 'good ecological potential' is sought.
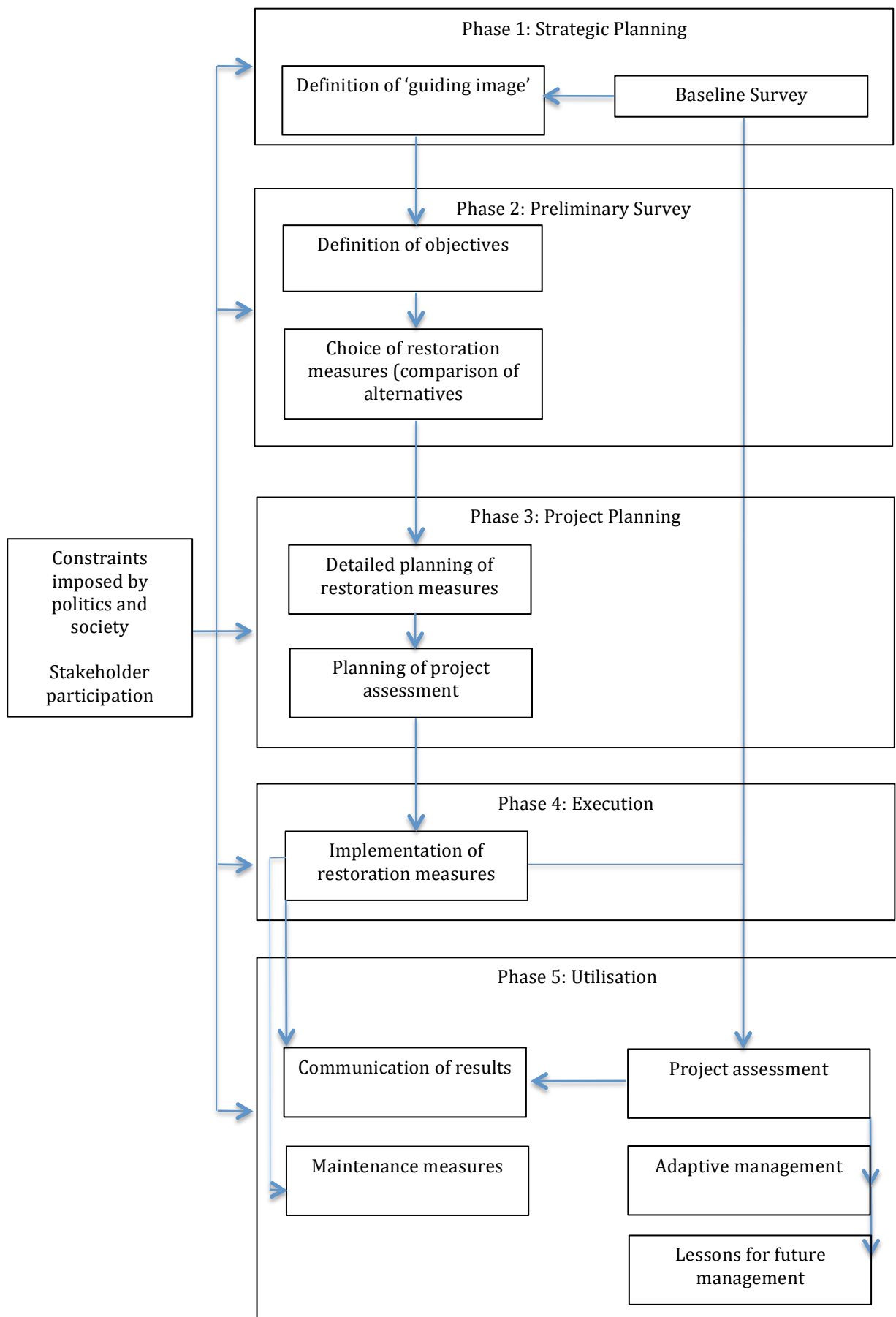
Figure 1.1. *Planning, implementation and structure of river restoration schemes. Modified from Woolsey et al. (2007).*

1.2. Key Drivers for Weir Removal-based River Restoration

There are a number of primary benefits of employing complete weir removal as a technique for river restoration. Fundamentally, such measures are applied in order to improve upstream and downstream ecological and hydrological longitudinal connectivity in streams that have been regulated by man-made structures. This may be displayed as benefits to a plethora of aquatic organisms, which are able to readily migrate and disperse throughout a river both as populations or individuals.

Additionally, removal of a barrier almost instantly restores natural sediment transport processes by initiating redistribution of impounded material. This eventually leads to complex, heterogeneous assemblages of habitat types, which further enhances biological functionality of streams. Moreover, as channel adjustment is initiated following barrier removal, a natural regimen of erosion and deposition is established, thus satisfying a range of criteria set out by the Water Framework Directive.

There are additional, anthropogenically-oriented benefits to removing weirs, most notably in the form of social and economic factors delivered in compliance of Ecosystem Services (a full and comprehensive overview of which can be found in Maltby *et al.* (2011)). Essentially, however, restoration by weir removal may contribute to the aesthetics of a river reach, in addition to general improvement of fauna and flora and potential for recreation. Moreover, reestablishing natural river processes may also reduce the risk of flooding, particularly as climatic changes further exacerbate extreme hydrologic events; thus, simply by removing an obsolete, outdated structure, a wide range of benefits can be achieved at relatively low cost and subsequent maintenance.

1.3. Shortfalls in Contemporary Monitoring and Appraisal Practices

Post-scheme monitoring and appraisal is integral to the success of river restoration (Skinner and Bruce-Burgess, 2005; Bernhardt *et al.,* 2007; England, 2008). Many projects, despite their increasing prevalence in the UK, fail to include sufficient evaluation methods that assess whether or not their objectives have been met (Wohl, 2005). Indeed, England (2008) identifies that many schemes are somewhat lacking precisely because their core objectives are not adequately outlined in the early stages of planning, and are thus destined to fail where monitoring is concerned. Furthermore, instances where monitoring has taken place, yet yielded results that may not correspond with initial aims, are rarely published. Morandi *et al.* (2014) found a lack of post-restoration feedback from French river restoration projects, particularly where communication of pre- and post-restoration references (i.e., biological metrics – such as floara and fauna survey data; and physical metrics – such as hydromorphology survey data). This is perhaps, in part, due to involvement of multiple stakeholders and pressure to maintain Good Ecological Status in compliance with government mandates.

Nevertheless, many river restoration schemes comprise a range of elements that have in some way been replicated elsewhere. It is therefore critical that results of successes *and* failings are shared among the river restoration community in order to: a) better understand river processes following remedial engineering; b) facilitate vital communication between practitioners, whose results can be compared; and c) maintain Good Ecological Status once achieved. Further, successful appraisal must encompass a wide-range of parameters in order to fully assess post-restoration developments. However, such appraisals must be implemented under adaptive management, defined by Kondolf and Downs (2002) as 'arguably the most suitable conceptual framework for planning restoration schemes'. River restoration should not be implemented in an 'all or nothing' approach (Palmer *et al.,* 2005) but rather as a set of adjustable milestones, realised through synthesis of quantified scientific observation (e.g., Florsheim *et al.,* 2005).

1.4. Potential for Remote Sensing and Computer Modelling as River Restoration Appraisal Methods

Remote Sensing

Various remote sensing techniques for evaluating natural river phenomena have emerged as a vital component in many riverine studies (Metres, 2002). Many such methods have existed since the launch of NASA's LandSat mission in 1972 (See Kirk 1982; Dekker *et al.,* 1997; Mertes *et al.,* 2002), leading to significant advancements in the exploitation of physical properties of light for informing various parameters of a variety of natural phenomena. However, space-borne instruments are limited in their spatial resolution in that only relatively large areas can be observed (Figure 1.2), and therfore, for the most part, cannot match spatial resolutions achieved by aerial- and terrestrial-based instruments.

Perhaps the most significant recent development in fluvial remote sensing is the advent of LiDAR (Light Detection And Ranging). Both aerially (Bowen and Waltermire, 2002; Charlton *et al.,* 2003; Jones *et al.,* 2007; Cavalli *et al.,* 2008; Vetter *et al.,* 2011) and terrestrially (Heritage and Hetherington, 2007; Entwistle and Fuller, 2009; Hodge *et al.,* 2009; Milan *et al.,* 2011; O'Neil and Pizzuto, 2011; Smith *et al.,* 2011) deployed LiDAR instruments have yielded excellent results, each offering their own particular advantages. Aerial LiDAR, for instance, provides highly accurate topographical data at spatial resolutions significantly greater (sub-metre) than that offered by space-borne instruments; however, it cannot provide the very high resolutions attained by terrestrial LiDAR.

Terrsetrial Laser Scanning, though limited by its spatial coverage, is able to gather topographic data at significantly finer resolution (sub-decimetre) in comparison to its aerially deployed counterpart. This permits a wide range of study, particularly where subtle alterations to the structure and composition of topographical features may elude convectional observation techniques. However, there a number of considerations that may limit TLS in its application, such as initial procurement cost of equipment and software; cumbersome scanners, difficult to maneuver in the field; and extensive post-processing time and computational requirements following data acquisition.

TLS methods have, historically, been employed in favour of more conventional techniques given the precision and accuracy offered by such instruments. However, recent developments in computer software have allowed for production of fine-scale digital elevation models (DEMs) similar to those derived from LiDAR, using conventional digital cameras. So-called Setructure from Motion (SfM) photogrammetry techniques have potential to instigate a new era in remote sensing, where traditional constraints, such as cost and specialised training, are no longer limiting factors for many river science applications. This thesis will encompass both TLS and Structure from Motion methods in a comparative, proof-of-concept quantitative study of grain size. For this reason, a patch-scale approach was selected in order to reduce time expenditure during data acquisition, post-processing, and analysis.
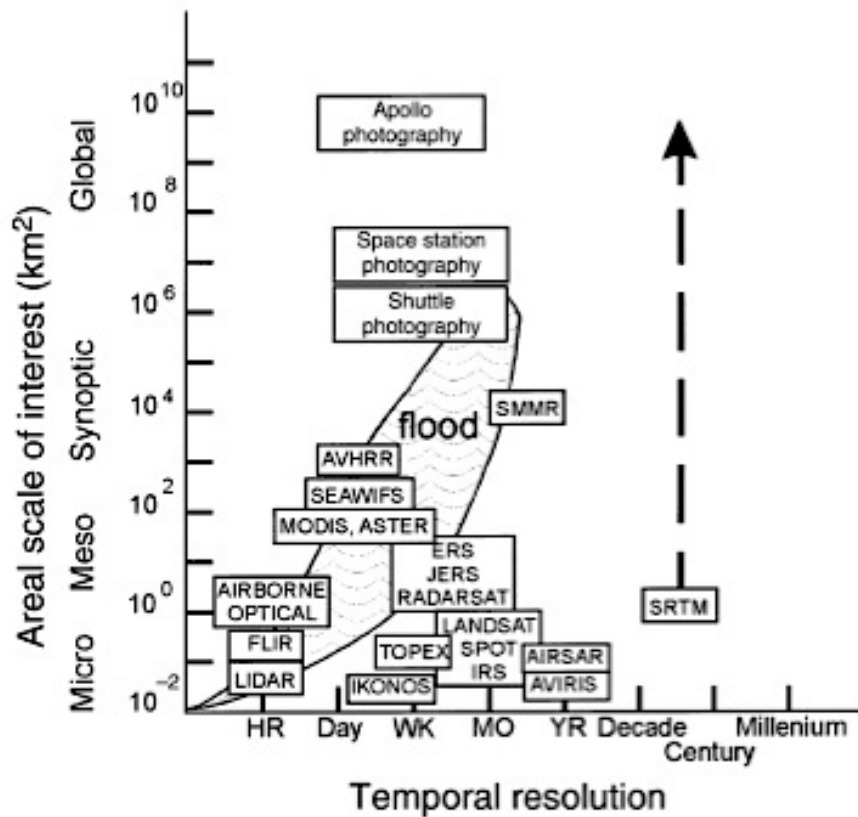
Figure 1.2 *Spatial and temporal scale of a range of remote sensing apparatus employed in riverine studies. After Mertes (2002).*

1.5. Roughness Elements of Rivers and the Quantification of Grain Size Distribution

The textural characteristics of river bedforms is important in controlling near-bed hydraulics, flow resistance and grain particle motion (Nikora *et al.*, 1998), and are defined by interactions between hydraulic roughness, flow parameters and sediment supply (Van Rijn, 1984). Quantification of bed roughness and its interrelationship with river flow is a fundamental element of hydraulic engineering and river restoration design, both as a physical, channel-forming component, as well as one that has important implications for aquatic ecology and habitat. However, bedforms are highly dynamic, moveable features, comprised of a complex arrangement of particle shapes and sizes, which are shaped and worked into an infinite configuration of packing, orientation, sorting and clusters, which, are therefore difficult to quantify.

Central to the formation of complex beforms is flow velocity and flow resistance, described by Knighton (1998. p, 101) as, 'one of the most important elements in the interaction between the fluid flow and the channel boundary'. For the purposes of this thesis, it is necessary to focus on 'boundary resistance', that is, friction created by bed morphology (Lawless and Robert, 2001), where, in streams whose bed is comprised of gravels and cobbles (i.e., particles ranging from 2 – 64mm and 64 – 256mm respectively), is derived from the shape and configuration of particles (Richards, 1982. p, 17), in addition to sediment size distribution.

Advancements in aforementioned remote sensing – namely, Terrestrial Laser Scanning – has offered perhaps the most substantial and influential recent shift in the ways in which grain size distribution is measured, providing a means of highly accurate grain size calculation with the exclusion of obstructive limitations associated with labor-intensive manual counting. A particularly beneficial advantage of TLS is that it is able to rapidly gather sub-cm topographic data over relatively large areas, thus illuminating the need for any strenuous manual surveying. Nevertheless, despite its success in topographic surveying, TLS at present is extremely financially expensive, with the cost of scanners being in the order of £100,000. Moreover, specialist training is required to operate such devices, and post-processing can be extensive and often requires considerable computing power.

More recently, modern photogrammetric techniques have allowed for acquisition of high-resolution topographic data. So-called Structure from Motion (SfM) photogrammetry derives reconstructed three-dimensional geometry through identification of conjugate points within two-dimensional digital images. Though the software packages that facilitate this technique are relatively new (for example, Autodesk 123D Catch; Microsoft Photosynth; VisualSFM; Photomodeler and, in this instance, AgiSoft PhotoScan Pro), the mathematical principles on which photogrammetric Structure From Motion derives its models has been in existence since the middle of the 20th Century, and, through extensive research and development, have evolved over the decades to eventually produce the aforementioned programs (Micheletti *et al.* 2015).

A primary benefit of SfM-photogrammetry is that the associated software performs the three-dimensional reconstruction process automatically: very little user training (compared to other techniques, for instance TLS and traditional photogrammetry) is required to produce a suitably accurate topographic model. The automated workflow – that is, image preparation; photo alignment; dense point-cloud construction; georeferencing; mesh construction; and DEM construction (see section 4.4) – is extremely intuitive, and the forgiving nature of SfM software means that processing is carried out with relative ease and efficiency. Whilst the georeferencing element of the SfM workflow is not essential for producing a representative model, fully georeferenced ground control points (GCPs), which are easily identifiable in each image, must be included in order to provide scale – which *is* essential if quantitative measurements are to be extracted from SfM-derived data (Micheletti *et al.,* 2015).

The final product of fully georeferenced SfM output data allows for full quantification of topography to the user's exact specifications, as one would with a model produced by aerial or terrestrial laser scanned data. Indeed, data produced by SfM-photogrammetry would be very familiar to anyone with experience of handling laser-derived topographic models. This is an important element of this study, whose main intention is to remotely and quantifiably characterise sediment characteristics of dry gravel.

Attaining sediment grain distribution, however, is particularly problematic. Commonly employed, traditional methods (e.g., Woman, 1954) require sampling of 100 randomly selected grain particles, from which a range of sediment size percentiles (16, 50, 84, and 99%, for example) can be derived. Though this technique is a ubiquitous feature of many geomorphic investigations, there are a number of fundamental shortcomings that have potential to yield erroneous data. Attempts have been made to eradicate such limitations: Leopold (1970), for instance, proposed a method whereby size frequency is obtained via a size-to-weight conversion in order illuminate bias towards larger particles during sampling. However, this technique is extremely laborious with similarly poor spatial coverage and insufficient sample size associated with that of the Wolman (1954) technique.

In addition, sediment features are often heterogeneous in form, comprising of many particle shapes and sizes, which are arranged in various configurations (e.g., amouring and imbrication) depending on the prevailing conditions. However, Buffington and Montgomery (1999b) demonstrate that gravel features are also commonly made up of homogenous patches or 'facies', 'distinguished by from one another by differences in grain size and sorting'.

1.6. Aims and Objectives of Thesis

Given that there are a number of shortfalls in the understanding of geomorphological channel modification following barrier removal, this thesis aims to present and examine several methods that can be used to observe a variety of geomorphic components fundamental to controlling river form and dynamics. Since sediment transport processes are essential in governing channel morphology, a new, innovative technique for quantifying sediment grain size characteristics will first be presented in a proof-of-concept approach. This will feature photogrammetric techniques to derive high-resolution digital elevation models (DEMs) from which a range of sedimentological parameters can be read. The technique has been applied in conjunction with traditional methods – which have previously been shown to yield insufficient data, yet which remains the industry standard – in addition to contemporary terrestrial laser scanning (TLS) methods (e.g., Entwistle and Fuller, 2009), which has previously yielded excellent results, but is expensive, cumbersome and requires considerable post-processing and user training.

Results from this new method will receive validation through the application of semi-variance analysis, i.e., multi-directional variograms, which has been validated as a viable statistical method in a number of studies that derive textural composition of dry gravel features in order to inform channel morphology and hydromorphologic processes. A full overview of the aims, objectives and structure of this thesis are described in Table 1.1.

Table 1.1. *Thesis objectives and the methods employed in order to achieve them.*

Objective	Method	Chapters
1. Present a novel, parsimonious, high-accuracy technique for quantitative examination of sediment grain size distribution on dry gravel features.	Use photogrammetric Structure from Motion techniques to build Digital Elevation models, from which sediment size distribution can be derived. Compare with existing TLS methods (e.g., Entwistle and Fuller, 2009) and manual counting techniques (e.g., Wolman, 1954).	4 and 5
2. Demonstrate how SfM-photogrammetry can be used to quantify sediment grain size to the same degree of accuracy offered by terrestrial laser scanning.	Quantifiably compare results by applying semi-variance statistics of TLS- and SfM-derived point-clouds in order to inform continuity (i.e., roughness).	4 and 5
3. Examine how development of a new method for quantifying sediment grain size – which has been used in conjunction with both traditional, empirical study and statistical analysis – will affect geomorphological investigations in the future, with specific reference to river restoration and engineering.	Critically evaluate findings from chapters four and five through comprehensive discussion. Present limitations to each aspect of the thesis and possible future recommendations. Provide a summarising conclusion.	6 and 7

1.7. Motivation

The stimulus for this investigation is a desire to provide a method for accurately quantifying sediment grain size by means of a remote sensing method that is accessible to those operating on modest budgets, yet who require a precise estimation of grain size distribution and sediment characteristics. Existing remote sensing methods, though highly accurate and strongly established as a viable method for micro-scale topographic estimation, are beyond the financial reach of many river restoration projects, particularly in a time of austerity at the time of writing. At the same time, methods for quantifying river restoration are highly sought after in an age where process-based restoration is widely ubiquitous in modified catchments.

1.8. Thesis Layout

This thesis is comprised of two distinct studies whose results will be integrated to form a single, cohesive argument. A generalised layout is provided in Figure 1.3., however, the broader rationale behind this arrangement is based on independent fractions of each study being assimilated through combined results. It is anticipated that this approach will assist the reader's referral to the presented material, in addition to creating a clear, intelligible paper.

Chapter Two provides a comprehensive review of the available literature regarding subjects touched upon throughout this thesis. This evaluation of existing works led to the establishment of experimental designs for each investigation presented herein, by allowing for identification of potential gaps in current knowledge, or of where improvements in technology may permit progression of existing research. Following this, a brief overview of the study site is provided in chapter Three, including descriptions of catchment characteristics – such as geology, land-use, precipitation, and elevation – in addition to a brief introduction of relevant maps, hydrological characteristics and a general historical background.

Chapter Four is separated into the two distinct elements that comprise this study: methods for quantifying sediment grain size distribution; and geo statistical analysis of data gathered using a range of techniques; including traditional, manual methods; laser scanning methods; and so-called SfM-photogrammetry methods. This separation is continued in chapter Five, where results from all the applied methods are presented. First, empirically-derived results from traditional, manual counting methods are provided, followed by findings from the application of both contemporary TLS, and SfM-photogrammetry. Next, results generated from geostatistical analysis are presented along with results from investigations of internal consistency within generated spatial data sets.

In Chapter Six, results produced from the aforementioned elements of the study are assimilated and examined in detail. A discussion of the derived results is provided, which contrasts each component as a method for quantifying sediment grain size; and explores the potential use of SfM-photogrammetry in river restoration schemes.

Finally, Chapter Seven provides an overall conclusion, presenting within it limitations of the methods and analysis employed in the study, in addition to possible future recommendations where applicable. Furthermore, the aims and objectives highlighted in section 1.5 will be referred back to and examined; demonstrating how this study may contribute in the future remote sensing of fluvial environments.
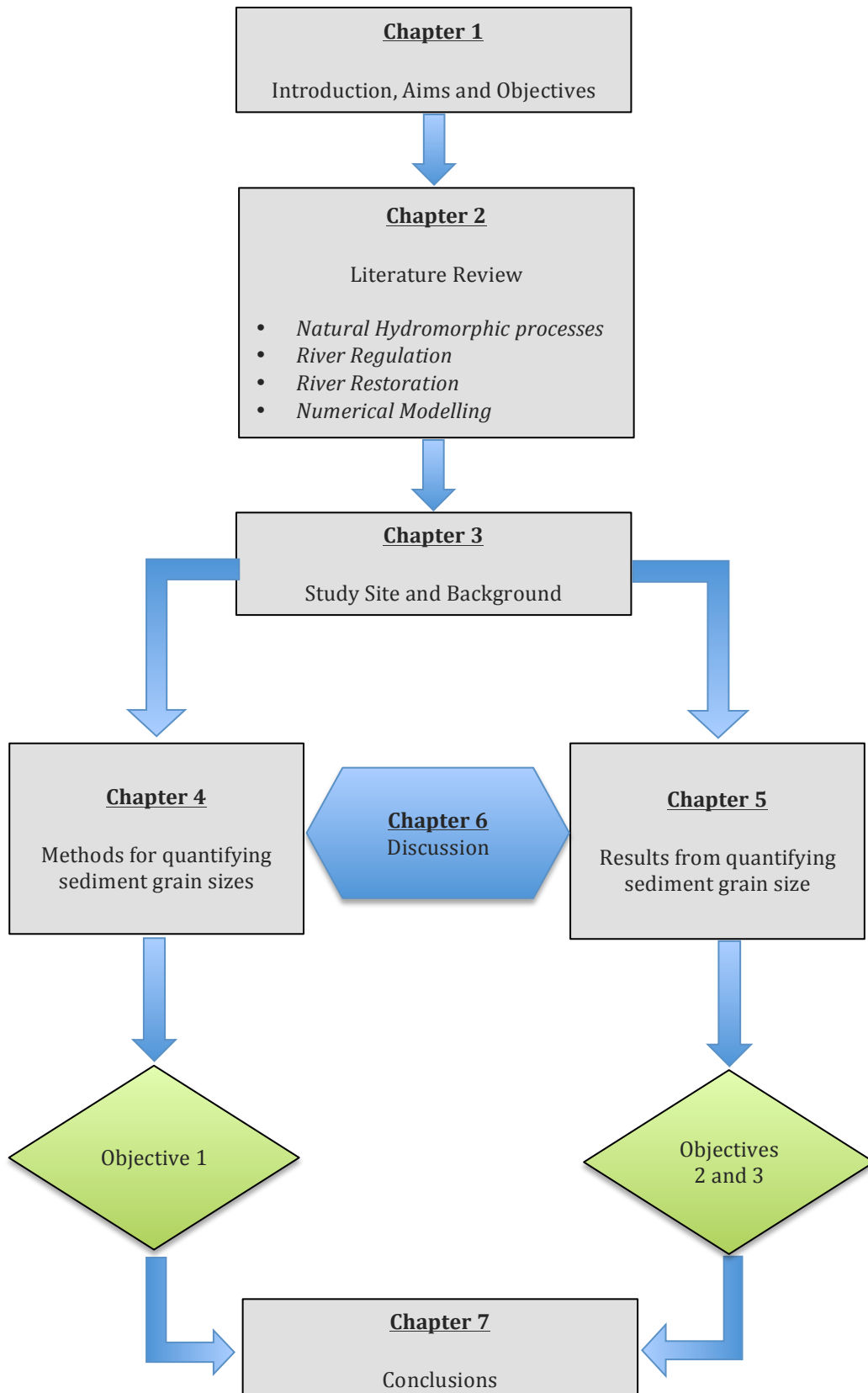
Figure 1.3. *A generalised thesis workflow highlighting its core aims and objectives and how they will be realised.*

Chapter 2: Literature Review

2.1. *Natural Hydromorphologic Processes of Gravel-Bed Streams*

Gravel-bed rivers are inherently complex systems, which encompass an intricate mosaic of in-stream habitat types and functions, and are shaped by interactions of fluid flow and erodible materials within the channel boundary (Knighton, 1998). Such systems comprise a diverse range of hydromorphologic processes; however, two primary forces acting upon water flowing within a channel's boundary define channel form: gravity, which facilitates movement of water in the downslope direction; and friction, which resists downslope motion (Leopold *et al.,* 1964; Van Rijn, 1984; Knighton 1998).

The flow of water in rivers is highly dynamic and undergoes periodic fluctuations of magnitude over timescales of 'hours days, seasons, years, and longer' (Poff *et al.,* 1997). Predictions of such events are permitted through analysis of long-term flow data derived from an extensive network of stream gauges, and is generally expressed as a daily mean average (although instantaneous values taken at 15 minute intervals may be available) usually in cubic metres per second (m^3s^{-1}).

Flow regimes exhibited by rivers are essentially dictated by precipitation events (Poff *et al.,* 1997), though catchment geology, soil typologies, and land cover can influence the timing, magnitude, frequency and duration of high and low discharge (Newson, 1994). Such fluctuations are important from a hydromorphologic perspective, since water flowing within a channel is the medium in which sediments and debris is transported, and thus facilitate morphological processes operating within the channel (Knighton, 1998). There is, then, a significant, optimal discharge for every river: a point at which sediment transport is initiated and channel-forming processes take place. 'Dominant Discharge', defined by Wolman and Miller (1960) as the discharge that performs most 'work' (i.e., sediment transport); and by Benson and Thomas (1966) as 'the discharge that over a long time period transports the most sediment', is a fundamental concept in fluvial geomorphology (Richards, 1982; Knighton, 1998).

In order for sediment transport to occur, river flow must first reach a sufficiently high discharge to initiate entrainment (the modes by which sediments are transported in a stream are described in figure 2.1). This may be described in the context of flow competence (Ashworth and Ferguson, 1989; Powell and Ashworth, 1995; Whitaker and Potts, 2007) and is expressed as stream power (Ω):

$$\Omega = \rho g Q S$$

More specifically, the entrainment, transport and deposition of non-cohesive alluvial sediments are fundamental for river morphology (Richards, 1982). Sediment transport processes may be separated into three distinct fractions: suspended load, comprised of fine, easily transported material; solute load, comprised of those products of weathering and erosion which are conveyed in the form of solutes; and bed-load, comprised of large sediment particles (gravels, cobbles and boulders) which form a river's substrate (Richards, 1982). The former two fractions represent the majority of material transported by a river at any given moment whilst the latter, despite contributing a smaller portion of total transported material, is important for defining channel form (Collins and Dunne, 1990) and thus will receive most investigation throughout this thesis. Bed-load transport is a phenomenon that occurs intermittently, during periods when discharge is sufficiently high to initiate entrainment and sustain transport, and is mediated through three primary mechanisms of conveyance: rolling, sliding and saltation (erratic jumping and bouncing of particles (Figure 2.1.)) (Van Rijn, 1984). Initially, some threshold must be achieved at which the aforementioned forces (gravity and friction) are balanced; either as critical shear stress (τ_{cr}) or critical velocity (v_{cr}). Mean boundary shear stress may be defined as:

$$\tau_0 \gamma R s$$

Where γ is specific weight of water, R is hydraulic radius and s is slope (after Knighton, 1998). Whilst this notion is broadly accepted, true transport processes require complex calculations in order to sufficiently describe them.

Numerous attempts have been made to fully encompass the entire range of variables that may influence bed-load transport, with DuBoys (1879) creating the first successful (albeit incomplete) numerical formula. Later works followed (see table 2.1. for a brief summary) (Schoklitsch, 1930; Shields, 1936; Einstein, 1942; Meyer-Peter, 1949; Einstein, 1950; Yalin, 1963; Nielsen, 1992) and have been subsequently tested under various conditions (Dietrich, 1982; 1989; Gomez, 1989; Gomez and Church, 1989; Lisle, 1995; Reid *et al.,* 1996; Buffington and Montgomery, 1997; 1999a; Yang and Huang, 2001; Barry *et al.,* 2004; Wilcock *et al.,* 2009; Recking *et al.,* 2012) (Figure 2.1b).

A.

B.

Drag force = $\pi_o/_n$ assuming n particles in a unit area

$X=^D/_2 \cos\phi$

$^D/_2$

ϕ

A

$Y=^D/_2 \sin\phi$

Y

Submerged weight =
$g(\rho_s - \rho)\,^\pi/_6\,D^3$
for a sphere of diameter D
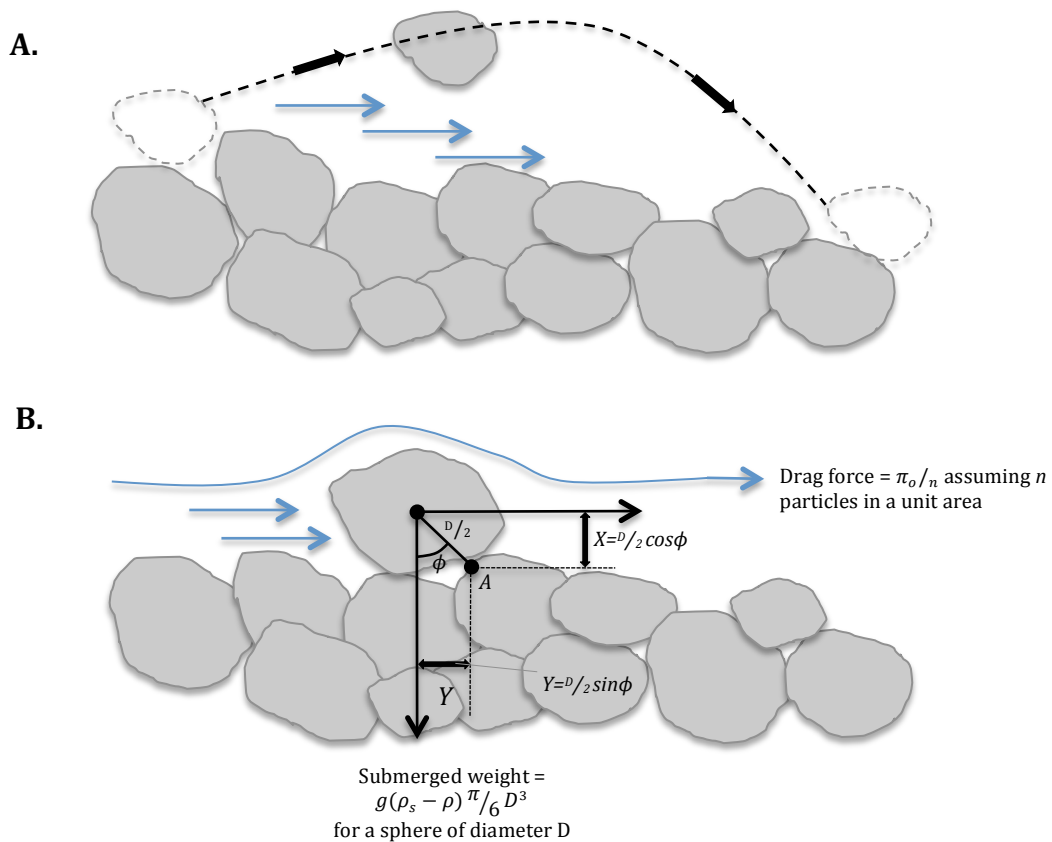
Figure 2.1. *Modes of sediment transport in gravel rivers. A: saltation; B: rolling and sliding. After Knighton (1998).*

Table 2.1. *Common equations used to describe sediment transport processes in open channels.*

Method	Equation	References
Du Boys (1879)	$q_s = \lambda\tau_o(\tau_o - (\tau_o)_c)$	Powell *et al.* (2001)
Shields (1936)	$\tau_c^* = \dfrac{\tau_c}{(\rho_s - \rho)gD}$	Vanoni (1964); Wiberg and Smith (1987);
Meyer-Peter (1948)	$q_b = 8(\theta - \theta_c)^{3/2}\sqrt{\left(\dfrac{\sigma g}{\rho g} - 1\right)gD^3}$	Wong and Parker (2006)
Bagnold (1966)	$q_b = \dfrac{a}{\tan\alpha}(u_* - u_{*c})(\tau_0 - \tau_c)$	Martin and Church (2000)

A river's substrate (or bed-load) can be loosely defined in the context of 'texture' or 'roughness' (Nikora *et al.,* 1998; Buffington and Montgomery, 1999b). However, whilst these appear to be qualitative observations, efforts have been made to objectively quantify streambed rugosity (e.g., Wolman, 1954), given that bed roughness is fundamentally interrelated with hydraulics and the supply and distribution of sediment particles within open channels (Buffington and Montgomery, 1999b). Moreover, texture can also refer to the immense variations of shape, size, weight and density of sediments that comprise bedforms – features similarly important in natural hydrogeomorphic processes (Gomez, 1993; Smart *et al.,* 2004; Qin *et al.,* 2013) – in addition to the many ways in which sediment can be configured (Milan *et al.,* 1999).

Flow velocity is one of the most important factors in controlling riverbed texture (Knighton, 1998) and relates to frictional resistance between fluid flow and the channel boundary. A number of formulae have been devised in order to account for such interactions, the most common of which are:

1) The Chezy (1769) Equation:

$$v = C\sqrt{Rs}$$

Where v is mean velocity (in m^3s^{-1}), C is the Chezy roughness coefficient, R is hydraulic radius and s is slope.

2) Manning's (1889) Roghness Equation:

$$V = \tfrac{1}{n}R^{2/3}S_e^{1/2}$$

Where V is mean flow velocity (in m^3s^{-1}), R is hydraulic radius (in m) S_e is slope of energy grade line (in m per m) and n is Manning's roughness coefficient.

3) Darcy-Weisbach equation:

$$ff = \frac{8gRs}{v^2}$$

Where ff is the Darcy-Weisbach friction factor, g is gravitational acceleration (9.81 m/s^2), R is hydraulic radius, s is slope and v is mean velocity.

Though the two former equations are pervasive in many river engineering operations, the latter is recommended 'for its directional correctness and sounder theoretical basis' (Knighton, 1998. p, 101). In rivers whose substrate is comprised of cobbles and gravels, grain roughness prevails as dominant factor of flow resistance, where grain roughness is a function of relative roughness:

$$\frac{1}{\sqrt{ff}} = c \log\left(a\frac{R}{D_x}\right)$$

Where c and a are constants, and D_x is a measure of the size of roughness elements.

In addition to small-scale sediment size distribution, a natural, longitudinal sorting of sediment likewise controls particle characteristics in gravel-bed streams (Hooke, 2003). Upper reaches of river catchments provide a source of coarse material, where the products of erosion are added to a continuous hydrogeomorphic cycle of bed-load transport, erosion and deposition (Kondolf, 1997). A consequence of the abovementioned modes of bed-load transport is that particles are gradually reduced in size by episodic periods of motion during high discharge.

Accordingly, forces acting upon bed-load material serves to lineally sort sediment along a river's length. The mechanisms by which sorting occurs is somewhat contended in the available literature; however, downstream fining is likely to be facilitated by a combination of selective sorting at varying discharge, and mechanical abrasion of particles during transit (therefore enhancing selective sorting) (Hoey and Ferguson, 1994; Paola and Seal, 1995; Dade and Friend, 1998; Gomez *et al.,* 2001; Constantine *et al.,* 2003; Wright and Parker, 2003; Gaspariani *et al.,* 2004). Hence, longitudinal changes in the structure of channel form are reflected by the myriad of habitat types along a river's course (Ward *et al.,* 2002).

2.2. River Regulation and its Impacts upon Natural Hydromorphic Processes and River Ecology

Most of the world's major rivers are in some way regulated by human intervention (Dynesius and Nilsso, 1994; Bednarek, 2001). Historically, such impacts result from the central role rivers played in the development and prosperity of civilizations. The most common way in which humans regulate rivers is through construction of dams and other hydraulic structures, usually for the purposes of flow diversion, flood control, irrigation, and hydroelectric power generation (Surian, 1999). The practice of building dams for water security developed 5,000 years ago (Petts and Gurnell, 2005; Gregory, 2006) thus prompting one of the oldest forms of engineering (Baxter, 1977), and has expanded considerably over the centuries, both in quantity and size: Bradt (2000) notes that 'in 1900, there were 427 large dams, i.e. higher than 15m, around the world, while in 1950 and 1986 there were 5,268 and 39,000 respectively' a number which, by the earlier 21st Century, had risen to between 45,000 (Marrenn *et al.,* 2014) and 48,000 (WWF, 2014) structures.

The importance of river regulation in human development is noteworthy indeed, and dams continue to be constructed in response to rapid growth in population. Whilst there exists a great many large impoundments, 168 of which are in the United Kingdom (BDS, 2014), there are likely to be millions of far smaller hydraulic structures constructed in rivers the world over. It is difficult to quantify how many of these lesser impoundments exist in UK streams, though Elbourne *et al.* (2013) suggest there could be up to 25,000 in-stream constructions. However, it is clear that many of these structures have become obsolete since the end of the industrial revolution and no longer serve the purpose for which they were constructed. Hence, profound alterations to natural hydromorphic processes arise from the addition of artificial barriers within rivers.

River impoundments disturb the two most determinant factors of channel size, shape and morphology: water and sediment (Grant *et al.*, 2003). Kondolf (1997) describes the river system as a continuous conveyor belt, which is defined by three distinct zones (erosion, transport and deposition), driven by the transfer of energy from 'steep, rapidly eroding headwaters' to lower level reaches below sea level (Schumm, 1977), and maintained by a dynamic, quasi-equilibrium (LaLeft ngbein and Leopold, 1964; Leopold *et al.,* 1964; Schumm and Lichty, 1965; Richards, 1982; Knighton, 1998).

Artificially modifying natural processes that facilitate transfer of water and sediments has profound influences on morphological, hydrological and ecological functions of rivers (Petts, 1977; Williams and Wolman, 1984; Knighton, 1989; Ligon *et al.,* 1995). The most important impacts of river regulation are alterations to natural water and sediment regimes brought about by a reduction in the timing, frequency and magnitude of low and high discharge events (Benke, 1990; Power *et al.,* 1996; Graf, 1999; Nislow *et al.,* 2002; Magilligan and Nislow, 2005; Rolls and Arthington, 2014). Church (1995) notes that, downstream from the point of regulation (where sediment is intercepted), degradation may occur providing that 'post-regulation flows remain competent to move bed material'. Similarly, Baxter (1977) highlights that the downstream impacts of impoundments are conversely mirrored upstream.

Hence, man-made impoundments represent a foremost disturbance to Kondolf's (1997) idealiased, conveyer-like river system, removing kinetic energy from the flow and severely adjusting post-impoundment quasi-equilibrium, therefore interrupting longitudinal connectivity within streams. Similarly, a reduction in peak flows ultimately reduces lateral connectivity with riparian environments –the zone that runs adjacent to river corridors (Marren *et al.,* 2014); and vertical connectivity – i.e., interactions between stream and groundwater resources (Ward, 1989). Diminution of the interaction between channel and floodplain may have significant impacts upon the morphology of rivers, since 'as much as half the annual sediment load of a river is deposited on its floodplain' (Renshaw *et al.,* 2014).

The purpose of dams is generally to control water for human requirements; however, a secondary effect is mass accumulation of sediments transported from upstream reaches either as fine material suspended in the water column, or as coarse-grained bedload, which intermittently rolls and cascades downstream and becomes impounded by the dam.

Though a maximum of only about 15% of sediment within a river is comprised of bedload material (Collins and Dunne, 1990), it is this which determines the character of alluvial channels, and what is more, Petts and Gurnell (2005) note that, 'for many rivers, the headwater catchment provides more than 75% of the river's sediment load'. Further, the efficiency with which hydraulic structures are able to impound sediment increases with size (Williams and Wolman, 1984); yet, although this thesis is concerned with small river weirs, the combined effects of many successive weirs may equal or exceed those imposed by very large constructions (Brandt, 2000).

In most cases, some form of channel adjustment will occur in response to flow and sediment impoundment, though the ways in which this is manifested, and the timeframe over which modifications occur, varies from one stream to the next (Surian, 1999). Due to the prompt impediment of sediment delivery from upstream, a regulated channel is likely to degrade since no new material is able to replace that which is entrained and transferred to lower reaches, often resulting in a coarsening of bed material or scour, before a newly-imposed equilibrium is achieved (Church, 1995). There is, then, a balance between form and process (Petts and Gurnell, 2005), a concept generally expressed by Lane (1955) as:

$$QS = fLbD$$

Where bed material load (Lb) and sediment size (D) is some function (f) of discharge (Q) and slope (S). Hence, alluvial river channel form (width, depth and gradient) is a product of the quantities of water and sediment supplies they receive and have adjusted to. Accordingly, a change in such parameters will permanently change channel form, and is likely to induce profound detrimental impacts to ecological functions of rivers.

The most abrupt and pervasive ecological impact of river impoundments is that they present a physical barrier to longitudinal movements of a plethora of aquatic organisms. Perhaps most marked are the impacts upon migratory species of fish, such as anadromous Atlantic salmon (*Salmo salar)* (Thorstad *et al.,* 2008) and catadroumous European eel (*Anguilla anguilla)* (White and Knights, 1997)*,* each of which requires unimpeded passage from sea to upstream reaches at some point in their life cycle. A diverse range of ecological impacts arises from changes to flow regimes, many of which are discussed by Ligon *et al.* (1995) and Bunn and Arthington (2002), though the entire range of such impacts are too numerous to mention in this thesis. What must be stated, however, is that reductions in the quality of riverine habitat is a major catalyst for many restoration projects in the UK (usually under the direction of European Law) and the interactions between natural hydromorphic processes are intrinsically linked with healthy river ecology (Clarke *et al.,* 2003).

2.3. Process-based River Restoration

River restoration design and implementation is, for the most part, governed by a desire to transform ecologically homogeneous streams back to complex, heterogeneous systems that display "good" or "desirable" (Roni *et al.,* 2008) ecological elements. This approach, though undertaken with the best intention, is often constrained by subjective judgment of river managers, who apply a preconceived interpretation of what constitutes a healthy river (Feld *et al.,* 2012). Moreover, governmental mandates (e.g., the European Union Water Framework Directive (EC, 2000)), which outline a finite set of parameters a river must display, further exacerbate this rigid approach (Beechie *et al.,* 2010).

Process-based river restoration aims to reinstate naturally occurring processes that have been heavily disrupted by anthropogenic influences (Becchie *et al.,* 2010), with an emphasis on remedying such impacts, as opposed to superimposing a predefined ideal. Gilvear (1999) identifies five fundamental component principles that ought to feature in corrective river engineering (table 2.2.). In addition to reinstating natural conditions (Poff *et al.,* 1997), applying such principles and allowing a river to respond naturally to a normative regimen of water a sediment supply – therefore establishing ecological heterogeneity – can also safeguard against any impacts that may emerge in the future (e.g., climate change) (Moss *et al.,* 2009; Beechie *et al.,* 2010).

Table 2.2. *Fundamental principles of remediative river restoration, from Gilvear (1999).*

Principle One	The river channel functions as a three-dimensional form with longitudinal, transverse, and vertical dimensions involving changes in morphology and fluxes of water and sediment
Principle Two	The river system functions in response to water inputs from the upstream catchment
Principle Three	The size, shape, and plan-form of a river normally varies through time, but the dynamics of natural channel adjustment varies between and along rivers
Principle Four	The geomorphic stability of a river system can be upset by such activities as river training, removing riparian vegetation, land use, and climatic change. The sensitivity of river channels to change varies between and along rivers
Principle Five	Fluvial landforms, substrates, and processes define habitats for biota while vegetation and woody debris play an important role in determining fluvial processes

Restoration by weir removal is becoming an increasingly common method for reestablishing natural functions of regulated rivers. Feld *et al.* (2010), however, identifies that much of the academic feedback has been of a qualitative nature (e.g., Kanehl *et al.,* 1997; Bushaw-Newton *et al.*, 2002; Hart *et al.,* 2002; Pizzuto, 2002; Shafroth *et al.,* 2002; Pollard and Reed, 2004; Doyle *et al*., 2005; Thomson *et al.,* 2005; Cheng and Granata, 2007; Maloney *et al.*, 2008; Burroughs *et al.* 2009; Tszydel *et al.,* 2009). The ways in which a river responds to removal of an impoundment varies over time, with longitudinal connectivity, and remobilisation and displacement of accumulated sediments being the most immediate results (Bednarek, 2001). Long-term effects, such as full ecological recovery and reestablishment of hydromorphic quasi-equilibrium, are more difficult to observe (Thomson *et al.,* 2008), particularly as distance from the site of regulation increases. It is for this reason that appraisals tend not to exceed five years' of observation.

Despite the impacts of weirs on natural geomorphic processes being fairly well understood, few studies have attempted to quantify such effects, with large dams in the United States receiving most academic attention (see Graf 1999; 2005; 2006 for a commentary of large dams in the US). Understanding how a river channel reacts following removal of an impoundment is highly sought after, since there could be implications for local infrastructure and flood risk. Moreover, fluvial geomorphology has emerged as a central component in river restoration, and has evolved to encompass hydrology and well as morphology; hence, 'hydromorphology' (Newson, 2002; Newson and Large, 2006; Sear *et al.,* 2008). Nevertheless, accurate restoration appraisal, particularly from a morphological perspective, is a feature that is lacking from many restoration schemes.

2.4. Emergence of the Digital Elevation Model and its Application in River Science

Remote sensing of fluvial environments has permitted study of complex process at resolutions previously unattainable by using conventional methods. The launce of NASA's Landsat platform in 1972 facilitated a change in the ways riverine systems are observed (Choudhury, 1991; Dekker *et al.,* 1997; Jenson, 1999; Mertes *et al.,* 2002; Chu *et al.,* 2006; Basar *et al.,* 2012). However, whilst space-borne platforms are able to observe large-scale fluvial features (e.g., Mertes *et al.,* 2005; Asner, 2001; Sheng, 2001) their application is limited given that spatial resolution is confined to studies of moderate- to large-scale observation (Smith, 1997; Mertes, 2002).

Emergence of the Digital Elevation Model (DEM) and Digital Terrain Model (DTM) has transformed ways in which riverine systems are observed, most principally phenomena that operate over sub-metre scales. In particular, the advent of LiDAR (Light Detection and Ranging) instruments has further enhanced fluvial studies (Notebaert *et al.,* 2009); however, a range of spatial scales may be further derived from LiDAR-based apparatus depending upon how such instruments are employed (i.e., Aerially- or terrestrially-based LiDAR), potentially yielding sub-decimetre scales (Flener *et al.,* 2013). For example, high-resolution, aerial LiDAR has been employed in a number of studies concerning river morphology (e.g., French, 2003; Thoma *et al.,* 2005; Jones *et al.,* 2007; Cavalli *et al.*, 2009; Vianello *et al.,* 2009).

Terrestrially-based LiDAR scanning (TLS) instruments have been similarly applied to a range of topographic analyses, which generally share a common theme: acquisition of very high spatial resolution data (Hohenthal *et al.,* 2011). Heritage and Hetherington (2007) provide a protocol for applying high-resolution terrestrial laser scanning in fluvial geomorphology. Using this method, the authors were able to achieve 0.01 resolution digital elevation data for a morphologically complex area of the upper River Wharfe, UK; thus successfully demonstrating the worth of TLS in river morphology observations (a more complete overview of which can be found in table 2.3).

Table 2.3. *A brief overview of recent published articles on the application of LiDAR in riverine environments*

Author(s)	Description
Entwistle and Fuller (2009)	Objective quantification of sediment size distribution using terrestrial LiDAR scanning techniques. In particular, identification of sediment facies within dry gravel features of the River South Tyne, Northumberland, UK. The authors employed two times standard deviation of grain protrusion to derive effective roughness and sediment homogeneous facies. In addition, traditional, manual counting methods were employed as a control.
Heritage and Milan (2009)	Quantification of full population grain roughness using TLS on dry gravel features of the River South Tyne, Northumberland, UK. Two times standard deviation of elevation was employed as a surrogate for grain roughness. Comparisons were made between results derived from TLS and conventional grid-by-number counting methods within eight 2m^2 regions.
Hodge *et al.* (2009b)	*In situ* characterization of grain size using terrestrial laser scanning techniques. Field- and laboratory-based experiments were conducted in order to elucidate errors introduced during laser scanning. The latter, controlled setting was used to quantify such errors.
Hodge (2010)	Accounting for errors in high-resolution terrestrial laser scanning. The author provides a threefold approach, investigating '(i) assess the effectiveness of the processing methodology at removing erroneous points; (ii) quantify the magnitude of errors in a digital surface model (DSM) interpolated from the processed point cloud; and (iii) investigate the extent to which the interpolated DSMs retained the geometric properties of the original surfaces'.
Milan *et al.* (2010)	Objective identification of hydraulically-defined biotopes using terrestrial laser scanning to detect water surface properties. Biotopes were defined based on local standard deviation to inform surface roughness and compared to an established classification scheme. In spite of absorptive properties of water upon contact with light, the sheer volume of laser pulses were sufficient to yield high-density data from which hydraulic habitats were mapped and classified.
Smith *et al.* (2011)	Patch-scale investigation of gravel beds using through-water terrestrial laser scanning. The effects of refraction on pulsed green (532nm) wavelength LiDAR were investigated both in a field- and laboratory-based setting.

Aerial and Terrestrial LiDAR instruments, whilst notably accurate and versatile in their application, are nevertheless restricted by several fundamental disadvantages. Procuring LiDAR apparatus and its computer software is currently financially expensive at approximately £100,00 (Large and Heritage, 2009). Similarly, it is expensive to hire specialist geomorphologists for their services – an option restrictive for most river studies, which often run on a sparing budget. Aerial LiDAR in the UK is available through the Environment Agency's Geomatics division (www.geomatics-group.co.uk); however, data is potentially equally as costly as hiring LiDAR specialists and spatial coverage may be restricted to 1m - 2m resolution data. In addition, LiDAR data sets are generally very large, given the fine scales instruments are able to observe. This ultimately requires increased computing power in order to post-process topographic data collected in the field (Large and Heritage, 2009).

Terrestrial and aerial LiDAR has traditionally surpassed the abilities of a range of river observation methods, such as EDM theodolite (Chappell *et al.,* 2003), Global Positioning Systems (Brasington *et al.,* 2000) and Photogrammetry (Baily *et al.,* 2003). Recent advances in computer software, however, have led to developments in the latter of these techniques, allowing digital photograph pixels (picture elements) to be transformed into *x, y, z* coordinates, thus producing point clouds analogous to those derived from LiDAR data (Large and Heritage, 2009). A comparable method developed by Heritage *et al.* (1998) was employed to produce DTMs of gravel features on the River Coquet and Kingwater stream, Northumberland, UK, to derive sediment grain size. Similarly, Church *et al.* (1998) used stereo photographs (taken by a camera suspended from a helium-filled blimp) to map sediments and derive D_{99} and D_{84}. These early developments, have since led to shift in the way riverine landscapes are mapped, along with considerable increase in accuracy, precision and adaptability.

Digital photogrammetry-derived Structure from Motion (SfM) is an increasingly attractive method in river science given the prevalence and low expense of photographic equipment (Fonstad *et al.,* 2013), and increasing computing capabilities of conventional desktop machines. Moreover, developments in the SfM automation process (Chandler *et al.*, 2002; Carbonneau, 2003) have yielded greater reliability, thus making SfM a viable competitor of LiDAR.

A full description of the Structure from Motion methodology can be found in chapter four (Figure 4.4), however Snavely *et al.* (2006) and Javernick *et al.* (2014) each provide an excellent overview of the workflow. In summary, though, SfM requires multiple images of feature of interest, from which 3-D topographic models are constructed. Complex algorithms, similar to the Scale Invariant Feature Transform (SIFT) (Lowe, 2004) embedded within computer software (in this instance PhotoScan Pro by Agisoft inc.) identify common points within an image and construct a model based on those points. Relatively few rivers related studies have thus far employed PhotoScan Pro, however Brown and Pasternack (2012; 2014) used PhotoScan Pro to mosaic and georectify images of the Yuba River, Ca, USA. Further, Javernick *et al.* (2014) were able to construct a DEM of a braided reach of the Ahuriri River, South Island, New Zealand. The Authors coupled DEMs derived from Agisoft PhotoScan with optical bathymetric mapping to produce a bathymetric model of the reach.

A primary benefit of Structure from Motion techniques is that, unlike SIFT methods and traditional photogrammetry, the image matching algorithms implemented to produce topographic models do so with such accuracy and computational efficiency that images can be loaded in any sequence (Woodget *et al.,* 2014). In addition, this method allows sub-centimetre accuracy with 'invariance to scale, orientation and illumination' (Woodget *et al.,* 2014).

Structure from Motion is likely to gain popularity in the future, particularly as a result of its superiority in areas that may be difficult to gain access to when transporting cumbersome laser scanning devices, or where acquisition of aerial LiDAR data is impossible due to flight restrictions or unsuitable terrain (Westoby, *et al.,* 2012), as well as its associated low cost and high accuracy, and its straightforward workflow.

In addition to sediment transport and river flow processes, numerical models and statistical analyses have also been developed for describing the configuration and roughness of sediment. Empirical studies have attempted to quantify streambed in terms of representative grain sizes for sediments (e.g., D16, D_{50}, D_{84} and D_{99}); D_{50} for instance, refers to the median sediment size, or 50% of those particles in a given sample that are smaller than a given D_{50} (Wolman, 1954; Hey and Thorne, 1983; Mosely and Tindale, 1985; Billi and Paris, 1992; Kondolf and Li, 1992; Bunte and Abt, 2001; Kappasser 2002).

It may be necessary for further, more robust statistical analyses to be performed, particularly when gravel features have been remotely sensed and subtle changes in bed composition may elude manually obtained samples. Entwistle and Fuller (2009) and Heritage and Milan (2009), for instance, determined sediment sizes from acquired terrestrial LiDAR data by calculating local standard deviation of elevation using a 0.3m and 0.15m moving window respectively, multiplied by a factor of two. Roughness analyses can be similarly derived from statistical investigation of spatial continuity or variability of topographic data sets. Semivariogram analysis is a branch geostatistics that accounts for physical irregularities in complex phenomena, such as grain roughness of a gravel bar, which, at first, may appear to be randomly varied, but in reality is physically determined (Oliver and Webster, 2014):

Vurdu *et al.* (2005) proficiently applied variogram statistics to high-resolution imagery in order to characterise sediment grain size, based on a modified semi-variance equation:

$$\gamma(h) = 1/\{2n(h)\} \cdot \Sigma\{DN(x_i) - DN(x_i + h)\}^2$$

'where $\gamma(h)$ is semi-variance at a defined distance (h)between pixels; *DN(x_i)* is the digital number of a pixel *i*, *DN(xi +h)* is the digital number of a pixel located at a distance h from pixel *i*, and *n(h)* is the number of pairs of pixels evaluated with separation distance *h*', (Vurdu *et al.,* 2005). This developed from earlier works by Lane (2000) and Carbonneau *et al.* (2003) who calculated grain size from digital photogrammetry using conventional semi-variance.

Dugdale *et al.* (2010) used very high-resolution aerial photographic data to produce grain size maps using 'photo-sieving' and semi-variance, though Carbonneau *et al.* (2005) highlight several flaws with the photo-sieving method. Semi-variance is geo-statistical method that may be employed in a range of scenarios where a comparison of topographic data is necessary and may incorporate LiDAR data (Glenn *et al.,* 2006). Hodge *et al.* (2009b) unified semi-variogram analysis with measurements of surface inclinations, surface slopes and aspects, and grain orientation in order to account for variables persistently overlooked in previous study, for instance the effects of imbrication and armouring.

Chapter 3: Study Site and Background

3.1. Introduction

The River Irwell is an archetypal example of a working river – one that has experienced a rich and significant industrial past, and which has suffered a heavy decline in natural hydrogeomorphologic and ecological functions as a consequence. Rapid expansion of manufacturing processes following the Industrial Revolution resulted in extensive flow regulation in the catchment through construction of hundreds of river weirs, as well as a number of large reservoirs, which supplied the growing population. Indeed, such a rapidly expanding population exacerbated the decline in natural river functions, particularly water quality (Williams *et al.,* 2010), as further pressure was exerted on the Irwell and its tributaries (Burton, 2003).

In addition to many in-stream barriers located within the Irwell Catchment, several widespread engineered structures feature commonly, including walled banks, straitened channels and extensive culverts (Lawson and Lindley, 2008). Moreover, considerable water abstraction practices take place at 29 locations within the catchment for public water supply, with numerous smaller consents for agriculture and small industry (Environment Agency, 2013). Each of these facets contributes to ecological and geomorphologic failings, and are of concern in many restoration schemes.
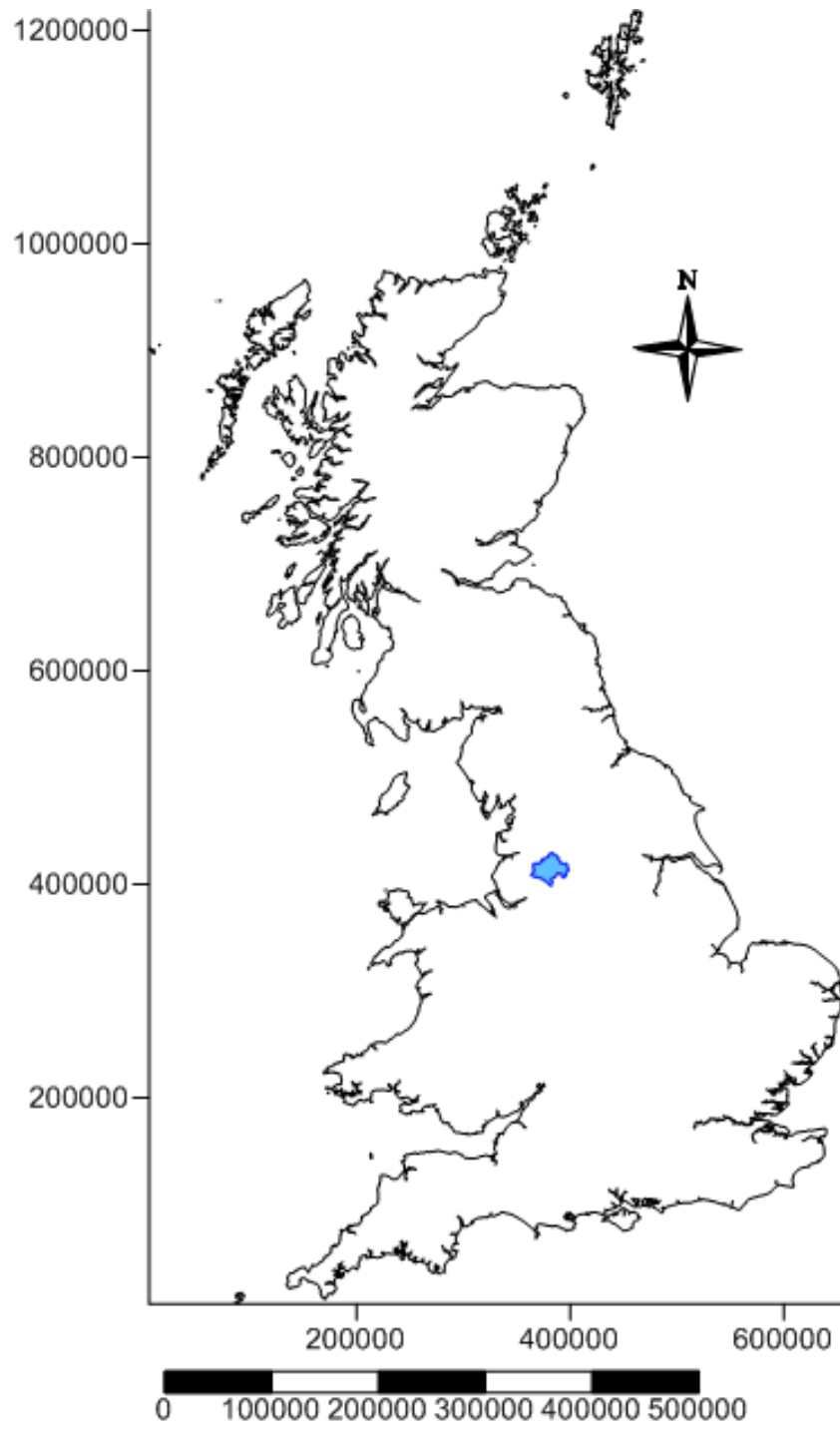
Figure 3.1. Geographical location of the River Irwell catchment, UK.

3.2. The River Irwell Catchment Background

The source of the River Irwell is located on Deerplay Moor, Lancashire, at a maximum elevation of approximately 400 m (Figure 3.2a), from where it rapidly descends through urban areas such as Bacup, Rawtenstall, Ramsbottom, Bury and Manchester, before its confluence with the Manchester Ship Canal at Salford Quays, Greater Manchester. A number of major tributaries join the Irwell along its course, most notably the rivers Croal, Roch, Irk and Medlock (all of which have been similarly impacted by historic human activity). Underlying geology is dominated by Carboniferous Pennine Lower Coal Measures, sandstones, gritstones and mudstones, with occurrences of Permo-Triasic formations in places. Extensive superficial deposits of Devensian glacio-fluvial material adorn much of the catchment, with alluvial clays, sands and gravels occupying river corridors (Figure 3.2b.)

Precipitation is generally frequent and profuse, particularly at high elevation, with 1941-1970 and 1961-1990 averages at 1249mm and 1257mm per annum respectively (Figure 3.2c). Land cover is predominantly grassland (50.8%), with large expanses of urban spaces occupying much of the low elevation areas (15.8%); and woodland (11.1%), Mountain/heath/bog (6.5%) and Arable/Horticultural covering the remainder (Figure 3.2d). Whilst 15.8% urban land cover appears moderate, in comparison to the UK average of 6% this figure is actually relatively high. Similarly, grassland represents just over half the UK average (25%); the two most dominant land cover types in the catchment are therefore likely to have important impacts on land drainage, manifested through decreased lag time (references). Hence, anthropogenic influences on the Irwell extend beyond those that are situated within the river itself.
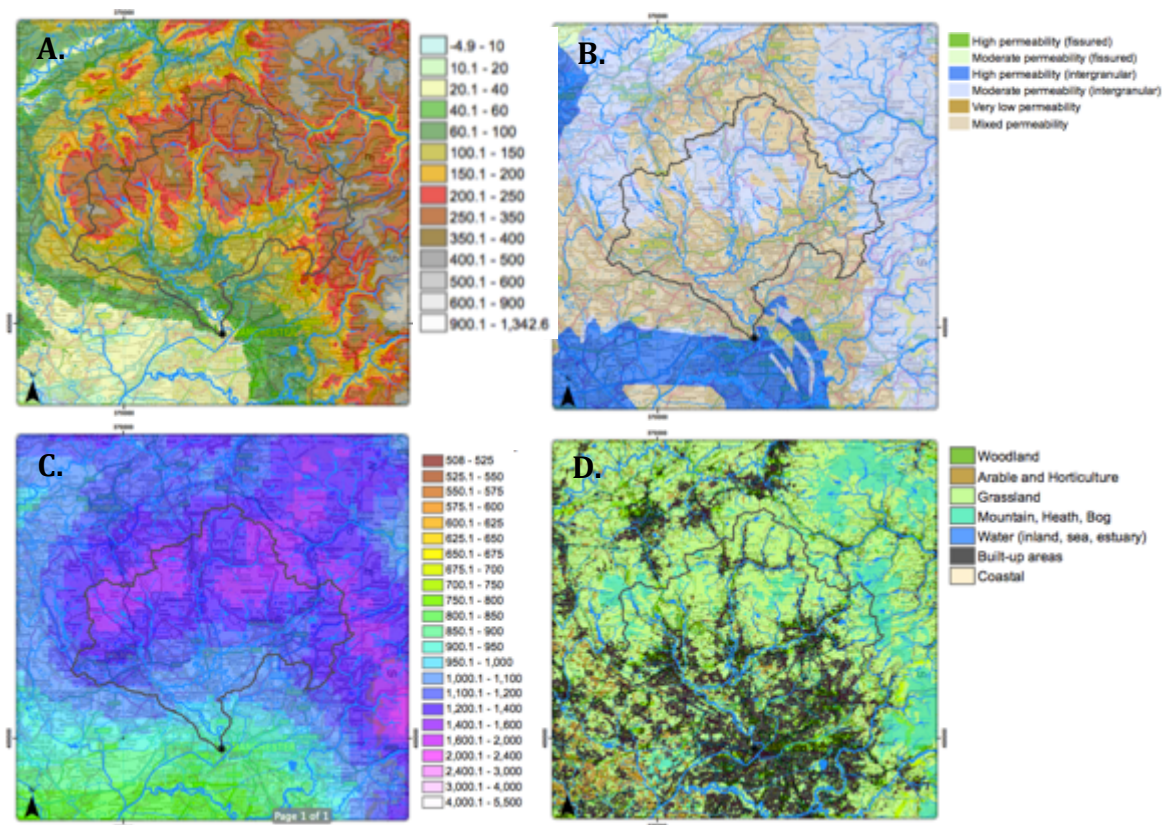
Figure 3.2. *Physical characteristics of the Irwell Catchment: A) Elevation; B) Surface permeability; C) Rainfall; and D) land-use. After Nerc, 2014.*

3.3. The River Roch Study Area

A 12-m² region of a large sediment point bar, situated on the River Roch, Bury, UK, was selected as the study site due to excellent visibility, low vegetation and good access. The River Roch is a stream typical of the wider Irwell catchment, in that it is highly regulated by man-made features such as a number of reservoirs situated at its upper reaches, in addition to numerous Eighteenth Century weirs, most of which are now obsolete. Indeed, the site has recently undergone substantial morphological change following failure of a weir located immediately upstream of the site, which is likely to have contributed to development of the gravel bar as previously impounded sediments were remobilised following removal. Additionally, sediments that comprise the feature are of considerable diversity, exhibiting a wide range of shapes, sizes and geologic materials, and were therefore expected to display distinct, physically-determined facies of homogeneous composition.
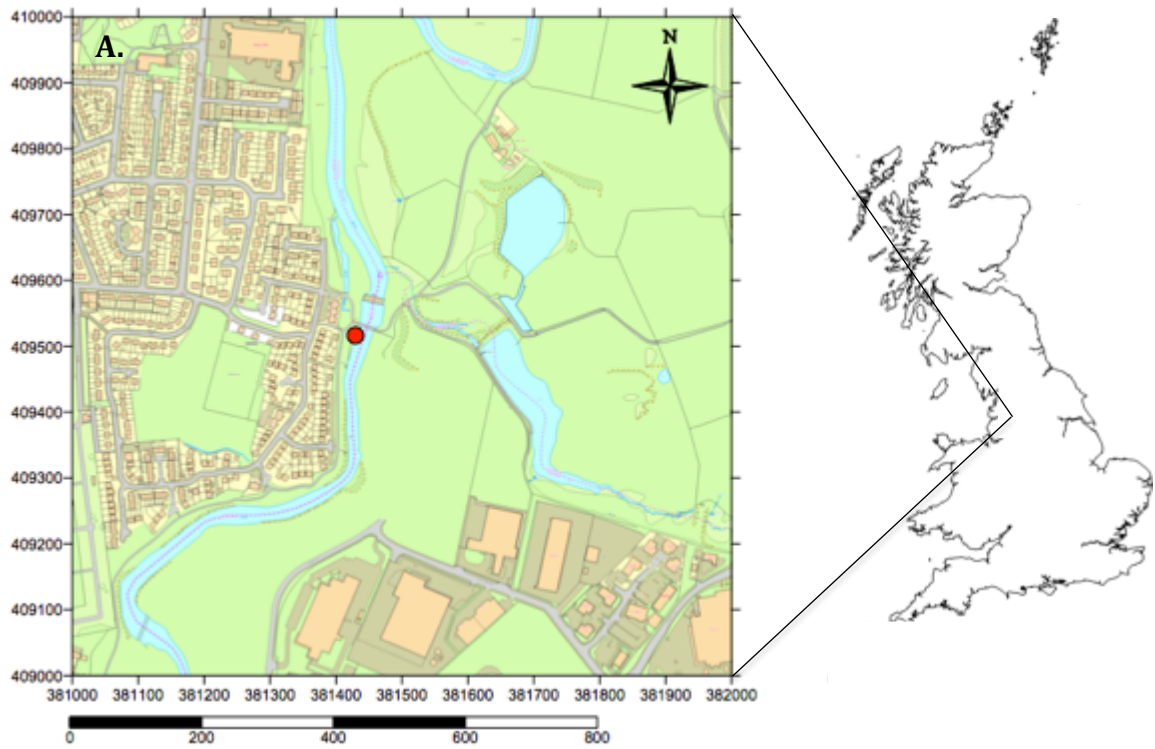
Figure 3.3. *A) Study site location; B) the sampled sediment bar; C) The TLS scanner and retro reflectors.*

Chapter 4: Methods

4.1. Introduction

A reliable method for full and accurate quantification of sediment grain size distribution, notwithstanding its fundamental importance in the understanding of geomorphic and hydromorphic river processes, has long eluded river scientists. The most widely employed technique, and perhaps that which can be considered an industry standard in river engineering, is Wolman's (1954) method of sampling one hundred randomly selected sediment particles from an area of interest (Leopold, 1970; Wohl *et al.,* 1996; Kondolf, 1997b; 2000; Olsen *et al.,* 2005). The intermediate (or 'b') axis for each particle is measured and graded using Wentworth's (1922) classification system, and a sediment frequency distribution curve is drawn from which a range of sample percentiles (for example, D_{16}, D_{50} (or median), D_{84}, and D_{99}), and estimates of roughness may be derived.

Despite common application of Wolman's (1954) method and relative ease with which it is carried out, there are a number of important limitations that inhibit precise measurement of grain size within a given area. First, assigning particles to a finite set of dimensions fails to integrate the immeasurable variation of sediment sizes in nature (Verdu *et al.,* 2005). This is further exacerbated by inclusion of one sediment axis only, and is demonstrated most profoundly when two particles, each at the opposing limit of a size class, are compared (Figure 4.1.) Second, river sediments are worked and configured into a complex assemblage of non-random uniformity, forming distinct patches or 'facies' (Buffington and Montgomery, 1999d; Latulippe *et al.,* 2001). These features, often subtle in their congregation, are likewise inadvertently disregarded by Wolman's (1954) method, which fails to observe ecologically important micro-scale habitats within gravel features. (Wittenberg and Newson, 2005).

Third, Wolman pebble counts are severely vulnerable to operational bias and human error (Marcus *et al.,* 1995); either as a result of failure to identify aforementioned patches of homogeneous composition, or, as emphasised by Bunte and Abt (2001), as a consequence of a tendency for operators to select larger sediment sizes. This is likely to yield results which do not adequately describe bed roughness, since a large proportion of particles may be omitted from the sampled area.

b clast axis = 90mm
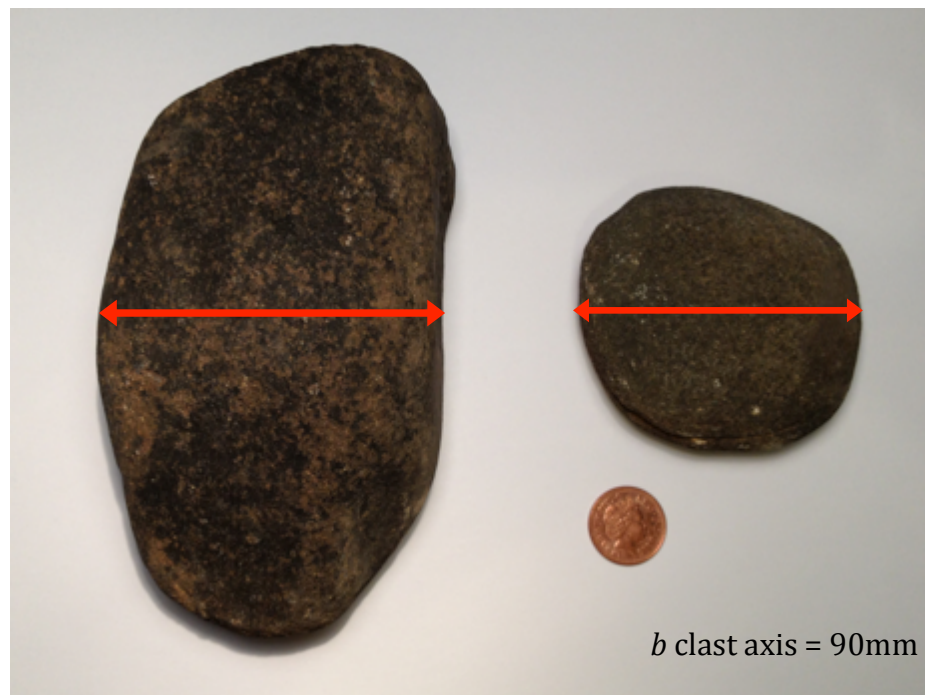
Figure 4.1*. A demonstration of the extreme difference in sediment dimensions between two clasts which belong to the same size class based on Wentworth's (1922) scale.*

Lastly, one hundred particles may not sufficiently encompass the entire range of sediment sizes in a study area, particularly when considering the array of associated limitations, which are likely to skew results at any rate. However, whilst both Brush (1961) and Mosley and Tindale (1985) conclude that fewer than one hundred particles (60 and 70 respectively) satisfactorily reveal sediment size distribution, Hey and Thorne (1983) and Olsen *et al.* (2005) oppose this hypothesis and assert that error is reduced with larger samples.

Advancements in micro-scale Digital Elevation Model (DEM) production, particularly with the arrival of Terrestrial Laser Scanning (TLS) instruments, have permitted highly accurate, quantified study of sediment grain size distribution and roughness (Heritage and Hetherington, 2007). However, whilst terrestrial laser scanning has been employed in a number of compelling studies (e.g., Heritage and Hetherington, 2009; Heritage and Milan 2009;), limitations such as initial of cost of instruments and software, extensive computing time during post-processing, and cumbersome scanners which are difficult to maneuver in the field, result in a technique that, whilst highly accurate, is a somewhat unrealistic procedure for many grain size investigations.

Prior to progressions in modern remote sensing apparatus, conventional technologies were used in efforts to remotely measure grain size. Photogrammetric methods have been utalised in several studies, which sought to gather sedimentological data and derive roughness. Initially, this was performed with traditional film cameras (Kellerhals and Bray, 1971; Church and Hassan, 1987) however Entwistle and Fuller (2009) highlight sources of error resulting from the effects of sediment imbrication and hiding. Nevertheless, Heritage *et al.* (1998) attained reasonable success in yielding course-resolution DEMs from which grain size was inferred.

Progresses in digital photographic technology achieved greater spatial resolutions than its analogue predecessor: Verdu *et al.* (2005) employed a combined geostatistical and digital photogrammetry analysis approach to determine roughness characteristics over a greater spatial extent than previously achievable. Similarly, Carbonneau *et al.* (2004; 2005) attained pixel resolutions of between 3 and 10cm to obtain D_{50}, whilst Dugdale *et al.* (2010) applied a photo-sieving approach for grain size mapping.

Recent developments in computer software packages have allowed users to construct fine-scale Digital Elevations Models from point-clouds analogous to those produced by LiDAR, at spatial resolutions equal to or exceeding data derived from such instruments. This study has employed PhotScan Pro by Agisoft Inc., which converts digital photograph pixels into *x,y,z* coordinates, in a Structure from Motion (SfM) based approach to derive sediment grain size and identify physically determined, non-random sediment facies.

Results from this emergent technique will be compared to those gathered using Terestrial LiDAR Scanning (e.g., Entwistle and Fuller, 2009), which is acknowledged herein as a reliable validation control.

4.2. Pebble Counts

A Wilco™ standard gravelometer was used to measure intermediate ('b') axes of sediment particles from a 12m^2 transect established on a gravel feature situated on the River Roch, UK. Spaces of the gravelometer comply with Wenthworth's (1922) classification scale, ranging from >2mm to <256mm, or –Log_2 diameter (Φ). One hundred sediment grains were selected at random using Wolman's (1954) instruction of choosing those particles that touch the toe of the sampler's boot, with averted eyes, and recorded. Percentage fines were derived from cumulative percentage frequency distribution curves, from which a range of sediment size parameters may be read.

The primary issue with manually sampling sediments, which represents the foundation of this study, is sample size. Manual sampling requires that: 1) a sufficient quantity of particles are surveyed in order to adequately represent the feature under investigation; whilst at the same time 2) care is taken that the amount labour involved does not become prohibitive (Bunte and Abt, 2001). Ideally, a full population of sediment particles from a given feature would be measured and recorded; however, this contravenes the second issue previously raised and is not practical when large features are being sampled. Instead, then, an appropriate compromise must be reached: a sample quantity that fits both rules neatly. A sample made up of 100 particles, as illustrated by Wolman (1954), requires minimal effort when coupled with a device such as a gravelometer, however there are limitations in its application when sampling large areas of *heterogeneous* composition (Bunte and Abt, 2001), where a varied array of particle shape, size and arrangement is present.

Therefore, in addition to conventional pebble counts, supplementary comprehensive assessments of grain sizes were simultaneously conducted to yield a fuller representation of sediment characteristics within the gravel feature.

250 particles were selected using the same heal-to-toe method described by Wolman (1954); however, each clast axis (*a, b* and *c)* (Figure 4.2.) was measured to the nearest millimetre and recorded without being assigned to a fixed size class. Cumulative percentage frequency curves were then drawn from the resulting data, from which the same range of parameters were read.

Figure 4.2. *Definition of A. B and C clast axes used in nearest millimetre sediment counts*

4.3. Data Acquisition

Terrestrial Laser Scanning

A Riegl LMS Z-390 LiDAR scanner was used to obtain sediment data from within the established transect. The scanner is capable of scanning up to 360° horizontally and 80° vertically, though specific settings can be selected depending on its required application. A pulsed infrared (0.9µm) laser is emitted from the instrument, which interacts with a feature surface. The outgoing pulse is reflected back to the instrument upon contact with a target, and recorded by a sensor rooted in the scanner. The return pulse carries information on distance and relative height (facilitated by a time-of-flight measurement), surface colour and reflectivity of most objects, however water surfaces readily absorb light in the infrared, as exploited by the Z-390.

Since LiDAR works on a line-of-sight arrangement, it is necessary to designate several positions from where scans can be conducted; in this instance, four scan positions were selected in order to acquire a complete, three-dimensional model of the sample sediments.

Point-cloud data from each scan position were combined using a TOPCON GTS-210N total station EDM theodolite system (Heritage *et al.,* 2005; Milan *et al.,* 2007; Hertiage and Hetherington, 2007) and meshed, thus yielding an accurate representation of grain structure and configuration of discrete sediment facies.

Digital Photogrammetry

Camera positions were established at the perimeter of the transect, facing inward and downward towards the sediments at a height of approximately two metres (Figure 4.3.) In total, 55 photographs were taken using a Canon 350d digital camera, at spacing of approximately 30cm, of which 51 met the appropriate standard for point-cloud generation. Agisoft Inc. recommend using a camera of moderate specification (>5 MPix), with an optimal focal length of 50mm. Photographs were taken in the RAW format converted to TIFF, at minimum ISO value and maximum resolution (Agisoft, 2014). It is not imperative that the entire area of interest does not appear in some of the photographs, providing that any missed features of interest are captured in others. Additionally, features that have mirrored or reflective surface yield poor data, as does shooting in poor light conditions.

In order to accurately fulfil georeferencing tasks (performed during post-processing), ten ground control points (GCPs), constructed from white plastic discs attached to heavy-duty tent pegs and painted with a distinctive target design for ease of identification during post-processing, were placed within the transect before photographic data was acquired. The position of each GCP was established using total station EDM theodolite techniques, data from which was also used in a tie-point system for LiDAR data. It is essential that a sufficient number of images are obtained during field sampling. Woodget *et al.* (2014), for instance, obtained an average of 48.75 images covering 2958.4 m^2 over four study areas, yielding 0.017 images per m^2. Similarly, Fonstad *et al.* (2013) acquired 304 images over a ~3600 m^2 area, yielding an average of 0.084 images per m^2. In comparison, this study yielded 4.167 images per m^2 providing sufficient coverage of the study area.

Camera
Positions
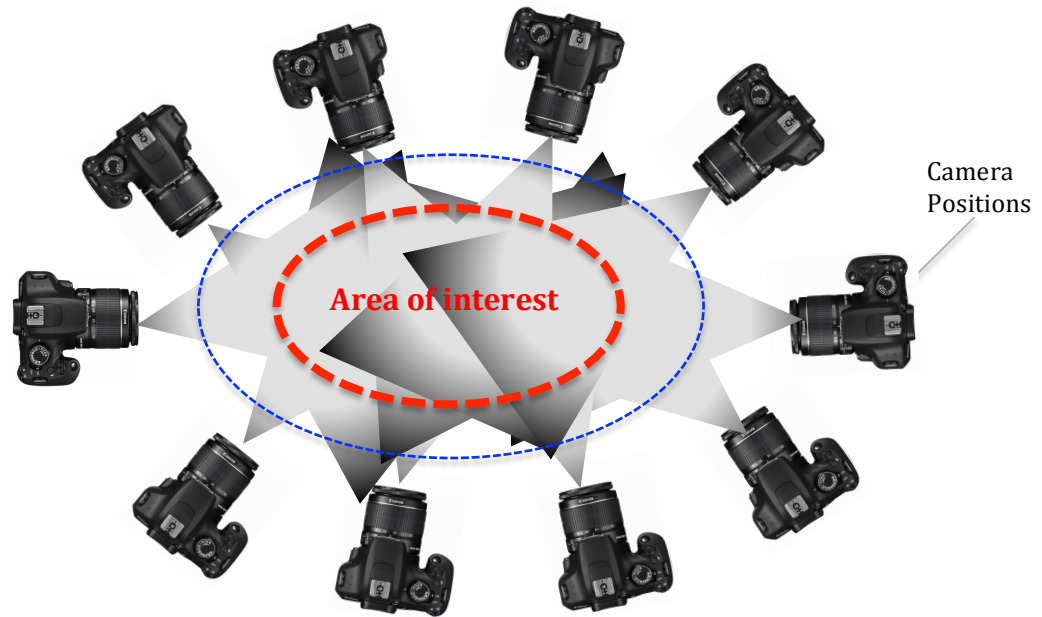
Area of interest

Figure 4.3. *Schematic of the shooting scenario employed in this study. Note: for each shot, the camera tripod is set at the same height with the camera facing down at the feature of interest at an oblique angle. Image overlap is achieved using divergent camera geometry – that is, numerous images of the same area, from different positions ensure sufficient coverage, which aids the SfM reconstruction process. The blue line represents areas that would likely yield some data; however it would be spurious, i.e., incomplete coverage or too poor a quality to include in the final model. Visual inspection allows the user to omit these from the model reconstruction during post-processing.*

4.4. Post-processing

Terrestrial Laser-scanned Data

Once data has been captured, it is instantaneously stored on a portable computer using the Z-390's accompanying software (RiScan-Pro) as *x, y, z* co-ordinate values based on the scanner's internal co-ordinate system. The precise locations of ten EDM theodolite points were manually identified in RiScan-Pro and used to merge point-cloud data to yield a complete three-dimensional model.

Further processing allowed for removal of unnecessary or spurious point data, such as unwanted vegetation, or points outside the area of interest (Heritage and Hetherington, 2007). Finally, point-cloud data was aligned to the project co-ordinate system based the ten EDM theodolite points. Examples of pre- and post-processed point data are demonstrated in Figure 4.4.

Figure 4.4. Raw x, y, z point data produced by A) Terrestrial Laser Scanning; and B) SfM-photogrammetry, with post-processed data inset. Note that spurious data, such as random points and points that lie outside the area of interest have been removed. Also note the extent to which TLS is able to detect points as a result of 'line of sight' sensing.

Photogrammetric Data

Prior to construction of the photogrammetry-derived point-cloud, acquired photographs were inspected for quality. This was performed first by manual examination to identify any poor-quality or o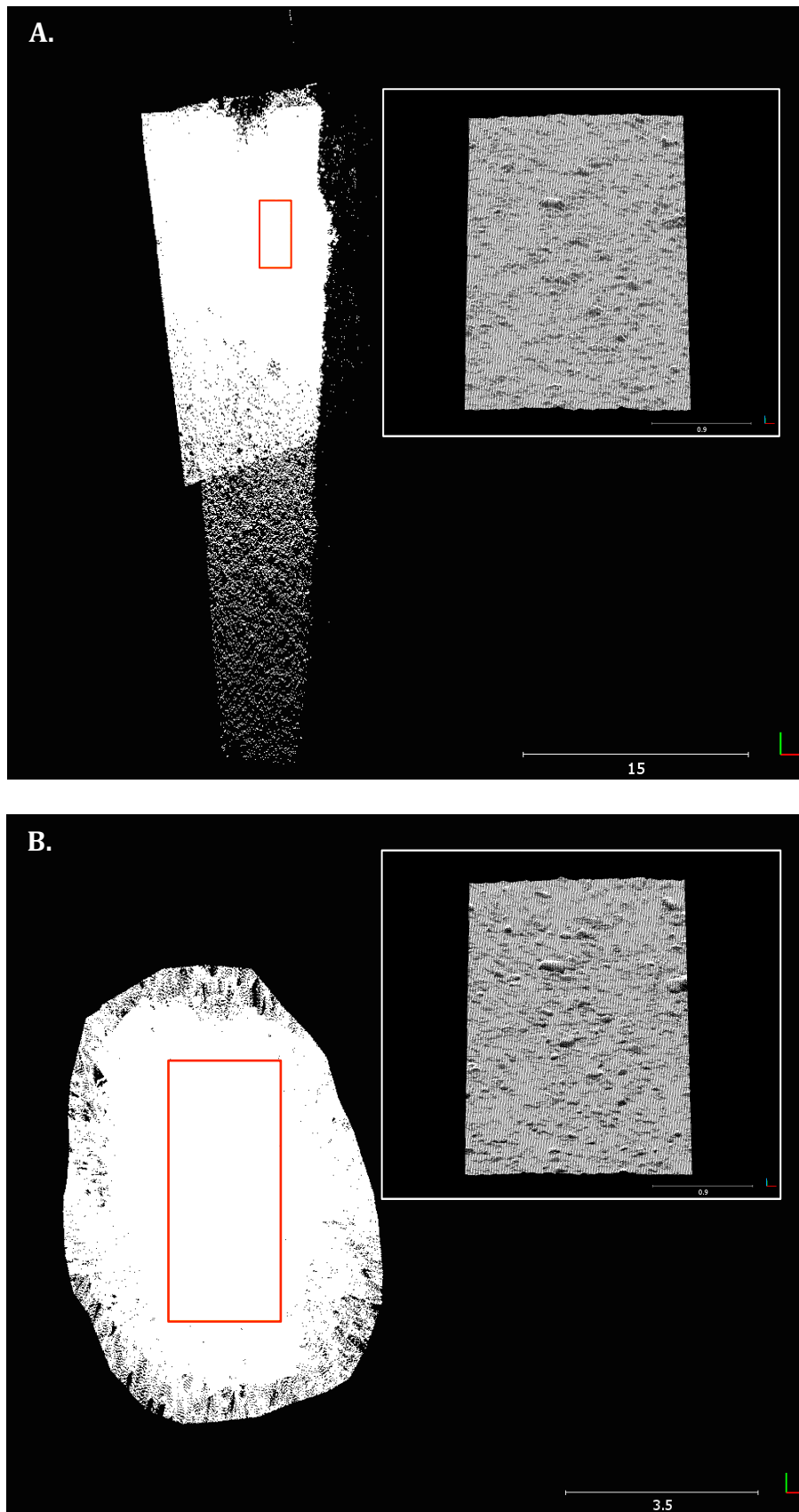ut-of-focus photographs; and second, by an automatic inspection feature included in AgiSoft PhotoScan Pro. Using this feature, photograph quality was estimated based on relative sharpness with respect to other images of the entire array, and presented as a number from 0 to 1 (a value calculated based on the most focussed part of each image). Photographs with estimated quality values of less than 0.5 were disregarded.

Ground control points (GCPs), whose precise location was obtained using EDM total station theodolite, were manually identified in one of the photographs, and each was assigned their respective *x,y,z* co-ordinate. PhotoScan Pro then automatically identified the same GCPs in the remaining images, thus facilitating complex triangulation algorithms employed by the software.

Images that were suitable for three-dimensional reconstruction were aligned: a process whereby common points within each image are automatically recognised by PhotoScan Pro, and used to build a preliminary sparse point-cloud. *High Accuracy* was selected and the point limit (that is, the maximum number of points to be taken into account on each image) was set to 100,000 in order to adequately match the level of precision gained using TLS, yet stay within the limits of reasonable computing time. Spurious data points were deleted at this stage in order to reduce computation time at subsequent stages of DEM construction.

Once the images were suitably aligned and geo-corrected, a dense point-cloud was constructed. *Ultra High Quality* was selected in order to yield maximal precision when reconstructing geometry. Similarly a *Mild* depth-filtering mode was selected in order to incorporate small-scale features and subtle changes in sediment configuration, thus fully representing complex heterogeneity of the gravel feature. The resultant high-resolution point-cloud was exported as an XYZ txt. file. A general workflow of three-dimensional reconstruction is described in Figure 4.5.

Action	Description	
1. Import digital images	1. Photos are imported into AgiSoft Pro where image quality can be generated based on the most focussed part of each image. 2. GCPs are easily identified in each photograph, where they are allocated their true location in preparation of photo alignment.	**A.**
2. Align Photos	1. The software identifies conjugate points within the image array to yield a sparse point-cloud. 2. This is generated using geo-referenced GCPs, whose precise location facilitates the addition of accurate scale to the subsequent dense point cloud.	**B.**
3. Build Dense Point-cloud	1. Prior to construction of the dense point-cloud (**A**), appropriate parameters are set in order to detect sufficient detail. The '*Mild*' depth filtering setting depicts micro-scale features (in this instance, minute differences in sediment protrusion), since there is no loss of detail during construction, however this substantially increases processing time.	
4. Build Mesh	Geometry is estimated based on the dense point-cloud previously constructed (**B**).	**C.**
5. Build Texture	Original raw images are draped over the constructed geometry to produce a Digital Elevation Model (DEM) (**C**). Additionally, fully orthorectified images are produced at this stage, each of which may be exported in a range of common formats.	
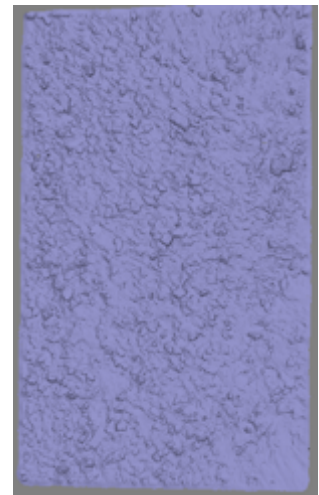
Figure 4.5. *The SfM workflow for reconstructing three-dimensional geometry from two-dimensional images.*

4.5 Grain-Size Analysis

For each point-cloud, a series of 0.19m moving windows (consistent with the largest manually sampled clast axis) were applied across the surface of the gravel feature to derive standard deviation of the elevation data (Gomez, 1993), which was then multiplied by a factor of two to yield effective sediment sizes (e.g., Entwistle and Fuller, 2009) from which sediment distribution curves were drawn and sediment size percentiles were read; in this instance, each percentile (ranging from D_1 to D_{99}) was calculated from every data set produced. The distribution curves constructed from the point-cloud data sets, in addition to the generated percentile data, were compared with those drawn from conventional Wolman (1954) samples and the fuller *a,b,c* axis counts, the latter of which provided further reference for sediment size distribution within the study area.

Geostatistical Analysis

Application of geostatistics permits observation of regionalised variables through a stochastic approach, which identifies spatial properties as random variables (Chappell *et al.,* 2003). Further, variogram analysis allows for the identification of spatial continuity (or roughness) of a data set consisting of elevation (*z*) values, which would otherwise be disregarded or misrepresented by conventional descriptive statistics. Since it is suggested here that grain protrusion (identified by local elevation data of the study area and revealed by two times multiplication of its standard deviation) is representative of sediment size distribution (Gomez, 1993), variogram analysis was performed in order to provide additional validation to the utilisation of photogrammetry-derived DEMs as a method for quantifying grain size distribution.

Separate variogram investigations were performed on elevation data generated from both point-clouds. Each was facilitated by Golden Software's SURFER 11, whose *Variogram* function is able to output graphical representations of both experimental variogram and the variogram model, broadly defined by:

$$\Upsilon(\Delta x, \Delta y) = \frac{1}{2}\varepsilon[Z(x + \Delta x, y + \Delta y) - Z(x, y)]^2$$

Where *Z(x,y)* is the value of interest at location (*x,y*) and ε [] is the statistical expectation operator.

Variograms are the graphical representation of half the average distance between two *Z* points as a function of the separation distance between those values. Multiple lag directions were applied at increments of 5°, with a maximum lag distance of 1.8 m, ranging from 0° to 175°. Each variogram generated was saved from as a .dat file, as (A) lag; (B) variogram; and (C) number of pairs. Both the *X* and *Y* location of each lag point was estimated by transforming the data as follows:

$$X = Lag*Cos(d2r(0))$$

Where Lag is the separation distance; *d2r* is the degree to radian; and *(0)* is the lag angle for each repeated variogram (altered to correspond with each lag direction). *Y* is

calculated using a similar equation, with the exception that the Cos function is substituted for the Sin function; and Z is denoted by the calculated variogram value. Each variogram (separated by 5° lag direction) was combined into one .dat file and 180° through 360° was represented simply by multiplying the values for X, Y and Z by -1. The resulting estimated X, Y, Z data for each lag direction was then drawn as krigged three-dimensional, 360° elevation map in order to diagrammatically represent all the generated variograms simultaneously.

Internal Consistency

Internal consistency within each data set was revealed using the same two-times standard deviation of elevation method previously described (Entwistle and Fuller, 2009). Five randomly selected regions of the study area within the SfM-photogrammetry data set (Figure 4.6.) were isolated using the '*Blank*' function in Golden Software's SURFER 11. The five resulting .BLN files ensured the exact same regions were selected when applied to the equivalent TLS-derived data set. Cumulative percentage frequency was plotted for each region and univariate statistics (maximum, minimum, mean, standard deviation, D_{16}, D_{50}, D_{84}, and D_{99}) were generated for direct comparison.
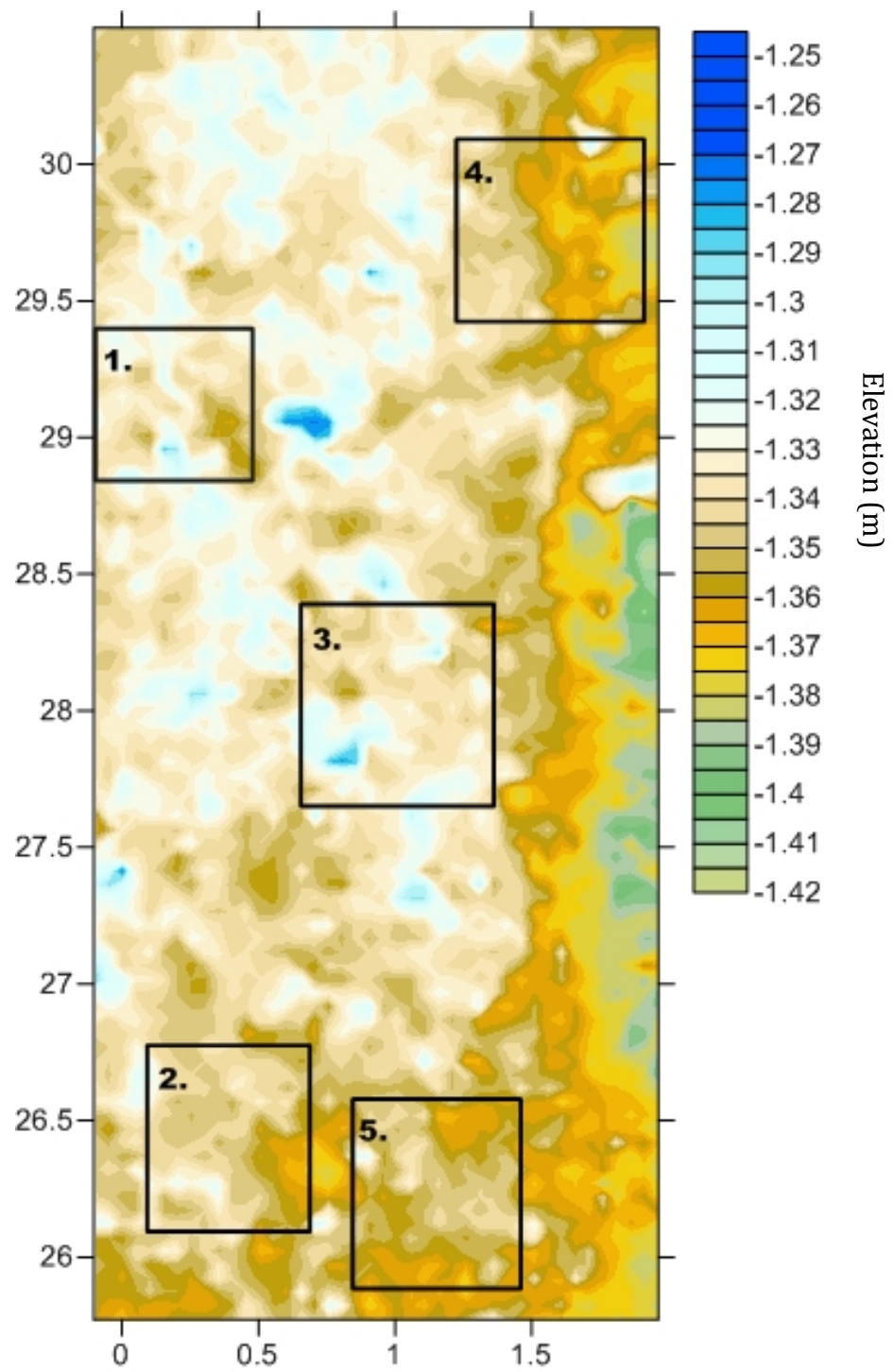
Figure 4.6. *Randomly selected, isolated regions within the study area that were tested for internal consistency.*

Chapter 5: Results

5.1. Introduction

The following chapter will present results gathered during field-based data collection, in addition to results derived from numerical, geostatistical analysis. To simplify examination and aid understanding for the benefit of the reader, results from each element of manually collated data will first be presented individually. Since, however, this study encompasses a proof-of-concept approach, a comparative investigation of remotely sensed data, using both SfM-photogrammetry and terrestrial laser scanning techniques data will follow, in order to; a) validate the newly developed methods, previously outlined in chapter 4; and b) fulfill the project aims and objectives.

5.2. Grain-Size Analysis

Wolman Pebble Counts

Performing traditional Wolman (1954) pebble counts at the study site produced a standard to which all subsequent analyses were compared due its wide spread application. A range of sedimentological parameters (D_{16}, D_{50}, D_{84}, and D_{99}) were derived from a cumulative frequency distribution curve drawn from the *b* clast axis of 100 randomly selected sediment particles (Figure 5.1), results from which are summarised in Table 5.1. The random, heal-to-toe approach associated with Wolman counts yielded sediments ranging from a minimum of <22.6mm to a maximum of <128mm with a median of <45mm.
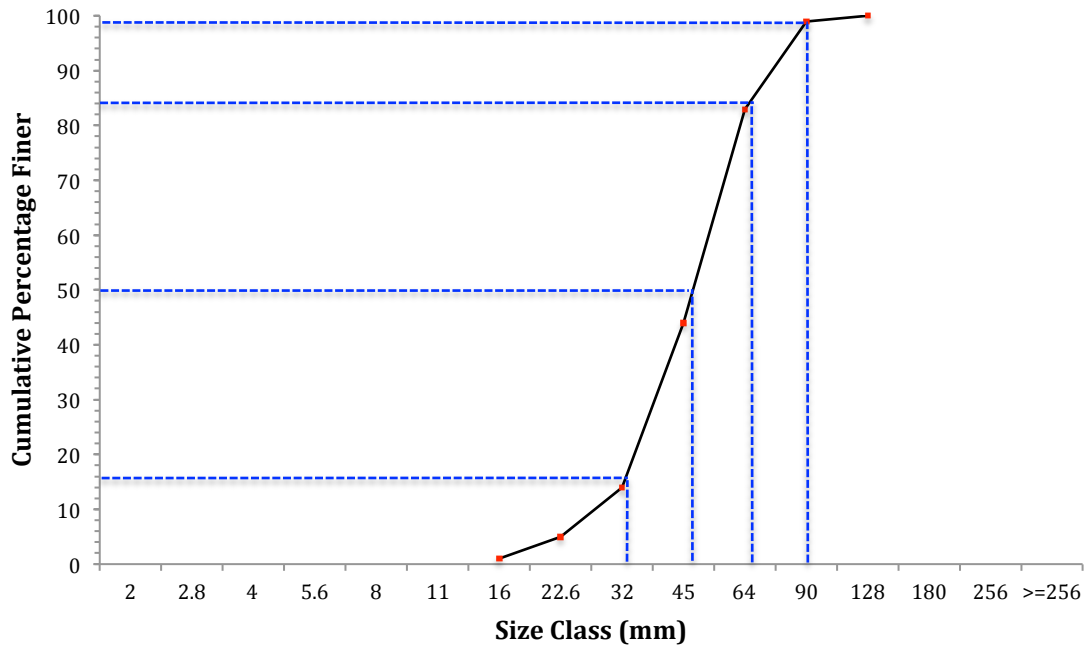
Figure 5.1. *Sediment size distribution curve drawn from Wolman Pebble count derived data.*

Table 5.1. *Percentile data derived from Wolman counts. Size classes are based on Wentworth's (1922) scale.*

Percentile	D_{16}	D_{50}	D_{84}	D_{99}
Size Class (mm)	32	45	64	90

53

Manual ABC Axis Counts

Wolman's (1954) Pebble count method, though commonly employed in river engineering, is vulnerable to a range of error brought about by aspects such as operator bias and insufficient sample sizes. As such, extensive, manual counts were performed on 250 sediment particles in order to yield a cumulative percentage curve for each *a, b* and *c* axis (Figure 5.2), from which the same sedimentological parameters were read (summarised in Table 5.2). In contrast to Wolman count data, however, the *a,b, c* clast data was not assigned to a fixed size class. Instead, each axis was manually measured to the nearest millimetre. These results exemplify a fuller depiction of sedimentary characteristics within the study area, and are therefore used as a more dependable reference of sediment size distribution over the gravel surface.
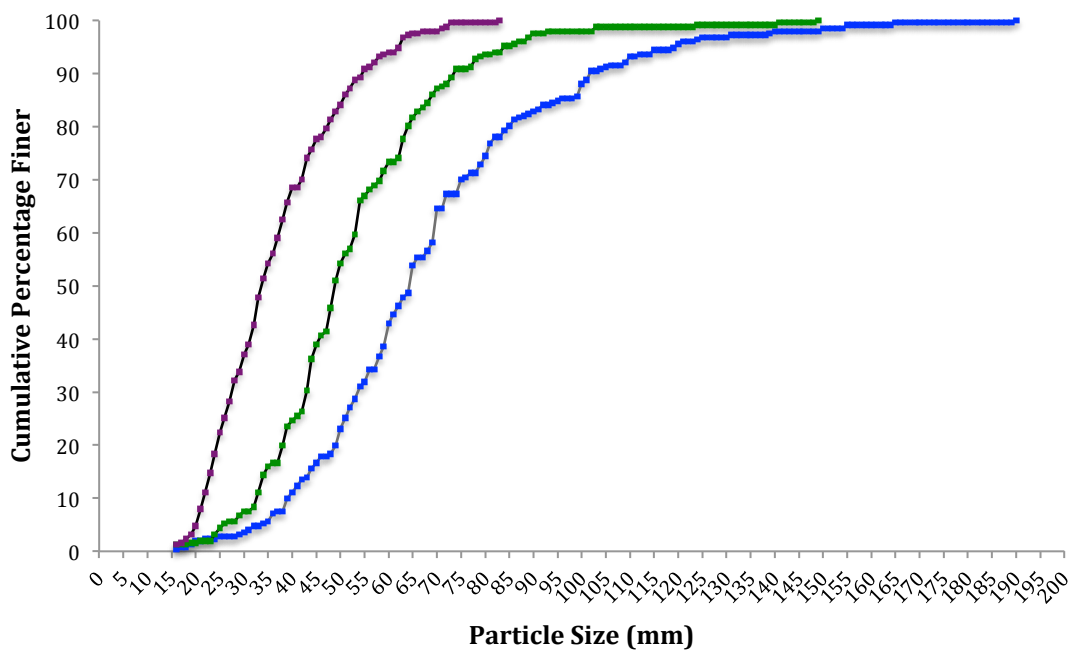
Figure 5.2. *Sediment distribution curve drawn from manually collected a(blue line), b (Green line),c (purple line) clast axis data.*

Table 5.2. *Percentile data derived from A, B, C clast axis counts.*

Axis	Percentile (mm)			
	D_{16}	D_{50}	D_{84}	D_{99}
A	45	65	93	160
B	31	45	64	128
C	11	21	38	60

Results from Terrestrial Laser Scanning (TLS) and Digital Photogrammetry, though visually similar when viewed as three-dimensional representations, are dissimilar in their raw data format. Firstly, the Digital Photogrammetry method that was employed yielded a significantly greater quantity of data points over the surface feature, and was therefore capable of representing considerably greater detail of micro-scale (sub-cm) bedforms. Consequently, estimates of D_{16} and D_{50} derived from each remote sensing method were substantially lower than baseline data gathered through manual Wolman and *a, b, c* clast axis counts. Whilst the lower fractions of these data (i.e., D_{16}, D_{50} and D_{84}) correspond extremely well, the upper fraction (D_{99}) is over-estimated in the SfM-derived data (see Table 5.3).

Terrestrial Laser Scanning methods produced D_{16} and D_{50} results more closely related to manually collected reference data, however the upper percentiles (D_{84} and D_{99}), were slightly lower. In either case, both generated optimal results when the *a* clast axis was considered (Figure 5.4).
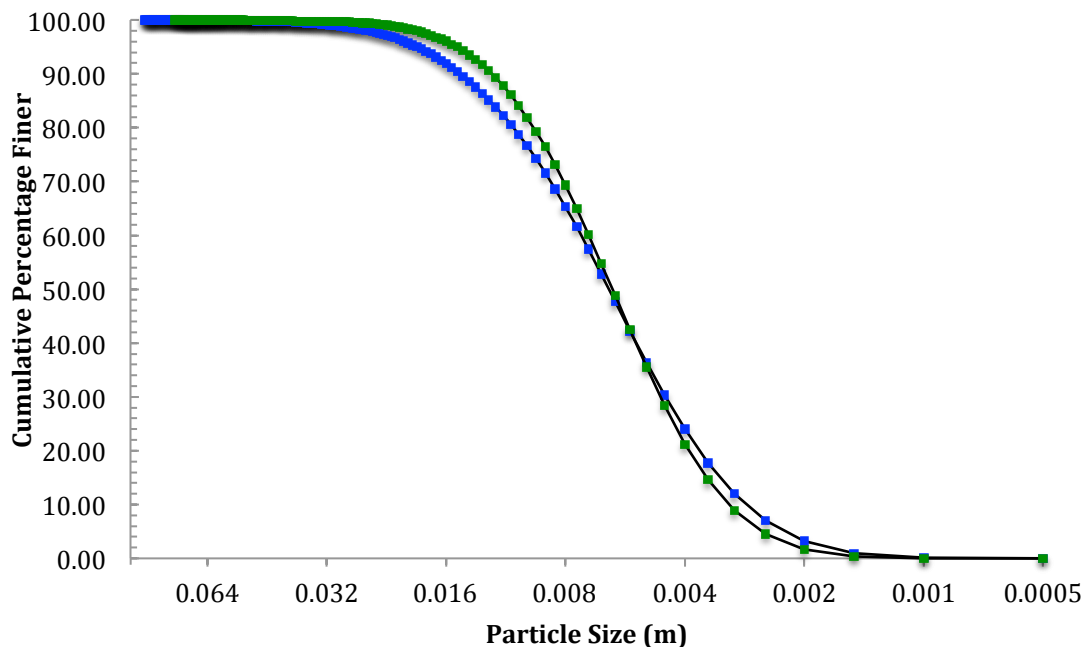
Figure 5.3. *Sediment distribution curves drawn from SfM-derived data (Blue line) and TLS-derived data (green line).*

Table 5.3. *Percentile data derived from SfM and TLS. The difference between each data set is provided.*

	TLS	SFM
D_{16}	0.003763422	0.003362662
D_{50}	0.006297654	0.006245015
D_{84}	0.010566588	0.011888701
D_{99}	0.022577136	0.030878672

Percentile data (ranging from D_1 to D_{99}) was calculated and compared in order to yield empirical relations between each sampling method – a technique similarly employed by Heritage and Milan (2009). Figure 5.4 denotes empirical relations between: A) percentile data generated from each remote sensing method; B) TLS-derived data and grid-by-number (a,b and c clast axis) data; and C) SfM-derived data and the same grid-by-number (a,b and c clast axis) data. The former has been generated in order to elucidate the excellent relation between existing TLS methods and the new SfM method; whilst the latter pair of graphs are presented in order relate remotely sensed, modelled data to those gathered from real-world surveys.
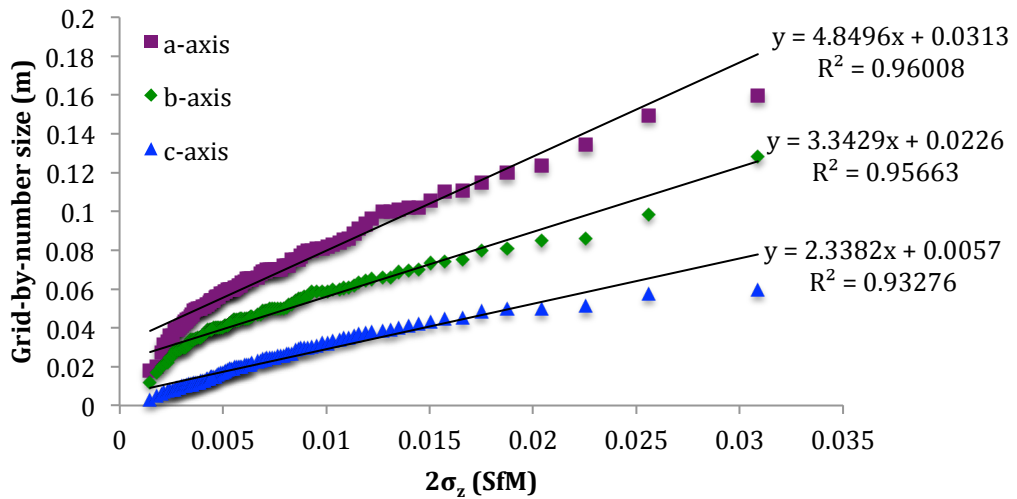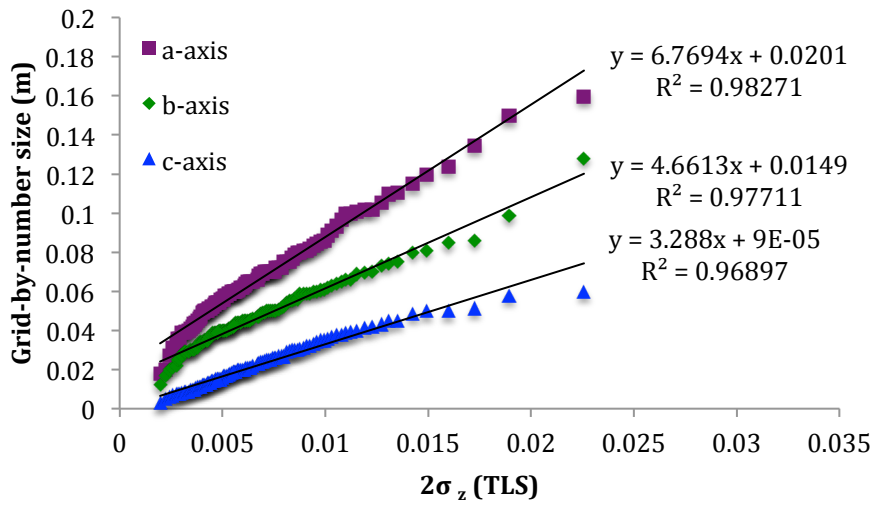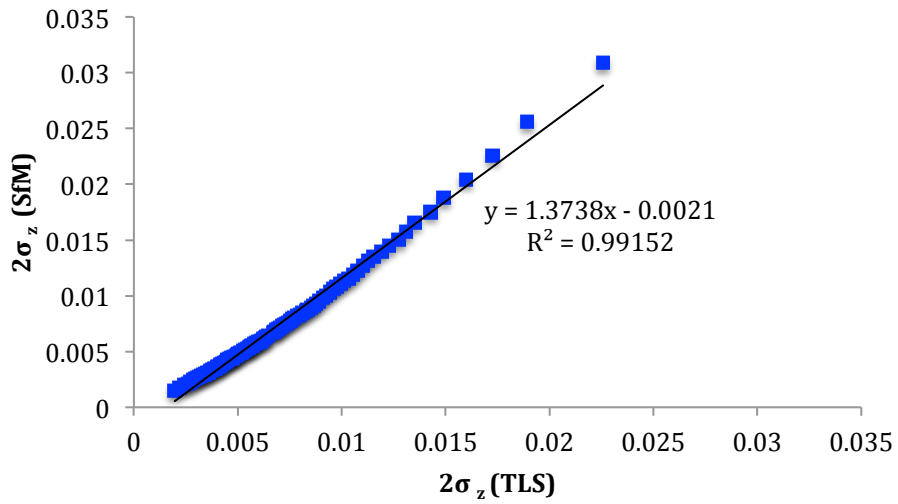
Figure 5.4. A) Empirical relation between $2\sigma_z$ data generated from each remote sensing method; B) empirical relation between $2\sigma_z$ generated from TLS Scanning and manual a- b- and c-axis surveys; and C) empirical relation between $2\sigma_z$ generated from SfM-photogrammetry and manual a- b- and c-axis surveys.

5.3. Geostatistical Analysis

The resulting raw data sets from terrestrial laser scanning and photogrammetry techniques yielded similar univariate statistics, such as mean, median and standard deviations of elevation data (Table 5.5), which, when displayed as an elevation map (Figure 5.5), produce notably similar images. However, since the DEM produced from photogrammetric data was constructed from a point cloud that was significantly denser than that produced from TLS data, it was revealed through variogram analysis that the SfM-photogrammetry-derived data has more variability in comparison to TLS-derived data, particularly in the Z direction from which roughness was inferred.
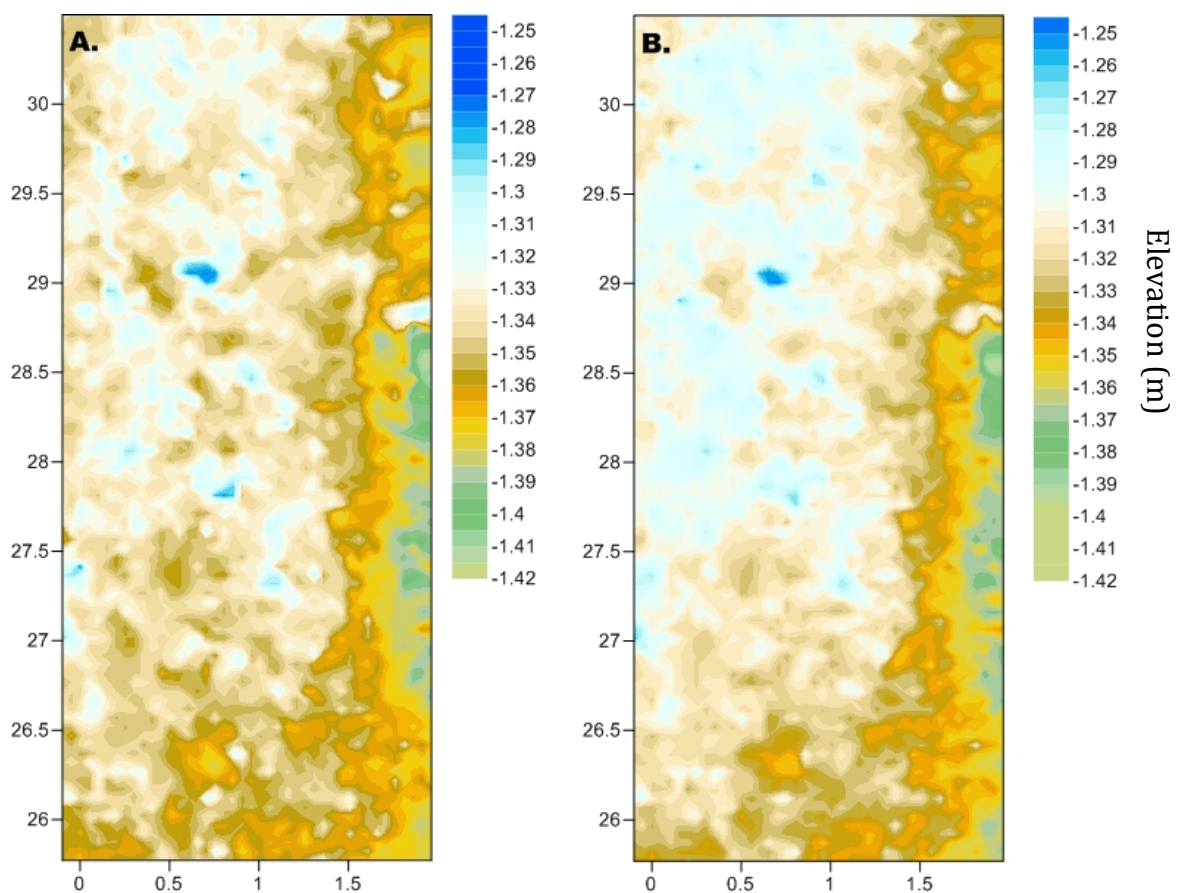
Figure 5.5. *Elevation maps of SfM (A) and TLS (B) data.*

Table 5.4. *Point quantity, density and univariate statistics drawn from each remote sensing method. Note the similar results for mean, standard deviation and median.*

Parameter	Data Acquisition Method	
	Terrestrial Laser Scanning	Digital Photogrammetry
Count	30,335	3,710,223
Point Density (per m²)	2,502.89	304,336.12
Mean	-1.323	-1.350
Standard Deviation	0.027	0.024
Median	-1.317	-1.346

Each data set (TLS and SfM) yielded comparatively similar omni-directional variograms at each lag direction (Figure 5.6 provides an summary of these at increments of 0°, 75°, and 150°). In either instance, the experimental variogram derived from each 5° iteration did not appear to level off; hence a linear model provided the best fit for each data set. However, data produced by SfM methods did not intersect the vertical (Y) axis at 0, thus a 'nugget' effect was applied; whereas data produced by TLS methods appeared to intersect the Y axis at 0. Results are presented as diagrammatic representations in Figure 5.7.
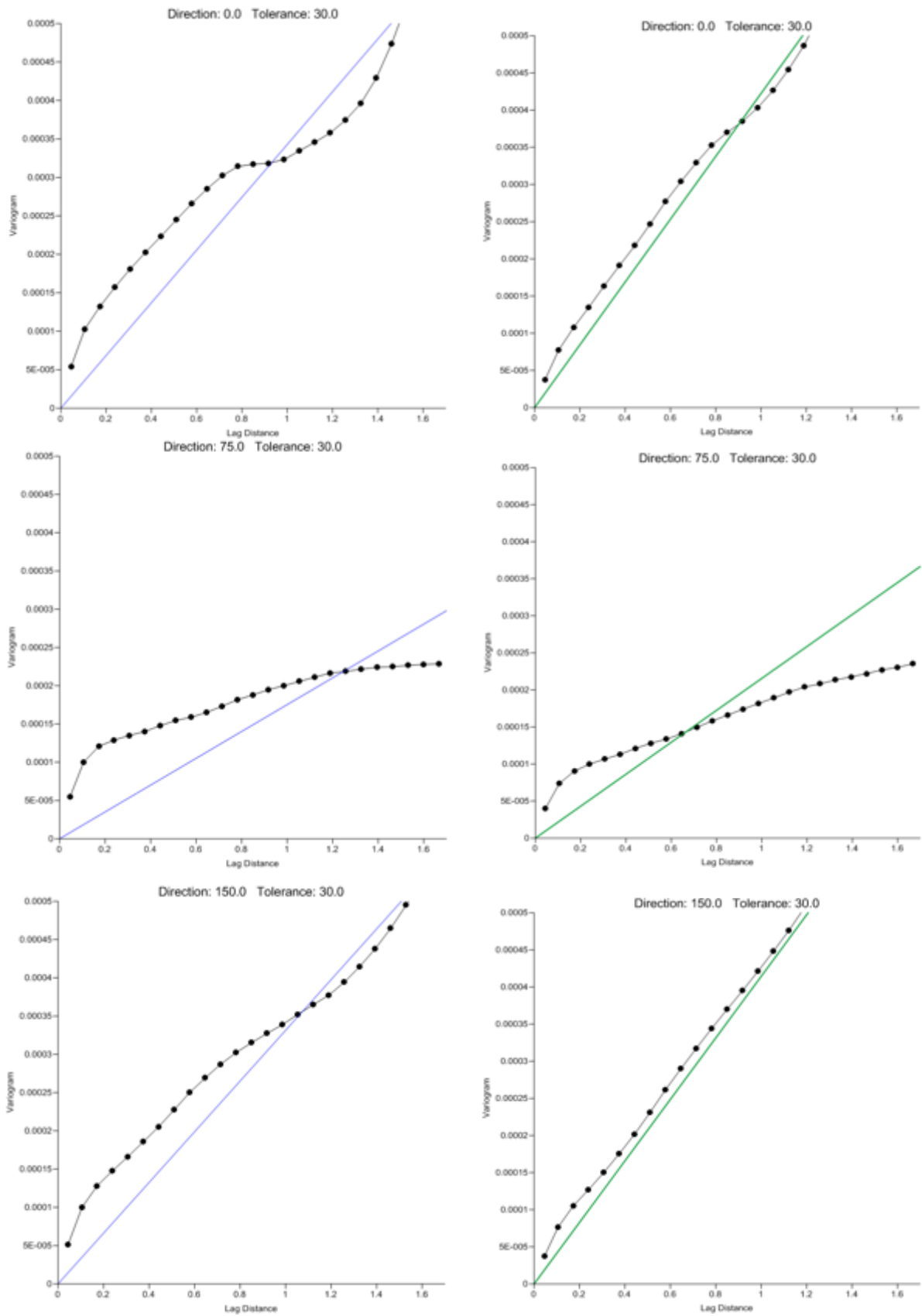
Figure 5.6. *Omni-directional variograms for SfM- (blue line) and TLS-derived (red line) sediment size data. Iterations of 0°, 75° and 150°.*
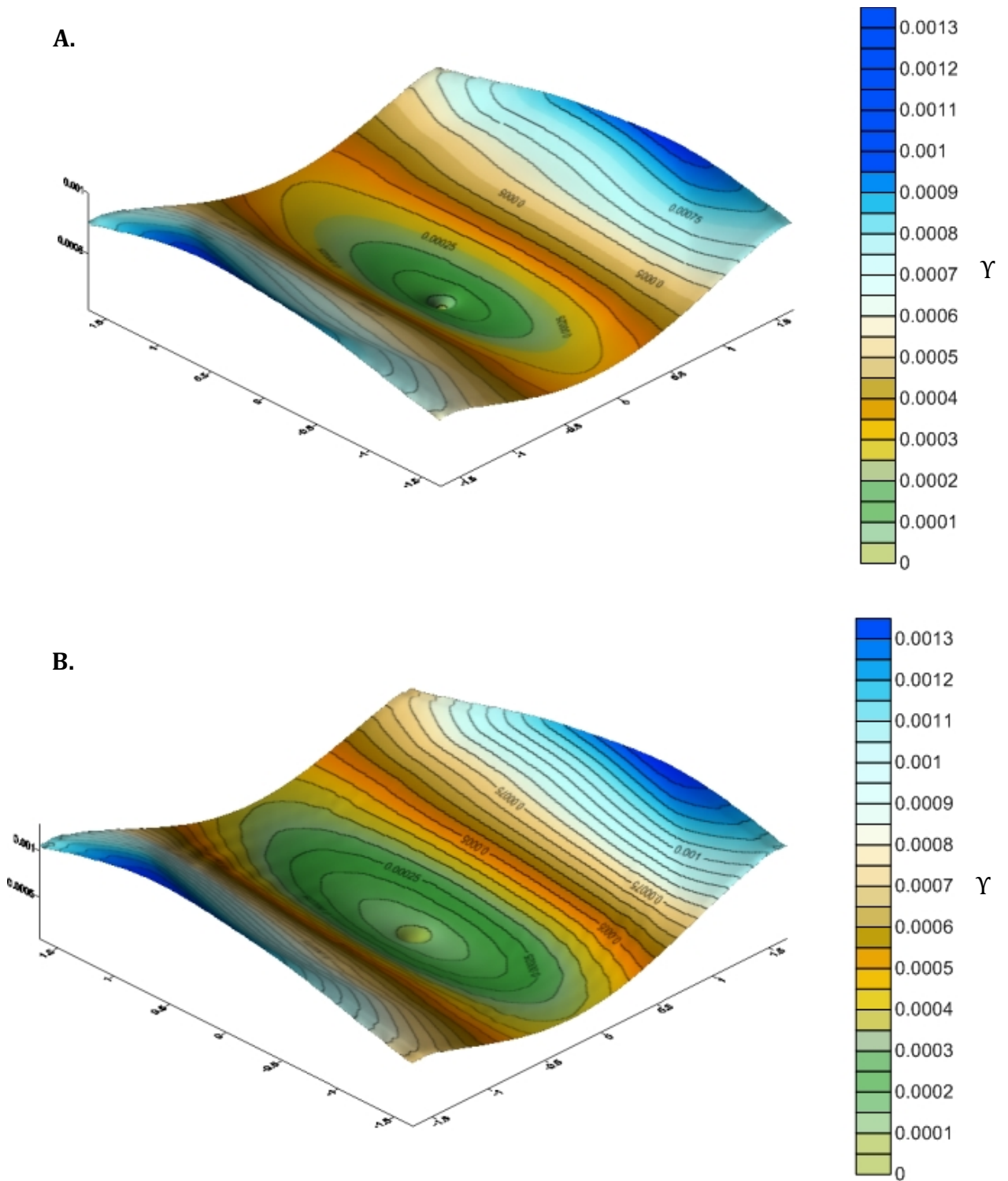
Figure 5.7. *Diagrammatic representations of 360° omni-directional variograms derived from A) SfM; and B) TLS data.*

Internal Consistency

Internal consistency, resulting from small, randomly selected areas within the entire data array provides validation of grain size results previously outlined. In each instance, SfM-photogrammetry-derived results are comparatively similar to those derived from TLS where the smaller percentiles are considered; whereas, conversely, the uppermost percentile (D_{99}) is consistently over-estimated at varying degrees and without exception. The mean difference between D_{99} values for each method over the five isolated regions (0.0102 m) is consistent with the difference in D_{99} values for the entire study area (0.012 m). However, direct comparison between each percentile derived from both data sets reveals that there is an excellent relationship between the two (R^2: 0.93396) (Figure 5.8).

Table 5.5. *Percentile data derived from the five random, isolated regions from within the study area.*

Percentile	Method									
	SfM-Photogrammetry					Terrestrial Laser Scanning				
	Region Number									
	1	2	3	4	5	1	2	3	4	5
D16	0.004	0.003	0.004	0.003	0.003	0.004	0.003	0.004	0.004	0.004
D50	0.007	0.005	0.007	0.006	0.006	0.006	0.005	0.007	0.006	0.006
D84	0.015	0.010	0.015	0.012	0.011	0.011	0.009	0.012	0.011	0.009
D99	0.032	0.020	0.042	0.036	0.028	0.023	0.018	0.022	0.027	0.017
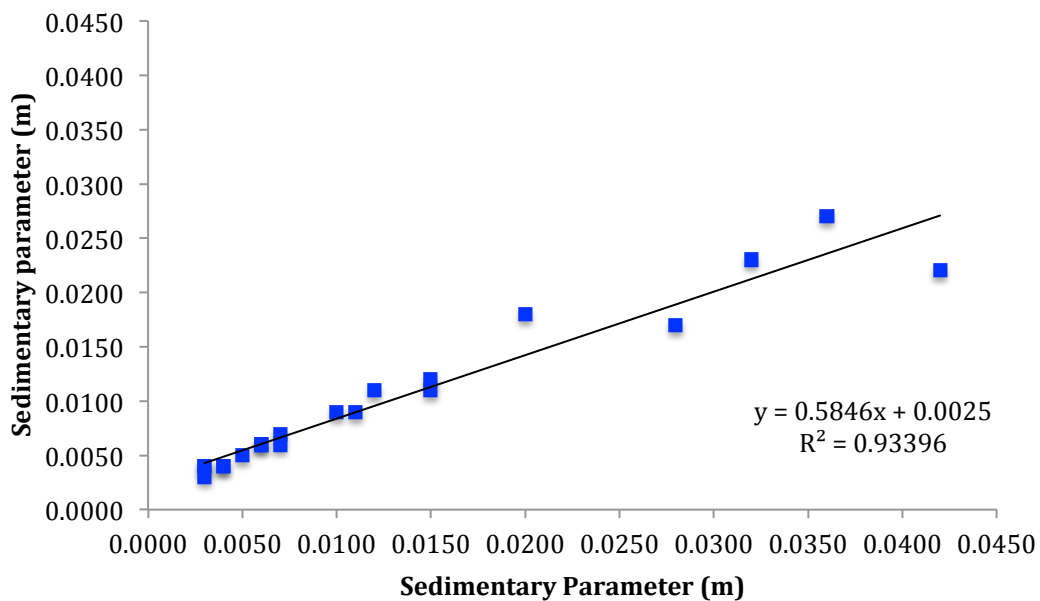
Figure 5.8. *Empirical relation between percentile data attained from each remote sensing method for the five isolated regions.*
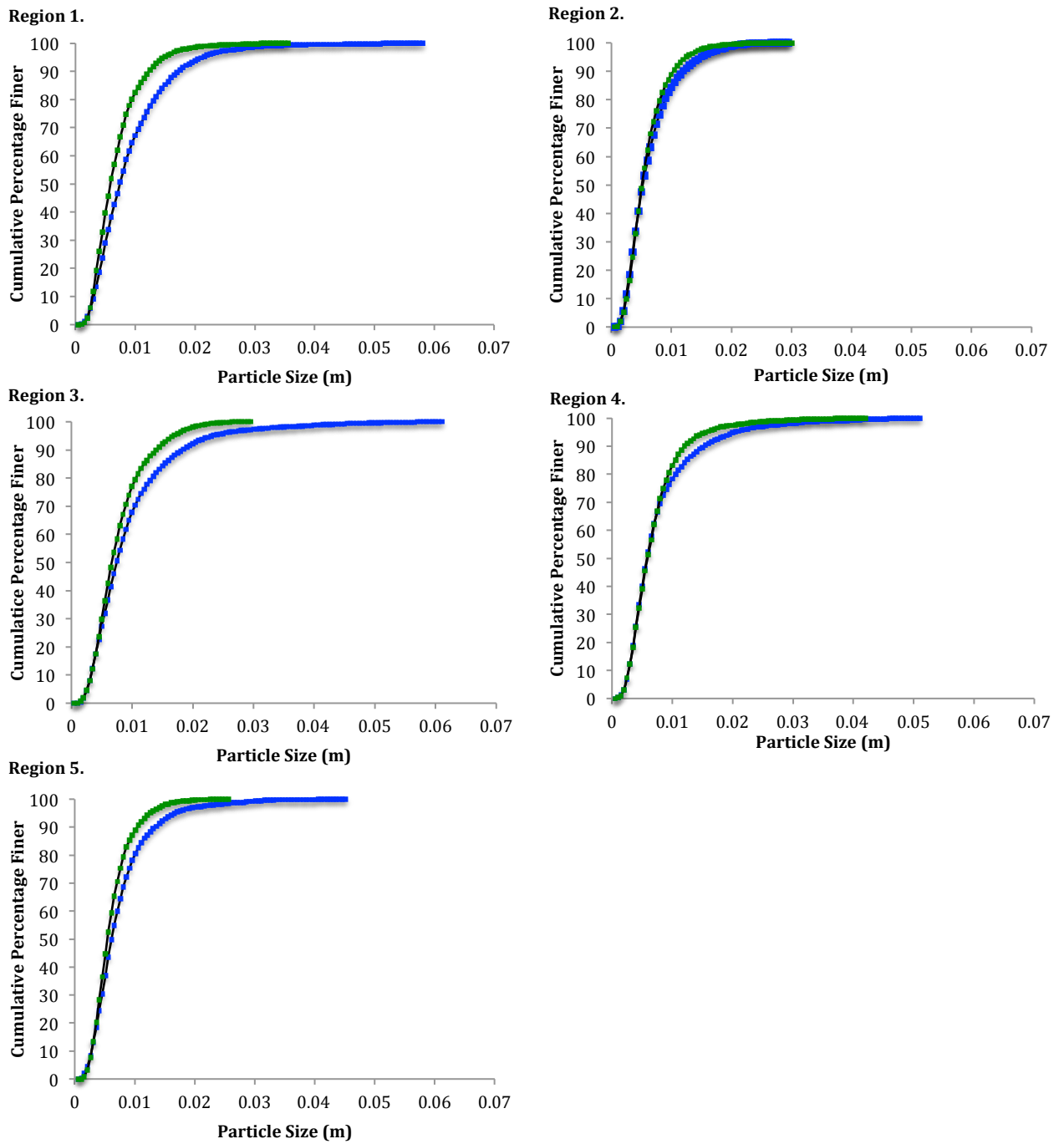
Figure 5.9. Direct comparisons of TLS- (green line) and SfM-derived (blue line) sediment size distribution within isolated regions 1 - 5.

Chapter 6: Discussion

6.1 Introduction

This chapter will comprehensively examine the major findings presented in previous chapters in order to fully elucidate questions posed in Chapter 1. Each element of the study will be discussed independently, with the intention of resolving a set of explicit aims and objectives, as follows: 1) Present a novel, parsimonious, high-accuracy technique for quantitative examining sediment grain size distribution on dry gravel features; 2) Demonstrate how SfM-photogrammetry can be used to quantify sediment grain size to the same degree of accuracy afforded by terrestrial laser scanning; and 3) Examine how development of a new method for quantifying sediment grain size – which has been used in conjunction with both traditional, empirical study and statistical analysis – will affect geomorphological investigations in the future, with specific reference to river restoration and engineering.

6.2. Issues surrounding traditional methods of quantifying grain-size

Despite a general awareness among the river science community that traditional counting methods do not fully represent true sediment size distribution, surface heterogeneity and micro-scale habitat types, they are nevertheless widely employed in fluvial studies, including: river restoration and engineering schemes (Sear *et al.,* 2003); habitat mapping and assessment (Pitlick and Van Steeter, 1998; Thompson *et al.,* 2003; Yarnell *et al.,* 2003); fluvial auditing (Sear, 1995; Sear *et al.,* 2003;); and hydraulics and sediment transport modelling (Verdú *et al.,* 2014).

Furthermore, the Wolman method stipulates that operators randomly select sediments in the field, thus exerting considerable disturbance to potentially delicate habitat systems. Indeed, Wolman pebble counts and manual clast *a,b,c* axis counts undertaken for this study were conducted following all remote sensing operations in order to preserve unspoiled bedforms.

It is noteworthy that performing extensive manual counts on gravel features, particularly those that are submerged, is capable of disrupting naturally imposed gravel configurations such armouring and imbrication, and therefore may have important implications for organisms that depend upon some degree of sedimentological permanence during incubation and maturation, for instance juvenile salmonids.

Results obtained from manual Wolman counts were consistent with concerns raised in the available literature, insofar as they appear to have overestimated true sediment size distribution within the study area (Kondolf 1997b). This was most probably brought about by a tendency for operators to select larger, protrusive particles and dismiss smaller, obscured grains when performing the sediment counts. Moreover, selecting just 100 sediment grains is likely to have exacerbated this misrepresentation, since attempting to yield a true illustration of roughness is somewhat implausible from such a comparatively small data set. Additionally, assigning particles to finite size classes, outlined by Wentworth (1922), also appears to have contributed to the general misrepresentation of true grain size distributions within the study area.

Manual Wolman count techniques scarcely take into account the shape, size, weight or arrangement of sediments, since just one clast axis is measured and allocated to a restricted range of size classes ranging from >2 mm to <256 mm, in addition to individual particles being chosen at random 'with eyes averted' (Wolman, 1954). Measuring each clast axis (*a, b* and *c*), as demonstrated in this study, serves to eliminate some of these shortcomings. For example, the *a, b* and *c* clast axis measuring technique not only accounts for all three axes, but operators also ensure that they measure them to the nearest millimetre, thus producing a truer representation of grain size distribution within a given area. This is reinforced by the fact that many more than the 100 particles necessary for Wolman counts can be incorporated. However, despite the apparent benefits of *a, b,* and *c* clast axis counts over conventional Wolman counts, this study produced notably similar results when clast *b* axis was considered. Again, this was perhaps partly due to operators selecting larger particles, and an insufficient sample size in either instance. Nevertheless, since each is method is a predominant feature of many riverine studies, they are presented herein as an initial control for subsequent remote sensing evaluations.

6.3. Terrestrial Laser Scanning for informing grain size distribution and identifying homogeneous sediment facies

Terrestrial Laser Scanning has been successfully employed in accurately attaining sediment grain size distribution (Heritage and Milan, 2009; Hodge *et al.,* 2009), identifying patches of homogeneous sediment facies (Entwistle and Fuller, 2009) and revealing sediment sorting processes (Milan *et al.,* 2009), at sub-decimetre scales. Where the Wolman (1954) method considers clast *b* axis, applying two times standard deviation ($2\sigma_z$) of TLS-derived elevation data provides a reliable, objective surrogate of sediment protrusion (i.e., roughness) and therefore takes into account clast *c* axis. Using clast *c* axis as an indication of sediment characteristics and grain roughness is expected to be more reliable than clast *a* or *b* axes, since river currents are likely to arrange sediment particles so that their *b* axes lie perpendicular to the flow and their *a* axes parallel (Figure 6.1).
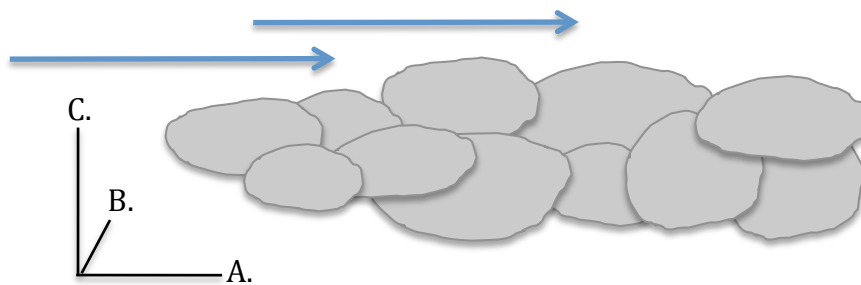
Figure 6.1. Typical sediment configuration of gravel-bed rivers. Clasts are arranged with their b axis aligned perpendicular to the flow.

Sediment distribution data derived from terrestrial laser scanning is not subject to the same errors proliferated by operator bias associated with traditional methods. This is because laser scanning instruments are capable of detecting a very large portion of the entire population of constituent surface sediments of a gravel feature (Heritage and Milan, 2009), providing they are within direct of line sight of the sensor. Furthermore, terrestrial laser scanning is generally carried out with minimal disturbance in the field, and is therefore ideal for observing quasi-stationary landscapes whose form shifts over time and space, as sediment particles are not required to be moved or disturbed in any way in order to quantify roughness.

Laser scanning results from the River Roch confirm that manual sediment counts fail to account for smaller particles. Where percentile data attained from frequency distribution curves drawn from Wolman and clast *b* counts relate remarkably well (respectively, D_{16}: 0.032 m and 0.031 m; D_{50}: 0.045 m and 0.045 m; D_{84}: 0.064 m and 0.064 m; D_{99}: 0.090 m and 0.128 m), TLS results indicate that a greater percentage of finer material is present within the gravel feature (D_{16}: 0.004; D_{50}: 0.0006; D^{84}: 0.01; D_{99}: 0.019), since errors brought about by operator bias and subjective selecting of particles has been removed.

6.4. SfM-photogrammetry for informing grain size distribution and identifying homogeneous sediment facies

Whilst TLS is a reliable, accurate method for acquiring high-resolution topographic data, LiDAR instruments and their respective computer software come at considerable financial cost. Moreover, though TLS instruments exert minimal disturbance in the field, they are nevertheless somewhat cumbersome, and acquiring data over large areas, particularly at higher resolutions, can be time-consuming and laborious. SfM-photogrammetry permits acquisition of topographic data at accuracies comparable to LiDAR with significantly reduced effort and time expenditure.

In order to capture sufficient coverage of the study area, 50 photographs were employed in the final meshing process (facilitated by AgiSoft's PhotoScan Pro). However, whilst just four laser scanning positions were sufficient to yield a complete, three-dimensional model, each scanning cycle took 12-minutes to complete; whereas capturing the necessary photographs to facilitate SfM reconstruction for the entire study area took considerably less time (approximately 10-minutes). Instead, the majority of time was spent on attaining the precise location of ground control points (GCPs) necessary for post-processing, using the EDM theodolite.

Since SfM point-clouds are constructed from digital photograph pixels, they are notably denser than those produced by LiDAR, even at moderate resolution. TLS methods obtained a point density 2,502.89 per m^2 compared to 304,336.12 per m^2 obtained by SfM-photogrammetry, which equates to mean spacing of 0.02 and 0.002 respectively. Consequently, SfM captured a far greater level of detail; however, this does not appear to have been reflected in the frequency distribution curve drawn from two times elevation data: percentile results from each method, for the most part, correspond extremely well. Nevertheless, from a purely subjective observation, the raw SfM-photogrammetry derived point data is significantly more texturally diverse than its TLS-dervied counterpart (Figure 6.2.)
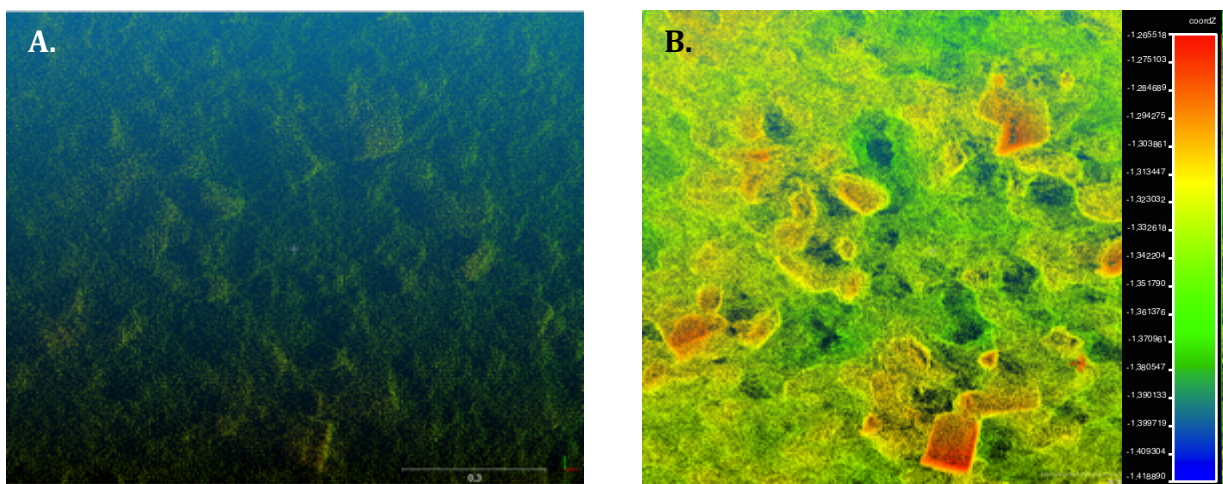
Figure 6.2. A comparison the textural properties of TLS (A) and SfM (B) derived raw point data. Note the greater density of the latter point data, which took a fraction of the time to gather. The represented data are taken from the exact same patch and are displayed as a colourised height filed in Telecom ParisTech and EDF's CloudCompare.

Where TLS methods revealed a higher percentage of smaller particles compared to manually collected data, so SfM-photogrammetry methods similarly revealed still a greater percentage of smaller particles compared to TLS. Moreover, assurance of correct elevation dimensions is offered by comparison of x and y between krigged contour maps (Figure 6.3), where features that appear on a two-dimensional, planar field precisely corresponds.
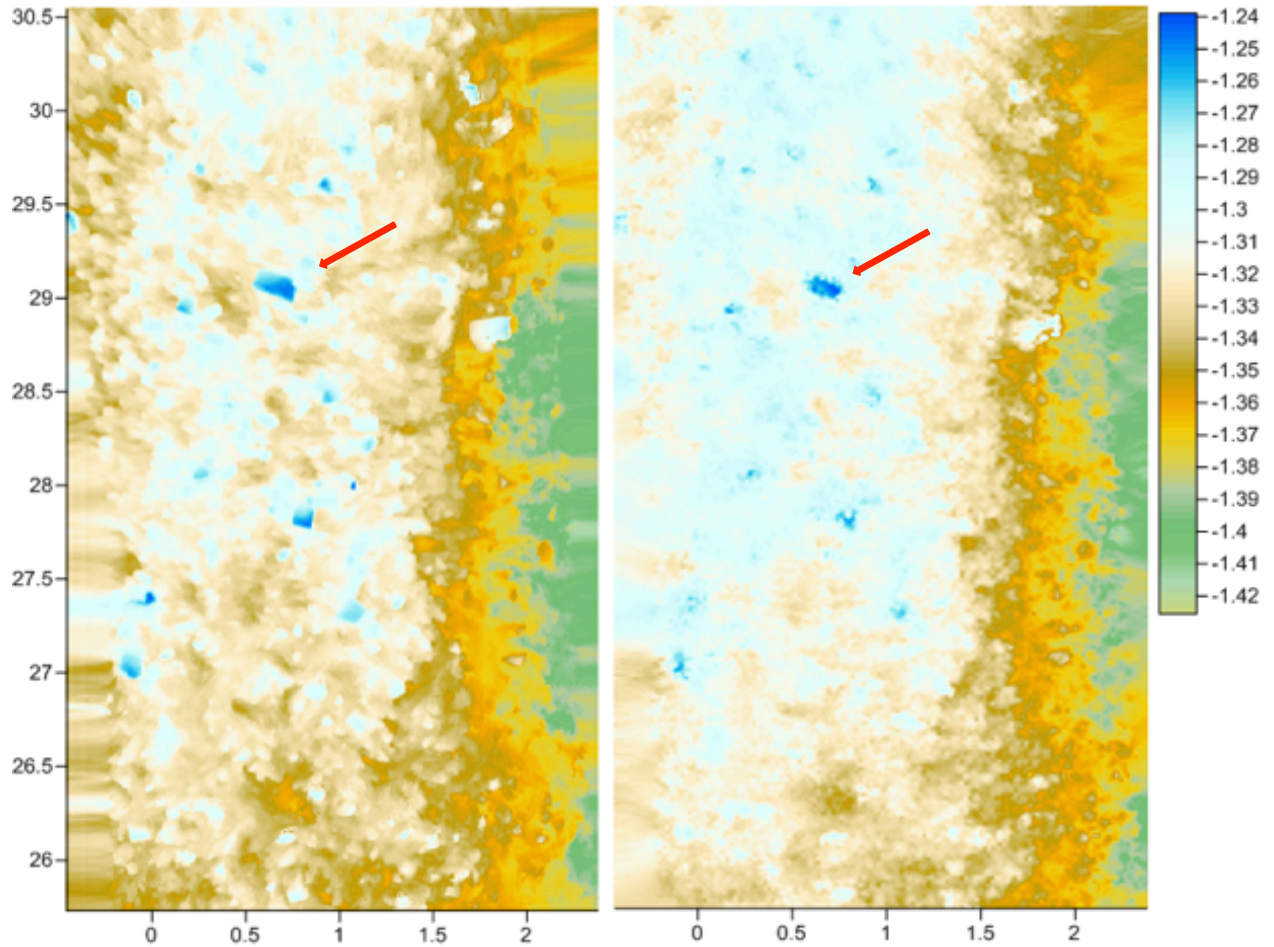
Figure 6.3. *Krigged contour maps of A) SfM-derived data; and B) TLS-derived data. Note the higher level of detail in the SfM-derived image compared to that produced by TLS.*

The dimensions of a standard house brick (215mm x 102.5mm x 65mm), which was situated within the gravel feature, were recorded for future reference following post-processing of each raw data set. This provided an easily identifiable target that could be straightforwardly located in SURFER 11, whose known measurements provided a reliable indication of accuracy following the meshing process, particularly for SfM data, since TLS has been widely demonstrated to be of high quality and accuracy. Accordingly, a greater level of detail is observable in the SfM-derived map, with considerably enhanced definition on individual sediment particles. Further, whilst univariate statistics for both data sets are similar, comparative variogram analyses reveal that, in actuality, there is a significantly higher degree of variability between the two data sets.

Investigations of internal consistency within each data set reveal that, over smaller, isolated regions, variability is reduced yet percentiles remain similarly equal in comparison to sediment size analysis of the entire study area (see Table 5.5 for a summary). As discussed by Fonstad *et al.* (2013), and reaffirmed by Micheletti *et al.* (2014), this is perhaps due to a reduction in errors that are propagated over larger areas. Nevertheless, within the five isolated regions, sediment size percentiles consistently reiterate those derived from the entire study region, insofar as the lower percentiles relate extremely well, with a constant over-estimation of D_{99} by SfM-photogrammetry.

6.5. Comparative Analysis of SfM-photogrammetry- and Terrestrial Laser Scanning-derived Sediment Data

Despite obvious differences in the quality of each remotely sensed data set – i.e., the considerably denser point-cloud yielded from Structure from Motion compared to that produced by terrestrial laser scanning – the sedimentary parameters derived from each method (D_{16}, D_{50}, D_{84} and D_{99}) have been shown compare extremely well. Manual *a, b, and c* clast axis counts were carried out as a control on each remote sensing method – despite TLS having been previously demonstrated to be a reliable method of quantifying sediment grain size distribution. However, results from these measurements reveal that each parameter has been overestimated considerably. This is possibly attributed by a tendency of operators to pick out mostly large, protrusive particles, and neglect to account for smaller sediment grains that are less likely to be selected due to their reduced size. It appears that the same can be said for percentile data produced by Wolman's (1954) method, though D_{16}, D_{50}, and D_{84} relate well, with a two-fold increase in D_{99} *b* clast axis count data. This, however, can be attributed to the fact that, during manual counting, sediment particles must be physically removed from their placing in order to be measured. Conversely, each remote sensing method utilised in this study infer sediment size distribution from grain protrusion. Hence, the effects of clast burial and imbrication are likely to have produced underestimates of the true size of those sediments that lie partly obstructed from view by the rest of the sediment sample population (Heritage and Milan, 2009), or which are partly buried.

It is suggested here then, that remote sensing methods serve to overcome many of the issues associated with manual sediment size measurements, instead providing a truer, more reliable quantification of sediment characteristics which influence hydraulics. The ability of the demonstrated remote sensing techniques clearly take into account smaller (>0.003 m) sediment grains (though it is acknowledged that operator bias is the most likely reason small particles were omitted during manual measurements). Whilst inclusion of small grains may not have significant implications for estimates of stream power and sediment transport capacity, understanding sediment characteristics at the lesser percentile ranges may have implications for assessment of invertebrate habitat or spawning gravel quality, for example.

Further quantitative examination of the difference between elevation models derived from each remote sensing method was performed using omni-directional semi-variogram analysis. At each 5° iteration, SfM-photogrammetric data consistently exhibited a greater degree of error than TLS, and hence a nugget effect was applied to each semi-variogram model drawn from SfM data. The nugget effect value is effectively the point at which the semi-variogram model intercepts the vertical axis, and is attributed to errors introduced by the type of measuring technique used – in this instance Structure from Motion-photogrammetry.

Variation between each data set is likewise readily observed when comparisons of cross-sectional elevation profiles are examined. Data derived from SfM-photogrammetry appear to have a greater range in elevation, in comparison to TLS-derived data, which generally remains within relatively small limits. This is possibly due to the increased quality and quantity (i.e., significantly larger point density) of data associated with the SfM reconstruction process taking into account a greater array of elevations within the resultant data set.

6.6. *Practical Application of SfM and its Benefit in River Restoration, Hydrogeomorphic Modelling and Habitat Assessment*

Attaining accurate sediment size, grain size distribution and particle configuration (i.e., homogeneous facies) is fundamental for aspects such sediment transport computation, hydraulic modelling and process-based river restoration design (Shields *et al.,* 2003). Despite the comparatively low-tech, field-based approach associated with this new method, and utilisation of ordinary, conventional apparatus (such as dSLR cameras Global Positioning Systems and EDM Total Station theodolites), the technique outlined in this study may have significant implications for the wider river restoration community and the ways in which DEMs are employed in understanding fluvial processes.

SfM-photogrammetry has been established as a plausible alternative to expensive, time-consuming remote sensing methods for quantifying sediment grain size. However, its potential applications may extend beyond those necessary exclusively for computer modelling and engineering design. It has been demonstrated that SfM-photogrammetry is able to detect detail previously unattainable by existing methods over the same timeframe; thus, it is reasonable to surmise that SfM may have a profound influence on the ways in which physical habitat is quantifiably assessed, monitored and managed.

Habitat assessments are a ubiquitous feature of river management practice (Thomason *et al.,* 2000), and developing methods for observing the physical habitat available to aquatic organisms is a fundamental component in evaluating river health, particularly where such assessment can be linked to specific, desirable biota. Further, ascertaining *quantified* information on the quality, complexity and diversity of riverine habitats – defined by geomorphic processes operating at a range of scales – has considerable value in river habitat restoration. Sfm-photogrammetry permits development of a multi-scalar habitat assessment approach, which can be applied to an array of river types, and provides a permanent, three-dimensional, geo-referenced model of a feature of interest, which can be subsequently manipulated in various GIS and computer modelling packages for further objective examination; for example, hydraulic evaluation, erosion and deposition monitoring and biotope assessment.

The method also has considerable potential for use in river restoration schemes that require some degree of monitoring prior and subsequent to restorative engineering. This is particularly beneficial where a river undergoing restoration is likely to experience significant morphological change, for example following removal of impoundments, channel re-profiling, or channel dredging.

Where traditional methods (for instance, fixed-point photography) (e.g., Chandler *et al.,* 2002) have been employed to monitor change subjectively, SfM-photogrammetry provides the opportunity to monitor morphologic readjustment *objectively,* since a permanent, high accuracy, three-dimensional model is produced. Moreover, the method also allows for rapid acquisition of quantitative baseline data before restoration takes place. This may then be used in subsequent studies where comparative analysis is necessary in order to reveal changes over time.

Chapter 7: Conclusion

7.1. Introduction

This thesis has presented a novel, parsimonious technique for detecting sediment grain size distribution of dry gravel features. Simultaneous investigations using both traditional, manual techniques, and established remote sensing techniques (terrestrial laser scanning and EDM theodolite) provided a two-fold benchmark to which results yielded from SfM-photogrammetry could be compared. It is anticipated that the key findings have potential to be applied in river restoration and monitoring schemes, providing a technique that is more practical than existing remote sensing methods of quantifying sediment characteristics of rivers, yet which remains significantly more accurate and time-saving than traditional methods.

7.2. Structure from Motion Photogrammetry for Informing Sediment Grain-Size Distribution

It has been demonstrated that SfM-photogrammetry is capable of detecting micro-scale variation in grain protrusion over a $\sim$12m^2 region of a gravel feature, using two times standard deviation of elevation ($2\sigma_Z$) data as a surrogate of grain size, previously established by Entwistle and Fuller (2009) and Milan $et\ al.$ (2009) as a reliable alternative to laborious and ultimately inaccurate manual counting. However, the level of detail produced by SfM-photogrammetry is significantly greater than that offered by Terrestrial Laser Scanning performed over similar timescales (though TLS is able to capture very dense point data, the amount of time necessary to yield a data set analogous to SfM would not be practical in the field.) Thus, the SfM method employed in this study detected greater detail, particularly of smaller (sub-cm) sediment particles when directly compared to TLS-derived data. Nevertheless, standard deviations of a 0.19m moving window yielded similar sediment rating curves, both for the entire study area, and five isolated regions within the data array, demonstrating that SfM-photogrammetry has the potential to rival TLS as a method for quantifiably examining sediment grain size distribution.

7.3. SfM-photogrammetry and its Relevance in Fluvial Geomorphology

The interaction between sediment and water is integral to the wider understanding of fluvial geomorphology. Central to this are the properties of sediment grain particles (i.e., size, shape and configuration), which interrelate with stream power to control sediment transport and channel form through flow resistance. The ability to identify bedforms, objectively quantify sediment size distribution, and detect homogenous sediment facies assemblages within gravel features is fundamental in geomorphological enquiry and, at present, is highly sought after among the fluvial science community. Results presented herein have considerable potential importance in elucidating morphological processes over various time frames, at greater accuracy offered by established techniques, and, crucially, at lower financial cost and time expenditure than that associated with contemporary laser scanning methods.

The methods which were employed in this thesis, and the results that were derived, are highly encouraging, particularly as current terrestrial laser scanning (though remaining a novel, albeit highly effective, luxury) is by no means easily accessible to many, either as a result of financial restraints, lack of user training or comprehensive knowledge of established fluvial remote sensing methods, or a combination of the two. SfM-photogrammetry, therefore, presents a noteworthy shift in topographic study of rivers and river dynamics, particularly as it can be performed with minimal guidance, using largely conventional apparatus (i.e., GPS and/or EDM theodolite). With this in mind, the method developed in this study and the ways in which it may be utilised extend far beyond simple *in situ* characterization of grain size and facies assemblage investegations. Indeed it has already proven its worth in reach-scale investigations where an aerial platform has provided greater spatial coverage.

7.4. SfM-photogrammetry as a New, Low-Cost, High Accuracy Method of River Restoration Monitoring

DEMs at scales achieved here are required in a multitude of riverine studies, not least those where some form of restorative measures have been undertaken, and a consistent, reliable monitoring program is required. Indeed, Fonstad *et al.* (2013) discuss viable applications of SfM-photogrammetry in a range of scenarios, including investigations of, 'bar and bank forms, woody debris geometry, and small- and medium-sized channel 3D morphology'.

A major advantage of SfM-photogrammetry is that data acquisition is extremely rapid compared to other techniques, and exerts negligible disturbance in the field, both in terms of time spent surveying and in physical disturbances. Moreover, from a practical perspective, SfM-photogrammetry is more easily applied than existing techniques, with minimal user training necessary to collect useful data, and can be very easily manipulated in the field.

This, therefore, ultimately contributes to the parsimonious nature of the technique, since less time is required in order to build accurate, three-dimensional topographic representations. However, care must be taken during the post-processing stage, where selection of pre-processing strictures – point limit; depth filtering; polygon count *etc.* – can determine the amount of time and computing power necessary for the reconstruction process.

7.5. Limitations

Despite encouraging results produced by Structure from Motion photogrammetry both in this study and other published works, there are a number of limitations that have emerged from such investigations. First, in order to capture sufficiently adequate photographs necessary for constructing three-dimensional representations, prevailing conditions must be optimal. This includes lighting conditions that are neither so bright that opaque shadows are cast, which may obscure features of interest; nor so dark that features do not appear at all. (Indeed, a benefit of LiDAR instruments is that they emit their own light source and therefore work in all light conditions). This is likely to have implications for sites covered by dense vegetation, where dappled light may obscure topographic detail and yield inaccurate or false results.

A further constraint of SfM-photogrammetry is that is limited in its application when observing immersed topographic fluvial features, though this is a similar restriction of LiDAR devices that emit eye-safe pulses of light, such as the instrument employed in this study. There are, nevertheless, terrestrially-based instruments available that employ light in the green wavelength (λ=532µm), whose emitted pulses are able to penetrate the water column and detect submerged topographic (Smith *et al.,* 2012). However, the oblique angles at which such instruments operate result in significant inaccuracies resulting from light refraction.

There is potential to resolve this issue using SfM-photogrammetry by gaining an elevated platform, thereby eliminating awkward, oblique shooting angles. Woodget *et al* (2014) employed an unmanned aerial vehicle (UAV), to acquire topographic data of both immersed and dry fluvial features, though clear, shallow water provided the best results, with optimal results gathered from depths of <0.2m.

Whilst the ability to remotely sense submerged fluvial topography and associated bedforms is of significant importance in geomorphological study, so too is the ability to measure water surface, particularly where identification of surface biotopes may support ecological monitoring.

Since, however, SfM requires several (theoretically, at least three) photographs of a feature, taken from several different locations, in order to facilitate three-dimensional reconstruction, it is not possible to capture water surface using the methods described in this thesis. Instead, photographs must be taken simultaneously in order to ensure the same water surface form is captured in each image, thus presenting some practical implications for use in the field if water surface features are the intended target.

The level of detail that SfM is able to capture, whilst notable, may present an issue at the post-processing stage. This is due to the sheer quantity of data that is captured by digital photographs: where TLS techniques yielded over 30,300 data points in this study, SfM yielded over 3,700,000 for the same area. Such an increase in data quantity results in considerably longer processing times when compared to TLS data collected over a similar period of time, especially when a large number of photographs and ground control points (as recommended by the software developers) are included.

Moreover, whilst the SfM-photogrammetric method is still in its infancy with regards to applications in the earth sciences, there is scope for investigations into the optimum settings for parameters such as number and configuration of GCPs and photographs, point limit during photo alignment, and the degree of accuracy necessary to replicate real-world phenomena whilst keeping computing time to a minimum, for example. Finally, the accuracy achieved in this study was only attainable with the inclusion of GCPs whose precise locations were acquired using EDM Total Station Theodolite. Though this method is also used in conjunction with liDAR instruments (see Heritage and Hetherington, 2007), this is to merely facilitate meshing procedures during post-processing – such apparatus produce accurate representations of real-world phenomena using their own internal co-ordinate system.

Structure from Motion, on the other hand, though capable of constructing representative three-dimensional models from photographs alone, cannot add accurate scale without inclusion of pre-measured ground control points, which are defined during the post-processing phase.

Whilst commercially available, off-the-shelf cameras with integrated GPS are available, the accuracy they offer is insufficient for micro-scale investigations that require sub-cm precision provided by dGPS and Total Station Theodolite.

7.6. The Future Direction of SfM-photogrammetry and Recommendations

The application of SfM-photogrammetry in fluvial sciences is potentially wide-ranging. However, limitations that have arisen in this study and others reveal that, despite encouraging initial results, the technique is still very much in its developing stages and more investigation is required so that SfM can reliably supersede traditional and expensive contemporary techniques. Once such method of acquiring photogrammetry data, which is starting to emerge as an alternative technique to ground-based remote sensing, is employment of unmanned aerial vehicles (UAVs). Such instruments provide an elevated platform from which photographs can be taken, thereby covering significantly greater areas than can be observed from the ground. However, there are no such investigations to date that test whether photographs taken from an oblique viewpoint yield better sediment size data than photographs taken from elevated, downward facing camera positions.

The use of UAVs, helium-filled blimps and other elevated platforms, however, has yielded promising results when observing riverscapes at larger spatial scales (see Fonstad *et al.,* 2013; Woodget *et al.,* 2014; Dietrich, 2015;). Moreover, the ease-of-use, minimal labour and presently less stringent operation aspects of employing such devices are common themes positively reported in the available literature; in addition to the intuitive and somewhat forgiving nature of post processing using structure from motion software packages. That said, however, since the SfM workflow relies on varied texture of the target object in order to produce a model; smooth, featureless areas – for instance: sand, silt and mud deposits that are uniform in character and form, such as estuarine environments for example – present a problem for adequately precise landscape mapping using SfM (Fonstad *et al.,* 2013), and hence may not be a viable remote sensing option in all environments.

Nevertheless, it is suggested that further direct comparison with established methods (e.g., terrestrial laser scanning) is required in order to understand the full potential of SfM-photogrammetry more completely. Similarly, TLS is able to yield three-dimensional representations of real-world phenomena, which can be subsequently manipulated in two- and three-dimensional modelling software.

Hence it is reasonable to surmise that there is great potential to input SfM-derived data in the same (or similar) modelling software packages, which simply require a three-dimensional mesh over which various hydrodynamic scenarios can be computed.

At the time of writing, there is no such study present in the available literature that incorporates both Structure from Motion *and* two- or three-dimensional flow modelling. However, this would be a highly valued asset among the river restoration community, particularly as the methods developed in this study are applied at considerably reduced financial cost and time expenditure compared to other techniques.

In addition to this, many flow modelling software packages are now open-source; hence, coupling inexpensive data acquisition methods with free or low-cost modelling software has the potential to eliminate many of the current inhibitive restrictions associated with riverine studies that comprise remote sensing and computation modelling elements. In a time of austerity and sparse funding opportunities, Structure from Motion offers great potential in reducing the presently high costs (both in terms of finance and effort) of river monitoring – particulalrly remote sensing – and thus may offer considerable benefits for the wider river restoration community. However, it has been demonstrated that SfM-photogrammetry is not merely a parsimonious compromise, but rather a viable, accurate and precise alternative to established remote sensing methods.

Whilst this thesis has considered one small, albeit fundamental, area of study, the number of published peer-review studies is increasing rapidly, with a diverse range of applications being presented. It is greatly anticipated that the method and results presented here will go towards supporting quantitative river monitoring in the future.

References

Aggett, G. R. and Wison, J.P. 2009. Creating and coupling a high-resolution DTM with a 1-D hydraulic model in a GIS for scenario-based assessment of avulsion hazard in a gravel-bed river. *Geomorphology.* **113:** 21-34.

AgiSoft LLC. 2014. Agisoft PhotoScan User Manual Professional Edition, Version 1.0.

Ashworth, P. J. and Ferguson, R. I. 1989. Size-Selective Entrainment of Bed Load in Gravel Bed Streams. *Water Resources Research.* **25 (4):** 627-634

Asner, G. P. 2001. Cloud cover in Landsat observations of the Brazilian Amazon. *International Journal of Remote Sensing.* **22 (18):** 3855-3862.

Baily, B., Collier, P., Farres, P., Inkpen, R., and Pearson, A. 2003. Comparative assessment of Analytical and Digital Photogrammetric Methods in the Construction of DEMs Of Geomorphological Forms. *Earth Surface Processes and Landforms.* **28:** 207-320.

Barry, J. J., Buffington, J. M., and King, J. G. 2004. A General Protocol for Predicting Bed Load Transport Rates in Gravel Bed Rivers. *Water Resources Research.* **40:** 1-22.

Basar, A., Baki, M., and Yew Gan., T. 2012. Riverbank Migration and Island Dynamics of the Braided Jamuna River of the Ganges-Brahmaputra Basin Using Multi-Temporal Landsat Images. *Quaternaery International.* **263:** 148-161.

Baxter, R. M. 1977. Environmental Effects of Dams and Impoundments. *Annual Reviews of Ecological Systems.* **8:** 255-283.

Bednarek, A. T. 2001. Undamming Rivers: A Review of the Ecological Impacts of Dam Removal. *Environmental Management.* **27 (6):** 803-814.

Beechie, T. J. Sear, D. A., Olden, J. D., Pess, G. R., Buffington, J. M., Moir, H., Roni, P., and Pollock, M. M. 2010. Processes-based Principles for Restoring River Ecosystems. *ioScience.* **60 (3):** 209-222.

Benson, M. A., and Thomas, D. M. 1966. A Definition of Dominant Discharge. *U.S Geological Survey.* 76-80

Bernhardt, E. S., Sudduth, E. B., Palmer, M. A., Allan, D. J., Meyer, J. L., Alexander, G., Follastad-Shah, J., Hassett, B., Jenkinson, R., Lave, R., Rumps, J., Pagano, L. 2007. Restoring Rivers One Reach at a Time: Results from a Survey of U.S. River Restoration Practitioners. *Restoration Ecology.* **15 (3):** 482-493.

Billi, P., and Paris, E. 1992. Bed Sediment Characterization in River Engineering Problems. *Erosion and Monitoring Programmes in River Basins (Proceedings of the Oslo Symposium).* 11-20.

Bowen, Z. H. and Waltermine, R. G. 2002. Evaluation of Light Detection and Ranging (LIDAR) For Measuring River Corridor Topography. *Journal of the American Water Resources Association.* **38 (1):** 33-41.

Brandt, A. S. 2000. Classification of Geomorphological Effects Downstream of Dams. *Catena.* **40:** 375-401.

Brasington, J., Rumsby, B. T., and McVey, R. A. 2000. Monitoring and Modelling Morphological Channel Change in a Braided Gravel-Bed River Using High Resolution GPS-Based Survey. *Earth Surface Processes and Landforms.* **25:** 973-990.

Brown, R. A., and Pasternack, G. B. 2012. Monitoring and Assessment of the 2010-2011 Gravel/Cobble Augmentation In The Englebright Dam Reach of the Lower Yuba River, Ca. Prepared for the U.S. Army Corps of Engineers, Sacramento District. University of California at Davis, Davis, CA.

Brown, R. A., and Pasternack, G. B. 2014. Hydrologic and Topographic Variability Modulate Channel Change in Mountain Rivers. *Journal of Hydrology.* **510:** 551-564.

Buffington, J. M., and Montgomery, D. R. 1997. A Systematic Analysis of EightDecades of Incipient Motion Studies, with Special Reference to Gravel-Bedded Rivers. *Water Resources Research.* **33 (8):** 1993-2029.

Buffington, J. M. and Montgomery, D. R. 1999a. Effects of Sediment Supply on Surface Textures of Gravel-Bed Rivers. *Water Resources Research.* **35 (11):** 3523-3530.

Buffington, J. M. and Montgomery, D. R. 1999b. A Procedure for Classifying Textural Facies in Gravel-Bed Rivers. *Water Resources Research.* **35 (6):** 1903-1914.

Bunn, S. E. and Arthington, A. H. 2002. Basic Principles and Ecological Consequences of Altered Flow Regimes for Aquatic Biodiversity. *Environmental Management.* **30 (4):** 492-507.

Bunte, K. and Abt, S. R. 2001. Sampling Surface and Subsurface Particle-size Distributions in Wadable Gravel- and Cobble-Bed Streams for Analyses in Sediment Transport, Hyrdaulics, and Streambed Monitoring. General Technical Rep. No. RMRS-GTR-74, U.S. Department of Agriculture Forest Service, Fort Collins, Colorado.

Burroughs, B. A., Hayes, D. B., Klomp, K. D., Hansen, J. F., and Mistak, J. 2009. Effects of Sronach Dam Removal on Fluvial Geomorphology in the Pine River, Michigan, United States. *Geomorphology.* **110:** 96-107.

Burton, L. R. 2003. The Mersey Basin: An Historical Assessment of Water Quality from and Anecdotal Perspective. *The Science of the Total Environment.* **314-316:** 53-66.

Bushaw-Newton, K.L., D.D. Hart, J.E. Pizzuto, J.R. Thom- son, J.Egan, J.T. Ashley, T.E. Johnson, R.J. Horwitz, M. Keeley, J. Lawrence, D. Charles, C. Catenby, D.A. Kreeger, T. Nightengale, R.L. Thomas, and D.J. Velinsky. 2002. An Integrative Approach Towards Understanding Ecological Responses to Dam Removal: The Manatawny Creek Study. *Journal of the American Water Resources Association.* **38:** 1581–1599.

Carbonneau, P. E., Lane, S. N., and Bergeron, N. E. 2003. Cost-Effective Non-Metric Close-Range Digital Phoogrammetry and its Application to a Study of Coarse Gravel Rivers Beds. *International Journal of Remote Sensing.* **24 (14):** 2837-2854.

Carbonneau, P. E., Bergeron, N. and Lane, S. N. 2005. Automated Grain Size Measurements from Airborne Sensing for Long Profile Measurements of Fluvial Grain Sizes. *Water Resources Research.* **41:** 1-9.

Cavalli, M., Tarolli, P., Marchi, L., Fontana, G. D. 2008. The Effectiveness of Airborne LiDAR Data in the Recognition of Channel-bed Morphology. *Catena.* **73:** 249-260.

Chandler, J., Ashmore, P., Paola, C., Gooch, M., and Varkaris, F. 2002. Monitoring River Channel Change Using Terrestrial Oblique Digital Imagery and Automated Digital Photogrammetry. *Annals of the Association of American Geographers.* **92 (4):** 631-644

Chappell, A., Heritage, G. L., Fuller, I. C., Large, A. R. G., and Milan, D. J. 2003. Geostatistical Analysis of Ground-Survey Elevation Data to Elucidate Spatial and Temporal River Channel Change. *Earth Surface Processes and Landforms.* **28:** 349-370.

Charlton, M. E., Large, A. R. G., and Fuller, I. C. 2003. Application of Airborne LiDAR in River Environments: The River Coquet, Northumberland, UK. *Earth Surface Processes and Landforms.* **28:** 299-306.

Cheng, F., and Granata, T. 2007. Sediment Transport and Channel Adjustments Associated with Dam Removal: Field Observations. *Water Resources Research.* **43:** 1–14.

Choudhury B. J. 1991. Passive Microwave Remote Sensing Contribution to Hydrological Variables. *Surveys in Geophysics.* **12:** 63–84.

Chu, Z. X., Sun, X. G., Zhai, S. K., Xu, K. H. 2006. Changing Pattern of Accretion/Erosion of the Modern Yellow River (Huanghe) Subaerial Delta, China: Based on Remote Sensing Images. *Marine Geology*. **227:** 13e30.

Church, M. 1995. Geomorphic Response to River Flow Regulations: Case Studies and Time-Scales. *Regulated Rivers Research.* **11:** 3-22.

Church, M., Hassan, M. A., and Wolcott, J. F. 1998. Stabilizing Self-Organized Structures in Gravel-Bed Stream Channels: Field and Experimental Observations. *Water resources Research.* **34 (11):** 3169-3179.

Clarke S. J., Bruce-Burgess, L., and Wharton, G. 2003. Linking Form and Function: Towards an Eco-Hydromorphic Approach to Sustainable River Restoration. *Aquatic Conservation of Marine and Freshwater Ecosystems.* **13:**439–50.

Collins, B., and T. Dunne. 1990. Fluvial Geomorphology and River Gravel Mining: A Guide for Planners, Case Studies Included. California Division of Mines and Geology Special Publication 98. Sacramento.

Constantine, C. R., Mount, F. F., and Florsheim, J. L. 2003. The Effects of Longitudinal Differences in Gravel Mobility on the Downstream Fining Patterns in the Cosumnes River, California. *The Journal of Geology.* **111:** 233-241.

Crowder, D. W. and Diplas, P. 2000. Using Two-Dimensional Hydrodynamic Models at Scales of Ecological Importance. *Journal of Hydrology.* **230:** 172-191.

Dade, B. W. and Friend, P. F. 1998. Grain-Size, Sediment-Transport Regime, and Channel Slope in Alluvial Rivers. *The Journal of Geology.* **106:** 661-675.

Dekker A. G., Hoogenboom H. J., Goddijn L. M. and Malthus T. J. M. 1997. The Relationship Between Inherent Optical Properties and Reflectance Spectra in Turbid Inland Waters. *Remote Sensing Reviews.* **15:** 59–74.

Dietrich, W. E. 1982. Settling Velocity of Natural Particles. *Water Resources Research.* **18 (6):** 1615-1626.

Dietrich, W. E., Kircher, J. W., Ikeda, H., Iseya, F. 1989. Sediment Supply and the Development of the Course Surface Layer in Gravel-Bedded Rivers. *Nature.* **340:** 215-217.

Doyle, M. W., Stanley, E. H., Orr, C. H., Selle, A. R., Sethi, S. A., and Harbor, J. M. 2005. Stream Ecosystem Response to Small Dam Removal: Lessons from the Heartland. *Geomorphology.* **71:** 227-244.

Downs, P. W., and G. M.Kondolf. 2002. Post-Project Appraisals in Adaptive Management of River Channel Restoration. *Environmental Management.* **29:**477–496.

Du Boys, P. 1879. Le Rhône et les rivièrs a lit affouillable, *Ann. Ponts Chausées Mem.* **5 (18):** 141–195.

Dugdale, S. J., Carbonneau, P. E., and Campbell, D. 2010. Aerial Photosieving of Exposed Gravel Bars for the Rapid Calibration of Airborne Grain Size Maps. *Earth Surface Processes and Landforms.* **35:** 627-639.

Dynesisus, M., and Nilso, C. 1994. Fragmentation and Flow Regulation of River Systems in the Northern Third World. *Science.* **266 (5186):** 753-762.

Einstein, H. A. 1942. Formulas for the Transportation of Bed Load. *Transaction of the American Society of Civil Engineering.* **107:** 561–597.

Einstein, H. A. 1950. The Bed-Load Function for Sediment Transportation in Open Channel Flows. *Technical Bulletin, United States Department of Agriculture.*

Elbourne, N., Hammond, D., and Mant, J. *Weir Removal, Lowering and Modification: A Review of Best Practice.* The Environment Agency. Bristol, UK.

England, J., Skinner, K. S., and Carter, M. G. 2008. Monitoring, River Restoration and The Water Framework Directive. *Water and Environment Paper.* **22:** 227-234.

Entwistle, N. S. and Fuller, I. C. . (2009). Terrestrial Laser Scanning to Derive the Surface Grain Size Facies Character of Gravel Bars. In: Heritage, G. L., Charlton, M. and Large, A. *Laser Scanning for the Environmental Sciences.* London : Blackwell Publishing . 102-114.

Ernst, J., Dewals, B. J., Detrembleur, S., Archambeau, P., Espicum, S., Pirotton, M. 2010. Micro-Scale Flood Risk Analysis Based on Detailed 2D Hydraulic Modelling and High Resolution Geographic Data. *Natural Hazards.* **55:** 181-209.

European Commission (2000) *Directive 2000/60/EC of the European Parliament and of the Council of 23rd October 2000: establishing a framework for Community action in the field of water policy.* Official Journal of the European Communities: Brussels.

Feld, C.K., Birk, S., Bradley, D.C., Hering, D., Kail, J., Marzin, A., Melcher, A., Nemitz, D., Pedersen, M.L., Pletterbauer, F., Pont, D., Verdonschot, P.F.M., et al. (2011). From natural to degraded rivers and back again: a test of restoration ecology theory and practice. Adv. Ecol. Res. 44, 119–210.

Flener, C., Vaaja, M., Jaakkola, A., Krooks, A., Kaartinen, H., Kukko, A., Kasvi, E., Hyyppä, H., Hyyppä, J., and Alho, P. 2013. Seamless Mapping of River Channels at High Resolution Using Mobile LiDAR and UAV-Photography. *Remote Sensing.* **5:** 6382-6407.

Florsheim, J. L., Mount, J. F., and Constantine, C. R. 2005. A Geomorphic and Adaptive Assessment Framework to Assess the Effect of Lowland Floodplain River Restoration on Channel-Floodplain Sediment Continuity. *River Research and Applications.* **22:** 253-375.

Fonstad, M. A., Dietrich, J. T., Courville, C., Jensen, J. L., and carbonneau, P. E. 2013. Topographic Structure from Motion: A New Development in Photogrammetric Measurement. *Earth Surface Processes and Landforms.* **38:** 421-430.

French, J. R. 2003. Airborne LiDAR in Support of Geomorphological and Hydraulic Modelling. *Earth Surface Processes and Landforms.* **28:** 321-335.

Gaspariani, N. M., Tucker, G. E., and Bras, R. L. 2004. Network-Scale Dynamics of Grain-Size Sorting: Implications for Downstream Fining, Stream-Profile Concavity, and Drainage Basin Morphology. *Earth Surface Processes and Landforms.* **29:** 401-421.

Gilvear, D. J. 1999. Fluvial Geomorphology and River Engineering: Future Roles Utilizing a Fluvial Hydrosystems Network. *Geomorphology.* **21:** 229-245.

Glenn, N. F., Streutker, D. R., Chadwick, J. D., Thackray, G. D., Dorsch, S. J. 2006. Analysis of LiDAR-Derived Topographic Information for Characterizing and Differentiating Landslide Morphology and Activity. *Geomorphology.* **73:** 131-148.

Gomez, B. 1993. Roughness of Stable, Armoured Gravel Beds. *Water Resources Research.* **29 (11):** 3631-3642.

Gomez, B. and Church, M. 1989. An Assessment of Bed Load Sediment Transport Formulae for Gravel Bed Rivers. *Water Resources Research.* **25 (6):** 1161-1189.

Gomez, B., Rosser, B. J., Peacock, D. H., Hicks, M. D., and Palmer, J. A. 2001. Downstream Fining in a Rapidly Aggrading Gravel Bed River. *Water Resources Research.* **37 (6):** 1813-1823.

Graf, W. L. 1999. Dam Nation: A Geographic Census of American Dams and their Large-Scale Hydraulic Impacts. *Water Resources Research.* **35 (4):** 1305-1311.

Graf, W. L. 2005. Geomorphology and American Dams: The Scientific, Social and Economic Context. *Geomorphology.* **71:** 3-26.

Graf, W. L. 2006. Downstream Hydrologic and Geomorphic Effects of Large Dams on American Rivers. *Geomorphology.* **79:** 336-360.

Grant, G. E., Schmidt, J. C., and Lewis, S. L. 2003. A Geological Framework for Interpreting Downstream Effects of Dams on Rivers. *A Unique River Water Science Application by the American Geophysical Union.* 209-225.

Gregory, K. J. 2006. The Human Role in Changing River Channels. *Geomorphology.* **79:** 172-191.

Hart, D. D., Johnson, T. E., Bushaw-Newton, K. L., Horwitz, R. J., Bednarek, A. T., Charles, D. F., Kreeger, D. A., and Velinsky, D. J. 2002. Dam removal: Challenges and opportunities for ecological research and river restoration. *Bioscience.* **52:** 669–681.

Heritage, G. and Hetherington, D. 2007. Towards a Protocol for Laser Scanning in Fluvial Geomorphology. *Earth Surface processes and Landforms.* **32:** 66-74.

Heritage, G. L. and Milan, D. 2009. Terrestrial Laser Scanning of Grain Roughness in a Gravel-Bed River. *Geomorphology.* **113:** 4-11.

Heritage, G. L., Fuller, I. C., Charlton, M. E., Brewer, P. A., and Passmore, D. P.1998. CDW Photogrammetry of Low Flow Relief Fluvial Features: Accuracy and Implications for Reach-Scale Sediment Budgeting. *Earth Surface Processes and Landforms.* **23:** 1219-1233.

Hey, R. D., and Thorne, C. R. 1983. Accuracy of surface samples from gravel bed material. *Journal of Hydraulic Engineering.* **109**: 842–851.

Hodge, R. A. 2010. Using Simulated Terrestrial Laser Scanning to Analyse Errors in High-Resolution Scan Data of Irregular Surfaces. *Journal of Photogrammetry and Remote Sensing.* **65:** 227-240.

Hodge, R., Brasington, J., and Richards, K. 2009a. Analysing Laser-Scanned Digital Terrian Models of Gravel Bed Surfaces: Linking Morphology to Sediment Transport Processes and Hydraulics. *Sedimentology.* **56:** 2024-2043.

Hodge, R., Brasington, J., and Richards, K. 2009b. *In Situ* Charaterization of Grain-Scale Fluvial Morphology Using Terrestrial Laser Scanning. *Earth Surfaces Processes and Landforms.* **34:** 954-968.

Hoey, t. B. and Ferguson, R. 1994. Numerical Simulation of Downstream Fining by Selective Transporn in Gravel Bed Rivers: Model Development and Illustration. *Water Resources Research.* **30 (7):** 2251-2260.

Hohenthal, J., Alho, P., Hyypaä, J., and Hyyppä, H.2011. Laser Scanning Applications in Fluvial Studies. *Progress in Physical Geography.* **35 (6):** 782-809.

Hooke, J. 2003. Coarse Sediment Connectivity in River Channel Systems: A Conceptual Framework and Methodology. *Geomorphology.* **56:** 79-94.

Horritt, M. S. 2002. Stochastic Modelling of 1-D Shallow Water Flows over Uncertain Topography. *Journal of Conceptual Physics.* **180:** 327-338.

James, S. C., Jones, C. A., Grace, M. D., and Roberts, J. D. 2010. Advances in Sediment Transport Modelling. *Journal of Hydraulic Research.* **48 (6):** 754-763.

Javernick, L., Brasington, J., and Caruso, B. 2014. Modelling the Topography of Shallow Braided Rivers Using Structure-from-Motion Photogrammetry. *Geomorphology.* dx.doi.org/10.1016/j.geomorph.2014.01.006.

Jensen J. R. 1999. Remote Sensing of Water. In: Remote Sensing Applications (Ed. J.R. Jensen). 379–406. Prentice-Hall, Inc., Upper Saddle River, NJ.

Jones, A. F., Brewer, P. A., Johnstone, E., and Macklin, M. G. 2007. High-resolution Interpretive Geomorphological Mapping of River Valley Environments Using Airborne LiDAR Data. *Earth Surface Processes and Landforms.* **32:** 1574-1592.

Jung, Y., Merwade, V., Yeo, K., Shin, Y., and Oh Lee, S. 2013. An Approach Using a 1D Hydraulic Model, Landsat Imaging and Generalized Likelihood Uncertainty Estimation for an Approximation of Flood Discharge. *Water.* **5:** 1598-1621.

Kanehl, P. D., Lyons, J., and Nelson, J. E. 1997. Changes in the Habitat and Fish Community of the Milwaukee River, Wisconsin, Following Removal of the Woolen Mills Dam. *North American Journal of Fish Management.* **17**: 387–400.

Kappesser, G. B. .2002. A Riffle Stability Index to Evaluate Sediment Loading in Streams. *Journal of the American Water Resources Association.* **38 (4):** 1061-1081.

Kellerhals, R., and Bray, D. I. 1971. Sampling Proceedures for Coarse Fluvial Sediments. *Journal of the Hydraulics Devision.* **97 (8):** 1165-1180.

Kngihton, D. 1998. *Fluvial Forms and Processes: A New Perspective.* Arnold. London, UK.

Kondolf, M. G. 1997. Hungry Water: Effects of Dams and Gravel Mining on River Channels. *Environmental Management.* **21 (4):** 533-551.

Kondolf, M. G. 2000. Assessing Salmonid Spawning Gravel Quality. *Transactions of the American Fisheries Society.* **129:** 262-281.

Kondolf, G. M., and Li, S. 1992. The Pebble Count Technique for Quantifying Surface Bed Material Size in Instream Flow Studies. *Rivers.* **3:** 80–87.

Lane,... 1955. The Importance of Fluvial Morphology in Hydraulic Engineering. *United States Department of the Interior Bureau of Reclamation.* Denver, Colorado.

Lane, S. N. 2000. The Measurement of River Channel Morphology Using Digital Photogrammetry. *Photogrammetric Record.* **16 (96):** 937-961.

Lane, S. N., Bradbrook, K. F., Richards, K. S., Biron, P. A., and Roy, A. G.1999. The Application of Computational Fluid Dynamics to Natural River Channels: Three-Dimensional Versus Two-Dimensional Approaches. *Geomorphology.* **29:** 1-20.

Langbein, W. B. and Leopold, L. B. 1964. Quasi-Equilibrium States in Channel Morphology. *American Journal of Science.* **262:** 782-794.

Large, A. R. G. and Heritage, G. L. 2009. Laser-Scanning – Evolution of the Discipline. In: Heritage, G. L., Charlton, M. and Large, A. *Laser Scanning for the Environmental Sciences.* London : Blackwell Publishing. 1-20.

Latulippe, C., Lapointe, M. F., and Talbot, T. 2001. Visual Characterization Tecnique for Gravel-Cobble River Bed Surface Sediments; validation and environmental applications Contribution to the programme of CIRSA (Centre Interuniversitaire de Recherche sur le Saumon Atlantique). *Earth Surface Processes and Landforms.* **26:** 307-318.

Lawson, N. and Lindley, S. 2008. A Deeper Understanding of Climate Induced Risk to Urban Infrastructure: Case Studies of past Events in Greater Manchester. *North West Geography*. **8 (1):** 4-18.

Leopold, L. B. 1970. AnImproved Method for Size Distribution of Stream Bed Gravel. *Water Resources Research.* **6 (5):** 1357-1366.

Leopold, L. B., Wolman, G. M., and Miller, J. P. 1964. *Fluvial Processes in Geomorphology.* W. H. Freeman and Company. San Francisco, CA.

Ligon, F. K., Dietrich, W. E., and Trush, W. J. 1995. Downstream Ecological Effects of Dams: A Geomorphological Perspective. *BioScience.* **45 (3):** 183-192.

Lisle, T. 1995. Particle Size Variations Between Bed Load and Bed Material in Natural Gravel Bed Channels. *Water Resources Research.* **31(4):** 1107-1118.

Magilligan, F. J. and Nislow, K. H. 2005. Changes in Hydrologic Regime by Dams. *Geomorphology.* **71:** 61 – 78.

Maloney, K. O., Dodd, H. R., Butler, S. E., and Wahl, D. H. 2008. Changes in Macroinvertebrate and Fish Assemblages in a Medium-Sized River Following a Breach of a Low-Head Dam. Freshwater Biology. **53:** 1055–1068.

Marcus, W. A., Ladd, S. C., Stoughton, J. A. and Stock, J. W. 1995. Pebble Counts and the Role of User-Dependent Bias in Documenting Sediment Size Distributions. *Water Resources Research.* **31 (10):** 2625 – 2631

Marren, P. M., Grove, J. R., Webb, J. A. and Stewardson, M. J. 2014. The Potential for Dams to Impact Lowand Meandering River Floodplain Geomorphology. *The Scientific World Journal.* **2014:** 1 –24

Mertes, L. A. K. 2002. Remote Sensing of Riverine Landscapes. *Freshwater Biology.* **47:** 799 – 816

Mertes, L. A. K., Dekker, A., Brakenridge, G. R., Birkett, C. and Lé Tourneau, G. (2002) Rivers and Lakes. In: Natural Resources and Environment, Manual of Remoté Sensing (Ed. S.L. Ustin). John Wiley and Sons. New York.

Mertes, L. A. K., Daniel, D. L., Melack, J. M., Nelson, B., Martinelli, L. A. and Forsberg, B. R. 1995. Spatial Patterns of Hydrology, Geomorphology, and Vegetation on the Floodplain of the Amazon River in Brazil from a Remote Sensing Perspective. *Geomorphology.* **13:** 215 – 232

Meyer-Peter, E., and Müller, R. 1949. Eine Formel zur Berechnung des Geschiebetriebs. *Schweizerische Bauzeitung.* **67(3):** 29–32.

Micheletti, N., Chandler, J. H., and Lane, S. 2015. Structure from Motion (SfM) Photogrammetry. *British Society for Geomorphology Geomorphological Techniques, Chap 2, Sec 2.2.*

Milan, D. J., Heritage, G. L., Large, A. R. G. and Brunsdon, C. F. 1999. Influence of Particle Shape and Sorting Upon Sample Size Estimates for a Coarse-Grained Upland Stream. *Sedimentary Geology.* **129:** 85-100

Milan, D. J., Heritage, G. L., Large, A. R. G. and Entwistle, N. S. 2010. Mapping Hydraulic Biotapes Using Terrestrial Laser Scan Data of Water Surface Properties. *Earth Surface Processes and Landforms.* **35:** 918 -931

Milan, D. J., Heritage, G. L., Large, A. R. G. and Fuller, I. C. 2011. Filtering Spatial Error from DEMs: Implications for Morpholigical Chang Estimation. *Geomorphology.* **125:** 160 –171.

Morandi, B., Piégay, H., Lamouroux, N., and Vaudor, L. 2014. How Is Success or Failure in River Restoration Projects Evaluated? Feedback From French Restroation Projects. *Journal of Environmental Management.* **137:** 178-188.

Mosley, M. P., and D. S. Tinsdale. 1985. Sediment Variability and Bed Material Sampling in Gravel Bed Rivers. *Earth Surface Processes and Landforms.* **10:** 465-482.

Moss, B., Herring, D., Green, A. J., Aidoud, A., Becares, E., Beklioglu, M., Bennion, H., Boix, D., Brucet, S., Carvalho, L., Clement, B., Davidson, T., Declerck, S., Dobson, M., van Donk, E., Dudley, B., Feuchtmayr, H., Friberg, N., Grenouillet, G., Hillebrand, H., Hobaek, A., Irvine, K., Jeppesen, E., Johnson, R., Jones, I., Kernan, M., Lauridsen, T. L., Manca, M., Meerhoff, M., Olafsson, J., Ormerod, S,m Papastergiadou, E., Penning, W. E., Ptacnik, R., Quintana, X., Sandin, L., Seferlis, M., Simpson, G., Triga, C., Verdonschot, P., Verschoor, A. M. and Weyhenmeyer, G. A. 2009. Climate Change and the Future of Freshwater Biodiversity in Europe: A Primer for Policy-Makers. *Freshwater Reviews.* **2:** 103 – 130

Nelson, P. A., Bellugi, D. and Dietrich, W. E. 2014. Delineation of River Bed-Surface Patches by Clustering High-Resolution Spatial Grain Size Data. *Geomorphology.* **205:** 102 –119

NERC. (2015). *Spatial Data.* Available: http://www.ceh.ac.uk/data/nrfa/data/spatialdata. Last accessed 2nd February 2015.

Newson, M. 1994. *Hydrology and the River Environment.* Oxford University Press. New York.

Newson, M. D. 2002. Geomorphological Concepts and Tools for Sustainable River Ecosystem Management. *Aquatic Conservation: Marine and Freshwater Ecosystems.* **12:** 365 –379.

Newson, M. D. and Large, A. R. G. 2006. 'Natural' Rivers, 'Hydromorphological Quality' and River Restoration: a Challenging New Agenda for Applied Fluvial Geomorphology. *Earth Surface Processes and Landforms.* **31:** 1606 – 1624.

Nielsen, P. 1992. Coastal Bottom Boundary Layers and Sediment Transport, World Scientific.

Nikora, V. I., Goring, D. G.. and Biggs, B. J. F. 1998. On Gravel-Bed Roughness Characterization. *Water Resources Research.* **34 (1):** 517 – 527

Nislow, K. H., Magilligan, F. J., Fassnacht, H., Bechtel, D., and Ruesink, A. 2002. Effects of Hydrologic Alteration on Flood Regime of Natural Floodplain Communities in the Upper Connecticut River. *Journal of the American Water Resources Association.* **38:** 1533-1548.

Notebaert, B., Verstraeten, G., Govers, G., and Poesen, J. 2009. Qualitative and Quantitative Applications of LiDAR Imagery in Fluvial Geomorphology. *Earth Surface Processes and Landforms.* **34:** 217-231.

Oliver, M. A. and Webster, R. 2014. A Tutorial Guide to Geostatistics: Computing and Modelling Variograms and Kriging. *Catena.* **113:** 56 – 69

Oliver, M. A. and Webster, R. 2014. A Tutorial Guide to Geostatistics: Computing and Modelling Variograms and Kriging. *Catena.* **113:** 56-69.

Olsen, D. S., Roper, B. B., Kershner, J. L., Henderson, R. and Archer, E. 2005. Sources of Variability in Conducting Pebble Counts: Their Potential Influence on the Results of Sream Monitoring Programs. *Journal of the American Water Resources Association.* 1225 - 1236

Orr, H. G., Large, A. R. G., Newson, M. D. and Walsh, C. L. 2008. A Predictive Typology for Characterising Hydromorphology. *Geomorphology.* **100:** 32 – 40

Palmer, M. A., Bernhardt, E. S., Allan, J. D., Lake, P. S., Alexander, S., Brooks, S., Carr, J., Clayton, S., Dahm, C. N., Follstad Shah, J., Galat, D. L., Loss, S. G., Goodwin, P., Hart, D. D., Hassett, B., Jenkinson, R., Kondolf, G. M., Lave, R., Meyer, J. L., O'Donnell, T. K., Pagano, L. and Sudduth, E. 2005. Standards for Ecologically Successful River Restoration. *Journal of Applied Ecology.* **42:** 208- 217

Palmer, M. A., Bernhardt, E. S. Allan, J. D. Lake, P. S. Alexander, G., Brooks, S., Carr, J., Clayton, S., Dahm, C. N., Follstad Shah, J., Galat, D. L., Loss, G., Goodwin, P., Hart, D. D., Hassett, B., Jenkinson, R., Kondolf, G. M., Lave, R., Meyer, J. L., O'Donnell, T. K. Pagno, L., and Suddoth, E.2005. Standards for Ecologically Successful River Restoration. *Journal of Applied Ecology.* **42:** 208-217.

Paola, C. and Seal, R. 1995. Grain Size Patchiness as a Cause of Selective Deposition and Downstream Fining. *Water Resources Research.* **31 (5):** 1395 – 1407

Paola, C., and Seal, R. 1995. Grain Size Patchiness as a Cause of Selective Deposition and Downstream Fining. *Water Resources Research.* **31 (5):** 1395-1407.

Petts, G. E. 1977. Channel Response to Flow Regulaltion: The Case of the River Derwent: Derbyshire. In: Gregory, K. J. *River Channel Changes.* Wiley. Chichester.

Petts, G. E. and Gurnell, A. M. 2005. Dams and Geomorphology: Research Progress and Future Directions. *Geomorphology.* **71:** 27 – 47

Pizzuto, J. 2002. Effects of Dam Removal on River Form and Process. *Bioscience.* **52:** 683–691.

Poff, N. L., Allan, J. D., Bain, M. B., Karr, J. R., Prestegaard, K. L., Richter, B. D., Sparks, R. E. and Stromberg, J. C. 1997. The Natural Flow Regime. *Bioscience.* **11:** 769 – 784

Pollard, A. I., and Reed, T. 2004. Benthic Invertebrate Assemblage Change Following Dam Removal in a Wisconsin Stream. *Hydrobiologia.* **513:** 51–58.

Powell, D. M. and Ashworth, P. J. 1995. Spatial Pattern of Flow Competence and Bed Load Transport in a Divided Gravel Bed River. *Water Resources Research.* **31 (3):** 741 – 752

Power, M. E., Dietrich, W. E. and Finlay, J. C. 1996. Dams and Downstream Aquatic Biodiversity: Potential Food Web Consequences of Hydrologic and Geomorphic Change. *Environment Management.* **20 (6):** 887 - 895

Qin, J., Zhong, D., Wang, G. and Ng, S. L. 2013. Influence of Particle Shape on Surface Roughness: Dissimilar Morphological Structures Formed by Man-Made and Natural Gravels. *Geomorphology* **190:** 16-26.

Recking, A., Liebault, F., Peteuil, C. and Joliment, T. 2012. Testing Bedload Transport Equations with Consideration of Time Scales. *Earth Surface Processes and Landforms.* **37:** 774-789.

Reid, I., Powell, D., and Loronne, J. 1996. Prediction of Bed-Load Transport by Desert Flash Flood. *Journal of Hydraulic Engineering.* **122 (3):** 170-173.

Renshaw, C. E., Abengoza, K., Magilligan, F. J., Dade, W. B. and Landis, J. D. 2014. Impact of Flow Regulation on Near-Channel Floodplain Sedimentation. *Geomorphology.* **205:** 120-127.

Richards, K. 1982. *Rivers Forms and Processes in Alluvial Channels.* Methuen and Co. New York.

Rolls, R. J. and Athrigton, A. H. 2014. How do Low Magnitudes of Hydrologic Alternation Impact Riverine Fish Populations and Assemblage Characteristics? *Ecological Indicators.* **39:** 179 – 188.

Roni, P., Hanson, K., and Beechie, T. 2008. Global Review of the Physical and Biological Effectiveness of Stream Habitat Rehabilitation Techniques. *North American Journal of Fisheries Management.* **28:** 856–890.

Saleh, F., Ducharne, A., Flipo, N., Oudin, L. and Ledoux, E. 2013. Impact of River Bed Mophology on Discharge and Water Levels Simulated by a 1D Saint-Venant Hydraulic Model at Regional Scale. *Journal of Hydrology.* **476:** 169 – 177.

Schoklitsch, A. 1930. *Handbuch des Wasserbaues.* Springer. Vinenna, Austria.

Schumm, S. A. 1977. *The Fluvial System.* Wiley. New York.

Schumm, S.A. and Lichty, R. W. 1965. Time, Space and Causality in Geomorphology. *American Journal of Science.* **263:** 110 – 119.

Sear, D. A., Hill, C. T. and Downes, R. H. E. 2008. Geomorpological Assessment of Riverine SSSIs for the Strategic Planning of Physical Restoration. *Natural England Research Report* NERR013.

Sear, D. S. Wheaton, J. M., and Darby, S. E. 2008. Uncertain Restoration of Gravel-Bed Riversand the Role of Geomorphology. In: Habersack, H., Piégay, H., and Rinaldi, M. *Gravel-Bed Rivers VI: From Process Understanding to River Restoration.*Elevier. BV.

Shafroth, P. B., Friedman, J. M., Auble, G. T., Scott, M. L., and Braatne, J. H. 2002. Potential Responses of Riparian Vegetation to Dam Removal. *Bioscience.* **52:** 703–712.

Sheng, Y., Gong, P. and Xiao, Q. 2001. Quantitative Dynamic Flood Monitoring with NOAA AVHRR. *International Journal of Remote Sensing.* **22 (9):** 1709 – 1724.

Shields, A. F. 1936. Application of Similarity Principles and Turbulence Research to Bed-Load Movement, vol 26. Mitteilungen der Preussischen Versuchsanstalt für Wasserbau und Schiffbau. Berlin. Germany.

Skinner, K. S. and Bruce-Burgess, L. 2005. Strategic and Project level River Restoration Protocols – Key Components for Meeting The Requirements of the Water Framework Directive (WFD). *Journal of Water and Environment.* **19 (2):** 135-142.

Smart, G., Aberle, J., Duncan, M. and Walsh, J. 2013. Measurement and Analysi of Alluvial Bed Roughness. *Journal of Hydraulic Research.* **42 (3):** 227- 237.

Smart, G., Aberle, J., Duncan, M., and Walsh, J. Measurment and Analysis of Alluvial Bed Roughness. 2004. *Journal of Hydraulic Research.* **42 (3):** 227-237.

Smith, L. 1997. Satellite Remote Sensing of River Inundation Area, Stage, and Discharge: A Review. *Hydrological Processes.* **11:** 1427- 1439.

Smith, M., Vericat, D. and Gibbin, C. 2012. Through-Water Terretrial Laser Scanning of Gravel Bed at the Patch Scale. *Earth Surface Processes and Landforms.* **37:** 411 – 421.

Snavely, N., Seitz, S. M. and Szeliski, R. 2006. Photo Tourism: Exploring Photo Collections in 3D. *Association for Computing Machinery.* 835 – 846.

Surian, N. 1999. Channel Changes due to River Regulation: The Case of the Piave River, Italy. *Earth Surface Processes and Landforms.* **24:** 1135 –1151.

Thoma, D. P., Gupta, S. C., Bauer, M. E. and Kirchoff, C. E. 2005. Airborne Laser Scaning for Riverbank Erosion Assessment. *Remote Sensing of Environment.* **95:** 493- 501.

Thomson, J. R., Hart, D. D., Charles, D. F., Nightingale, T. L., and Winter, D. M. 2005. Effects of Removal of a Small Dam on Downstream Macroinvertebrate and Algal Assemblages in a Pennsylvania Stream. Journal of North American Benthological Society. **24:** 192–207.

Tszydel, M., Grzybkowska, M., and Kruk, A. 2009. Influence of Dam Removal on Trichopteran Assemblages in the Lowland Drzewiczka River, Poland. *Hydrobiologia* **630:** 75–89.

Van Rijn, L. C. 1984. Sediment transport, Part I: Bed load transport. *Journal of Hydraulic Engineering.* **110:**1431-1456.

Vetter, M., Hofle, B., Mandlburger, G. and Rutzinger, M. 2011. Estimating Changes of Riverine Landscapes and Riverbeds by using Airborne LiDAR Data and River Cross-Sections. *Zeitschrift fur Geomorphologie.* **55 (2):** 51 – 65.

Vianello, A., Cavalli, M. and Tarolli, P. 2009. LiDAR-Derived Slopes for Headwater Channel Network Analysis. *Cantena.* **76:** 76 – 106.

VurduJ. M., Batalla, R. J., Martinez-Casanovas, J. A. 2005. High-Resolution Gran-Size Characterisation of Gravel Bars Using Imagery Analysis and Geo-Statistics. *Geomorphology.* **72:** 73-93.

Verdú, J. M., Batalla, R., J., Martínez-Casasnovas, J. A. 2014. Assessing River Dynamics from 2D Hydraulic Modelling and High Resolution Grain-size Distribution. *Zeitschrift für Geomorphologie.* **58 (1):** 95-115.

Ward, J. V. 1989. The Four-Dimensional Nature of Lotic Systems. *Journal of the North American Benthlogical Society.* **8 (1):** 2-8.

Ward, J. V., Tockner, K., Arscott, D. B. and Claret, C. 2002. Riverine Landscape Diversity. *Freshwater Biology.* **47:** 517-539.

Wentworth, C. K. 1922. A Scale of Grade and Class Terms for Clastic Sediments. *The Journal of Geology.* **30 (5):** 377 – 392.

Werner, M. G. F. 2001. Impact of Grid Size in GIS Based Flood Extent Mapping Using a 1D Flow Model. *Phsycial Chemical Earth.* **26 (7-8):** 517 – 522.

Westoby, M. J., Brasington, J., Glasser, N. F., Hambrey, M. J. and Reynolds, J. M. 2012. 'Structure-From-Motion' Photogrammetry: A Low-Cost, Effective Tool for Geoscience Apllications. *Geomorphology.* **179:** 300 – 314.

Whittaker, A. C. and Potts, D. 2007. Analyis of Flow Competence in an Alluvial Gravel Bed Stream Dupuyer Creek, Montana. *Water Resources Research.* **43:** 1-16.

Whitaker, A. C., and Potts, D. F. 2007. Analysis of Flow Competence in an Alluvial Gravel Bed Stream, Dupuyer Creek, Montana. *Water Resources Research.* **43:** 1-16.

White, E. M. and Knights, B. 1997. Dynamics of Upstream Migration of the European Eel, Anguilla Anguilla (L.), in the Rivers Severn and Avon, England, with Special Reference to the Effects of Man-Made Barriers. *Fisheries Management and Ecology.* **4:** 311 –324.

Wilcock, P., Pitlick, J. and Cui, Y. 2009. Sediment Transport Primer: Estimating Bed Material Transport in Gravel-Bed Rivers. *General Technical Report RMRS-GTR-226. Fort Collins, CO: U.S. Department of Agriculture, Forest Service, Rocky Mountain Retail Station.* 1 – 78.

Williams, G. P. and Wolman, G. M. 1984. Downstream effects of dams on alluvial rivers. In: Geological Survey Professional Paper 1286 U.S. Government Printing Office. Washington, DC.

Williams, R. D., Brasington, J., Vericat, D. and Hick, D. M. 2014. Hyperscale Terrain Modelling of Braided Rivers: Fusing Mobile Terrestrial Laser Scanning and Optical Bathymetric Mapping. *Earth Surface Processes and Landforms.* **39:** 167 – 183.

Williams, R. D., Brasington, J., Vericat, D., and Hicks, D. M. 2014. Hyperscale Terrain Modelling of Braided Rivers: Fusing Mobile Terrestrial Laser Scanning and Optical Bathymetric Mapping. *Earth Surface Processes and Landforms.* **39:** 167-183.

Wohl, E. Angermeier, P. L., Bledsoe, B., Kondolf, M. G.,MacDonnell, L., Merritt, D. M. Palmer, M. A., Poff, L. N., and Tarboton, D. 2005. River Restoration. *Water Resources Research.* **41:** 1-12.

Wohl, E. E., Anthony, D. J., Madsen, S. W. and Thompson, D. M. 1996. A Comparison of Surface Sampling Methods for Coarse Fluvial Sediments. *Water Resources Research.* **32 (10):** 3219 –3226.

Wolman, M. 1954. A Method of Sampling Coarse River-Bed Material. *Transactions, American Geophysical Union.* **34 (6):** 951 – 956.

Wolman, M. G. and Miller, J. P. 1960. Magnitude and Frequency of Forces in Geomorphic Processes. *Journal of Geology.* **68:** 54 – 74.

Wong, M. and Parker, G. 2006. Reanalysis and Correction of Bed-load Relation of Meyer-Peter and Mueller using Their Own Database. *Journal of Hydraulic Engineering.* **132:** 1159-1168.

Woolsey, S., Capelli, F., Gonser, T., Hoehn, E., Hotmann, M., Junker, B., Paetzold, A., Roulier, C., Schweizer, S., Tiegs, S., Tockner, K., Weber, C. and Peter, A. 2007. A Stratgey to Assess River Restoration Success. *Freshwater Biology.* **52:** 752 – 769.

Wright, S. and Parker, G. 2003. Modelling Downstream Fining in Sand-Bed Rivers I: Formulation. *Journal of Hydraulic Research.* **43:** 612-619.

Wu, W., Sanchez, A. and Zhang, M. 2011. An Implicit 2-D Shallow Water Flow Model on Unstructured Quadtree Rectangular Mesh. *Journal of Coastal Resarch.* **59:** 15 – 26.

Wu, W., Shields Jr., F. D., Bennett, S. J. and Wang, S. S. Y. 2005. A Depth-Averaged Two-Dimensional Model for Flow, Sediment Transport, and Bed Topography in Curved Channels with Riparian Vegetation. *Water Resources Research.* **41:** 1-15.

WWF. (2014). *Dam facts and figures.* Available: wwf.panda.org. Last accessed 20 July 2014.

Yalin, M. S. 1963. An Expression for Bed-Load Transportation, Proc. ASCE. **89:** 221-250.

Yang, C. T., and Huang, C. 2001. Applicability of Sediment Transport Formulas. International Journal of Sediment Research. **16:** 335–353.